이학박사 학위논문

Responses of marine organisms at multiple levels of organization to diverse anthropogenic activities in the Yellow Sea

황해 해양환경 내 다양한 인간활동이
해양생물에게 미치는 영향에 관한 연구

2020년 2월

서울대학교 대학원
지구환경과학부
노 준 성

Responses of marine organisms at multiple levels of organization to diverse anthropogenic activities in the Yellow Sea

지도 교수 김 종 성

이 논문을 이학박사 학위논문으로 제출함

2020년 2월

서울대학교 대학원

지구환경과학부

노 준 성

노준성의 이학박사 학위논문을 인준함

2020년 2월

위 원 장 _____ (인)

부위원장 _____ (인)

위 원 _____ (인)

위 원 _____ (인)

위 원 _____ (인)

ABSTRACT

Marine ecosystems are continuously influenced by multiple stressors by anthropogenic activities, and the effects can be assessed through the ecological responses of various marine organisms. In the present study, ecological responses focused on marine organisms against anthropogenic influences were assessed in varying spatiotemporal scales through four case studies in the Yellow Sea; 1) benthic primary production and benthic-pelagic coupling in large marine ecosystem, 2) food web dynamics in a closed estuary by sea dike, 3) distribution characteristics of fish assemblages in natural and artificial reefs, and 4) bioaccumulation and biodegradation in oil-contaminated marine environment.

On the benthic primary production study covering the Yellow Sea region, which is continuously influenced by various human activities, the benthic production and productivity in the Yellow Sea were confirmed, and the benthic-pelagic coupling was revisited. In particular, this study suggested benthic-pelagic coupling boundary which is estimated until ~10 km offshore in the Yellow Sea, and tidal energy was the dominant factor to transport benthic production toward the pelagic zone. These results indicated that the indiscriminate development and alteration of coastal environments could have resulted in a collapse of entire marine ecosystem productivity. The closed estuarine food web dynamics indicated that relatively limited utilization of terrestrial particulate organic matter to estuarine benthos than marine origin food sources. In particular, microphytobenthos (MPB) was the major food source for marine clams following growth and seasonal variations. In the study of artificial reefs, relatively abundant fish individuals were observed in artificial reef habitats compared to control sites, and specific fish assemblages showed preferences on certain environmental conditions (temperature, reef materials, and bottom sediment properties) in artificial reefs. However, potential impacts were also found in some of the artificial reef habitats such as community shift and very low effectiveness of artificial reef installation. The result showed that bioaccumulation by oil-suspended particulate matter aggregates (OSAs) in marine bivalve was remarkable during 30 days, and then depuration of the OSAs accumulation was observed after 30 days until 50 days. Simultaneously, great blooms of oil-degrading microbes were observed in the OSAs contaminated environment which indicating

biodegradation of OSA by microbial activities.

The present study provided marine ecosystem responses in the Yellow Sea through the case studies in different time and space. Of note, the anthropogenic influences have altered the structure and/or function of marine organisms, nevertheless, the marine ecosystem of the Yellow Sea showed that very productive benthic primary production and the adaptable capacity against anthropogenic influences in this study. However, increasing and continuous anthropogenic pressures cause the weakening of marine health, consequently, it could lead to a series of declines in the diversity and proliferation of marine lives. Therefore, a better scientific understanding of sustainable management in the Yellow Sea region or elsewhere will be necessary for the future plan for a healthy marine environment.

Keywords: Marine ecosystem, Anthropogenic influences, Marine organisms, Coastal development, Marine pollution, Sustainability

Student Number: 2015-30104

TABLE OF CONTENTS

LIST OF TABLES

LIST OF FIGURES

CHAPTER 1.

INTRODUCTION

1.1. Backgrounds

Human well-being including the basic material needs for a good life, health, security, abundant social relations, and freedom of choices and actions is significantly related to ecosystem health (Millennium Ecosystem Assessment Synthesis Report, 2005). Humans are fully dependent on Earth's ecosystems and their services that they support, such as food, clean water, climate regulation, disease regulation, and spiritual/aesthetic recrations. Therefore, it is important to use strategically finite resources efficiently for the sustainability of ecosystem services. Indiscriminate development and human activities will return to humans due to various environmental problems such as famine, water scarcity, climate change, pollution, and multiple environmental issues (Fig. 1.1).

During the last decades, the global marine ecosystems have undergone dramatic changes under the strong influences of anthropogenic activities, in particular, coastal areas have been intensively developed and altered following by increase of human population. The anthropogenic activities can produce numerous and multiple stressors such as overfishing, pollution, habitat fragmentation and destruction, invasion of alien species, climate changes, and ocean acidification that have varying impacts to the marine ecosystems on different spatio-temporal scales (Jackson et al., 2001; UNEP, 2010; Rombouts et al., 2013; Boldt et al., 2014). The anthropogenic impacts to marine ecosystem possess a high risk of biological extinction and loss of diversities on habitat and biota, and lead to a collapse of entire ecosystem structure and function.

Various types of anthropogenic stressors affect to marine ecosystem along the Yellow Sea coast. For examples, oil spill accident is one of the most catastrophic disaster to marine ecosystem in local scale. Crude oil and oil-derivatives not only contain toxic components, such as polycyclic aromatic hydrocarbons (PAHs), but can also be spread widely and persist and be accumulated into food chains. In particular, detrimental effects of oil spills such as PAHs bioaccumulation to marine organisms over an extended period can be significant (Table 1.1). The habitat alteration of the estuarine and coastal areas such as straightening, dike or dam construction, coastal reclamation, etc. can occur at various scales and could have resulted in significant ecosystem deterioration. (Table 1.2). As efforts to manage and

enhance damaged marine ecosystem, sometimes artificial reefs are widespread installed along the coastal area. Practically, previous studies have reported varying influences on the artificial reef installation which are generally focused on positive effects (Table 1.3). Although there are such evidences to enhance marine biodiversity by artificial reefs, the disturbances caused by the installation of artificial structures by humans in the ecosystem should not be overlooked. In particular, the artificial reefs were installed along with a wide area of the coastal environments, thus, the side effects should be considered.

A recent study founded that at least 40% of the global oceans are heavily disturbed by human activities (IOC/UNESCO et al., 2011). Likewise, rapidly developing East Asia countries; China and Korea, resulted in increasing anthropogenic pressures to estuary, coast, and eventually open sea of the Yellow Sea large marine ecosystem (YSLME) during the past decades (Jeppesen et al., 2011; Ryu et al., 2014). Considering sustainable management of marine resources in the Yellow Sea, the comprehensive monitoring and concrete management strategies to understand on ecological responses of marine ecosystem against impacts of anthropogenic activities would be needed in various types, time and space.

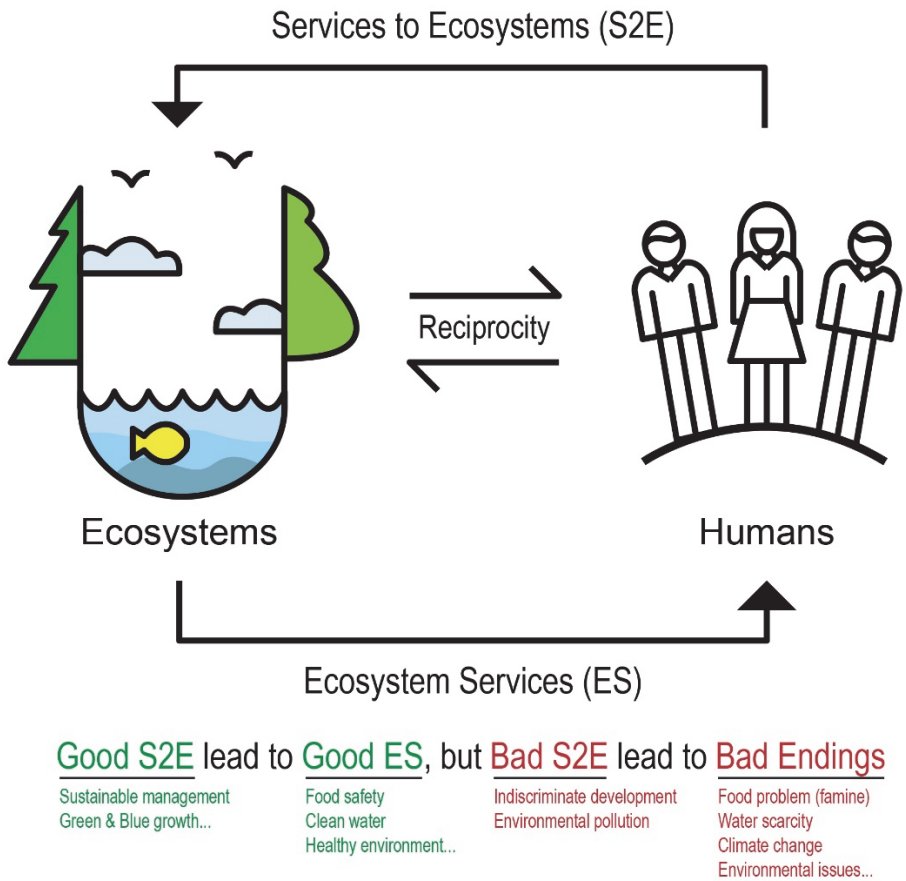

Fig. 1.1. Illustration of reciprocal feedback loop between ecosystems and humans.

Table 1.1. Mini-review of bioaccumulation of PAHs in marine organisms (fish and bivalves), data from in situ measurements.

Species	Region	Dominating Mol. Mass	ΣPAHs (ng/g)	Reference
Fish				
Clupea pallasii	Puget Sound, Washington, USA	LMM[a]	1.1–140	West et al., 2014
Mullus barbatus	Mediterranean Sea	LMM	14.7–49.6	Baumard et al., 1998
Serranus scriba	Mediterranean Sea	LMM	23.6–139	
Micropogonias furnieri	Bahía Blanca Estuary, Argentina	LMM	34.87	Oliva et al., 2017
Cynoscion guatucupa	Bahía Blanca Estuary, Argentina	LMM	98.25	
Anguilla anguilla	Biertze Lagoon, Tunisia	LMM	114.5–133.7	Barhoumi et al., 2016
Scophthalmus maximus	Laboratory	LMM	121	Baussant et al., 2001
Cynoglossus senegalensis	Gulf of Guinea, Ghana	LMM	67–163	Bandowe et al., 2014
Drepane africana	Gulf of Guinea, Ghana	LMM	136–453	
Pomadasys perotaei	Gulf of Guinea, Ghana	LMM	163–252	
Sarotherodon mossambicus	Pearl River Estuary, Hong Kong	LMM	184–194	Liang et al., 2007
Ramnogaster arcuata	Bahía Blanca Estuary, Argentina	LMM	182.35	Oliva et al., 2017
Mustelus schmitti	Bahía Blanca Estuary, Argentina	LMM	308.96	
Anguilla anguilla	Amsterdam, Netherlands	LMM	11,000–39,000	van der Oost et al., 1994

Table 1.1. Continued.

Species	Region	Dominating Mol. Mass	ΣPAHs (ng/g)	Reference
Bivalves				
Chlamys farreri	Yellow Sea, China	NA[c]	ND[d]	Liu et al., 2008
Cyclina sinensis	Yellow Sea, China	NA	ND	
Neptunea arthritica	Yellow Sea, China	NA	ND	
Neverita didyma	Yellow Sea, China	NA	ND	
Anadara kagoshimensis	Yellow Sea, China	NA	ND	
Siliqua pulchella	Yellow Sea, China	NA	ND	
Bullacta exarata	Yellow Sea, China	HMM[b]	23.5	
Euspira gilva	Yellow Sea, China	HMM	23.5	
Solen grandis	Yellow Sea, China	HMM	23.5	
Mytilus edulis	Yellow Sea, China	HMM	ND–29.3	
Saccostrea cucullata	Yellow Sea, China	HMM	29.7	
Magallana gigas	Yellow Sea, China	HMM	24.7–30.3	
	Pacific Coast, Japan	LMM	370	Onozato et al., 2016
Leukoma jedoensis	Yellow Sea, China	HMM	26.5–39.7	Liu et al., 2008
Anadara broughtonii	Yellow Sea, China	HMM	41.9	

Table 1.1. Continued.

Species	Region	Dominating Mol. Mass	ΣPAHs (ng/g)	Reference
Mytilus galloprovincialis	Gironde Estuary France	LMM, HMM	49.8–101.5	Bodin et al., 2004
	Pacific Coast, Japan	LMM	301	Onozato et al., 2016
	Arachon Bay, France	HMM	279–2420	Baumard et al., 1998
Meretrix meretrix	Yellow Sea, China	LMM	28.3–108.0	Liu et al., 2008
Ruditapes philippinarum	Pacific Coast, Japan	LMM	244	Onozato et al., 2016
	Yellow Sea, China	HMM	24.8–302.0	Liu et al., 2008
Brachidontes rodriguezi	Bahía Blanca Estuary, Argentina	LMM	ND–482.4	Oliva et al., 2017
Mytilus galloprovincialis	Mediterranean Sea	LMM	25.1–337	Baumard et al., 2001
	Biertze Lagoon, Tunisia	LMM	107.4–430.7	Barhoumi et al., 2016
	Urdaibai Estuary, Spain	HMM	21–64	Orbea et al., 2002
Magallana sp.	Urdaibai Estuary, Spain	HMM	31–218	
Mya truncata	Svalbard Fjord	LMM	200,080*	Camus et al., 2003

*Analyzed in lipid extracts from *Mya truncata*.

[a]lower molecular mass, [b]higher molecular mass, [c]not available, and [d]Not detected.

Table 1.2. Mini-review for studies on the spatiotemporal changes in ecological responses of marine organisms to habitat alteration by artificial structures or reclamation (Abbreviations are corresponding; Sp: spring, Su: summer, F: fall, W: winter, Re: region, St: station, and Sv: survey).

Study area		Type	Target		Sampling information								Remark	Reference
					Period	Season				Number of				
Country	Region		Organism	End-point	(yr)	Sp	Su	F	W	Re*	St	Sv		
China	Chongming Island	Reclamation	Nematode	Density, richness, diversity	<1				v	1	12	1	Reclamation altered nematode community structure.	Wu et al., 2005
China	Yancheng	Reclamation	Macrobenthos	Abundance, richness	<1	v				1	4	1	Biodiversity and functional composition of macrofauna was significantly affected by dike age in the reclaimed coast.	Ge et al., 2016
China	Yellow River delta	Tidal barrier	Macrobenthos	Density, biomass	<1	v		v		1	18	2	The macrobenthos communities differed greatly on opposite sides of tidal barriers.	Yang et al., 2017
Bahrain	Sitra island	Reclamation	Macrobenthos	Survival, burrowing	<1	v				1	10	1	Reclamation diminished abundance and distribution of macrobenthos	Naser, 2011
Netherland	Oosterschelde	Storm-surge barrier	Macrobenthos	Abundance, density, biomass	1–3		v			1	305	2	The impact of barrier construction on the macrofauna was relatively smaller than climate effects.	Meire et al., 1994
France	Bay of Biscay	Reclamation	Macrobenthos	Abundance, richness	1–3		v			1	6	3	After restoration (return land to the estuary), rapid recovery of benthic communities was observed.	Marquiegui & Aguirrezabalaga, 2009
Austarlia	Eastern Hunter River	Weir, dam	Fish community	Abundance, density	1–3		v			4	3	2	The barriers within river networks resulted in varying connectivity loss.	Rolls, 2011
India	Mumbai	Reclamation	Polychaete	Abundance, biomass	1–3			v		1	12	15	Reclamation caused the decrease of polychaete community.	Quadros et al., 2009

Table 1.2. Continued.

Study area		Type	Target		Sampling information								Remark	Reference
						Number of								
Country	Region		Organism	End-point		Sp	Su	F	W	Re*	St	Sv		
China	Tianjin	Reclamation	Phyto- and zooplankton, benthos	Density, biomass	1–3	v	v			1	8	3	Reclamation decreased the biodiversity and changed the structure of marine communities.	Li et al., 2010
China	North to south China coasts	Coastal infrastructures	Macrobenthos	Abundance, density, biomass	1–3		v		v	26	1	3	Artificial structures provided habitats for rocky shore species.	Dong et al., 2016
Korea	South coasts	Dike	Macrobenthos	Stable isotopes (food web)	1–3	v		v		2	4	2	Dike (local scale) induces changes in basal resource availability and faunal composition.	Park et al., 2017
UK	Sedgeunkedunk Stream	Dam	Fish community	Density, biomass	>3	v	v			1	8	9	Dam removal has enhanced the fish assemblage by undisrupted stream gradient.	Hogg et al., 2015
The Netherlands	Oosterschelde	Storm-surge barrier	Macrobenthos	Abundance, density, biomass	>3		v	v		1	6-305[a]	2-18[a]	Climate caused more disturbance than barrier construction in the macrofaunal population.	Coosen et al., 1994
Korea	Saemangeum	Reclamation	Macrobenthos	Density, richness	>3	v	v	v	v	1	11-38[b]	12	Dike construction caused the change of benthic communities.	An et al., 2006
Korea	Seamangeum	Reclamation	Macrobenthos	Abundance, density, richness	>3	v	v	v	v	1	7	15	Since the closure of the dike, the number of species of macrobenthos	Koo et al., 2008

*The number of regions depending on geographical grouping by river-catchments, estuaries, or coasts.

[a]The number of stations, study period, and field survey differed depending on the dataset (total three datasets used).

[b]The number of stations differed depending on sampling date.

Table 1.3. Mini-review for the previous artificial reef studies summarizing the major environmental factor(s) influencing the effectiveness of artificial reefs in fish community, data given by region and target organisms.

Region	Target organism	Response	Environmental factor	Reference
Oahu, Hawaii	Sessile organisms	Community development	Seasonal variation (summer and winter) Reef materials (concrete, car tire, and steel)	Fitzhardinge & Bailey-Brock, 1989
Southern California, USA	Infaunal benthos	Species density	Grain-size distribution of sediment Foraging by predators (assumption of authors)	Ambrose and Anderson, 1990
Adriatic Sea, Italy	Fish	Abundance, richness, and density	Artificial vs. natural reef Reef size Variation in bottom habitat (sand-muddy and rocky)	Bombace et al., 1994
Adriatic coast, Croatia	Fish, mollusc, and crustacean	Richness, diversity, and catch composition	Artificial reef vs. control site Seasonal variation	Fabi and Fiorentini, 1994
Loano, Italy	Sessile organisms	Community development	Seasonal variation Development-climax-interaction with fish pattern instages (3 years)	Relini et al., 1994
Gulf of Mexico, USA	Fish (juvenile, adult)	Abundance and diversity	Vertical (in depth) distribution Diel periodicity Seasonal variation	Rooker et al., 1997
Southern Eilat, Israel	Fish	Abundance, richness, and diversity	Reef size and complexity Vertical (in depth) distribution Temporal variability	Rilov and Benayahu, 1998
Rio de Janeiro, Brazil	Fish	Species, individuals, and weight	Seasonal variation Hydrological features (rainfall, river outflow, water clarity, and salinity)	Godoy et al., 2002
Florida, USA	Fish	Abundance, richness, and biomass	Reef design (void space, complexity, and floating attractants)	Sherman et al., 2002
Southern Eilat, Israel	Sessile organisms	Community development	Structural design and spatial orientation Reef age (successional species variation)	Perkol-Finkel & Benayahu, 2004

Table 1.3. Continued.

Region	Target organism	Response	Environmental factor	Reference
Tortola, UK	Fish	Abundance and richness	Reef complexity (rugosity, hard substrate, and small refuge holes)	Gratwicke and Speight, 2005
Ft. Lauderdale, USA	Fish	Abundance and richness	Reef space and size (module positioning experiment)	Jordan et al., 2005
Rio de Janeiro, Brazil	Fish	Density, richness, diversity, and dominance	Seasonal variation Reef complexity (with and without holes) Reef cover (with and without benthos)	Brotto et al, 2006
Jeju, Korea	Fish	Abundance and species composition	Seasonal variation Reef type (five shapes of artificial reef)	Oh et al., 2010
Jeju, Korea	Fish	Species composition	Seasonal variation Reef type (two types of artificial reefs and a natural reef)	Kim et al., 2011
Parana coast, Brazil	Fish	Species composition (richness and abundance)	Reef complexity (shape and holes)	Hackradt et al., 2011
Cape Verde, Senegal	Fish	Richness, diversity, dominance index, and equitability	Artificial vs. natural reef Reef rugosity and depth	Santos et al., 2013
Gulf of Mexico, USA	Fish (Red snapper)	Density and size distribution	Depth	Jaxion-Harm & Szedlmayer, 2015
Sydney, Australia	Fish	Species and abundance	Distances from the reef Reef type (five shapes of artificial reef)	Scott et al., 2015

1.2. Objectives

In this dissertation, an overarching research question is ***"How do anthropogenic activities affect to marine organisms?"***. It is impossible to assess the response of marine organisms to all anthropogenic influences, thus, four case studies were foucused to address the responses of marine organisms to anthropogenic influences such as development or pollution pressures in this study. In particular, the Yellow Sea Coast, which is known as an area where the pressure on the coast has increased markedly by the rapid economic growth of China and Korea in the last half century, was selected as a research area. Specific subtopic, objectives and structure of the studies are stated as follows (Fig. 1.2, 1.3, & Table 1.4):

1. ***Benthic primary productivity and benthic-pelagic coupling of the Yellow Sea.***
   As a case study for very fundamental function by marine producer, we measured the primary production by microphytobenthos in the entire intertidal area and then estimated a range of the productive zone toward open sea in the Yellow Sea (in **Chapter 2**).

2. ***Benthic food web dynamics in a closed estuary by sea (estuarine) dike.***
   As a case study to understand food web dynamics between producers (potential food sources) and consumers in an estuary which was interrupted freshwater discharge by man-made construction (dike) (in **Chapter 3**).

3. ***Distribution characteristics of fish assemblages in artificial reef areas***.
   As a case study to assess structure of fish communities (consumer) in natural and artificial reefs and find environmental fators to attract specific fishes, and also to diagnose potential impacts of artificial reef installation (in **Chapter 4**).

4. ***PAHs bioaccumulation and biodegradation by marine organisms.***
   As a case study to evaluate PAHs bioaccumulation to the marine bivalve (consumer) and PAHs biodegradation by marine microbes (decomposer) in oil-suspended particulate matter aggregates contaminated environments.

The detailed topics in this dissertation are intended to supplement information on the responses of marine organisms to anthropogenic influences that have not been reported previously or are lacking. Finally, discussion and implication including a coherent conclusion and contribution of this study under the overarching research question and future research directions for the better understanding and sustainable management of marine ecosystem are provided in **Chapter 6**.

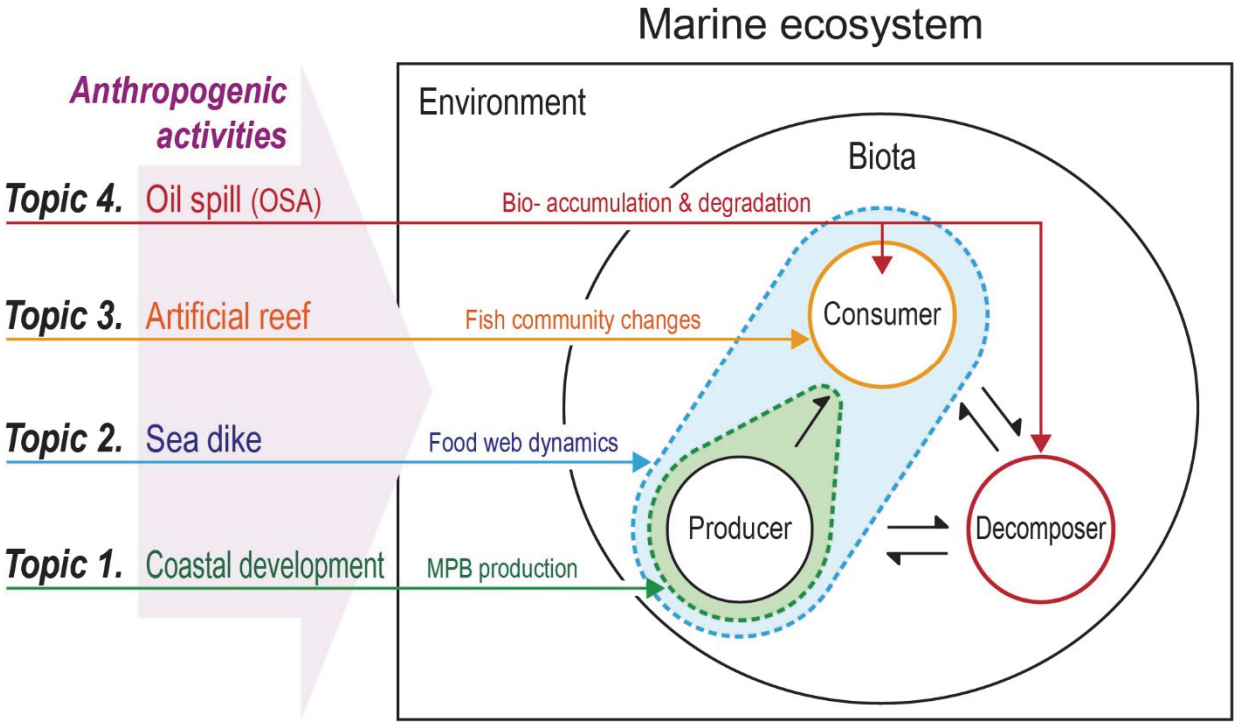

Fig. 1.2. Schematic diagram of marine ecosystem components (environment and biota) and external influences by anthropogenic activities. Four topics consist of subchapters in this PhD dissertation.

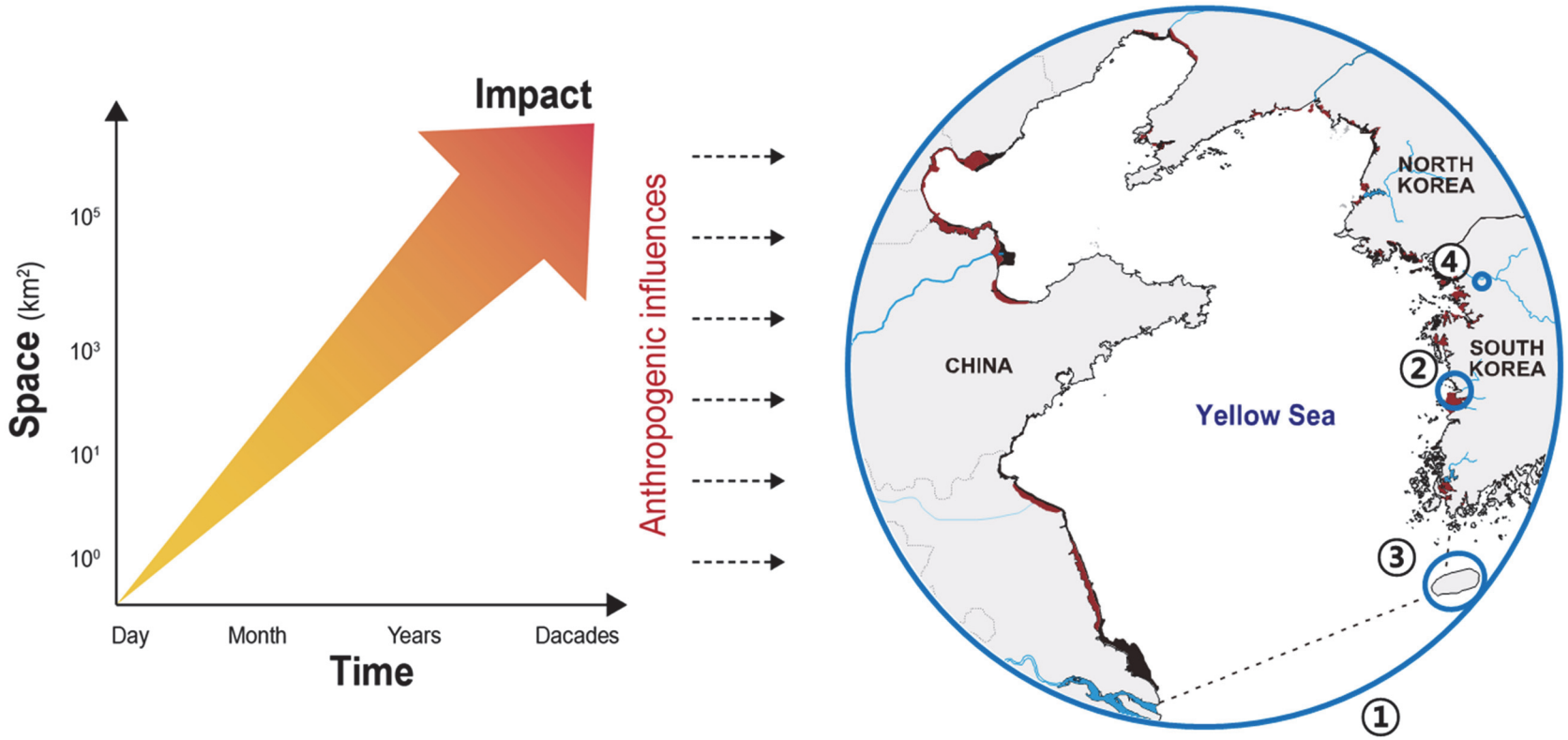

Fig. 1.3. (**left**) Schematic diagram of ecological impacts by anthropogenic influences in different time and space. (**right**) Map showing the spatial scales following case studies (①–④) conducted in the Yellow Sea for the present study. Details of each case study given in Table 1.4.

Table 1.4. Spatiotemporal scale, target organism, and end-point of case studies in the present study. Each number of case studies is (①–④) corresponding to Fig. 1.2.

Topic	Time scale	Sptial scale	Target organism			End-point
			macro	micro	Details	
① MPB production	Summer season (~ 1 month)	Large marine ecosystem (Yellow Sea)		v	**Microphytobenthos**	Biomass (chlorophyll-*a*) & primary production
② Food web dynamics	Seasonal survey for 3 yrs	Estuarine area (Geum-river)	v	v	**Microphytobenthos** **Macrofauna**	Isotope signatures ($\delta^{13}C$, $\delta^{15}C$)
③ Artficial reef fishes	2 times per a year	Coastal area (Jeju Island)		v	**Fish communities**	Community structure
④ Oil spill (OSA)	50 d experiment	Lab-mesocosm	v	v	**Microbial communities** **Bivalve (*Mactra veneriformis*)**	PAHs

CHAPTER 2.

Ecological role and significance of microphytobenthos on the benthic-pelagic coupling: A case study in the Yellow Sea

This chapter has been prepared for submission.
Noh, J., Kwon, B.-O., Yim, J., Zhou, Y., Yoon, S.J., Lee, C., Wang, T., Nam, J., Lee, S.Y., Ryu, J., Hong, S., Park, J., Lu, Y., Khim, J.S., 2019. A global microphytobenthic primary production and marine benthic-pelagic coupling revisited. (in preparation).

2.1. Introduction

Marine ecosystems are widely interconnected by carbon flows with complex biological processes of varying sptiotemporal scales (Gounand et al., 2018). From intertidal to pelagic zone, oxygenic photosynthesis by primary producers is practically the summation of all the biochemical production of organic matter (Falkowski et al., 1998). Atmospheric carbon, in the process, is to be fixed as primary producer's biomass then transferred to the first heterotrophic level in an ecosystem (Lindeman, 1942; Field et al., 1998; Middelburg et al., 2000). Microphytobenthos (MPB), one of primary producers mainly inhabit in soft bottom sediments, possess ubiquitous coastal habitats (Macintyre et al., 1996; Cahoon, 1999), can contribute up to 50% of total coastal carbon budgets (Underwood & Kromkamp, 1999).

The diverse MPB is a key primary producer significantly supporting marine ecosystem services. Its pivotal socioecological roles from sediment stabilization, nutrient cycling, and to trophic energy transfer are well documented (Macintyre et al., 1996; Miller et al., 1996; Harison et al., 2013). In particular, the MPB resuspension, a major process involved in benthic-pelagic coupling (BPC), is controlled by a complex set of interactions among biological, physical, and chemical components (De Jonge & Beusekom, 1995; Koh et al., 2006; Ubertini et al., 2015). The resuspended portion of MPB can be transported away from intertidal to offshore zone (De Jonge & Beusekom, 1995), which potentially allow a number of pelagic organisms to utilize the benthic-originated food sources (Herman et al., 2000). Likewise, the correspondence between sedimentary Chl-a during exposure and water Chl-a during flood, have evidenced the entrainment of sedimentary Chl-a to the water column during by tidal resuspension (Koh et al., 2006). However, a global or large-scale assessment of MPB primary production (PP) has yet been emphasized. In the meantime, what remain unclear so far is to which extent benthic production can further reach out in a global or large marine ecosystem scale.

2.2. Materials and Methods

2.2.1. Global data collection

All data were originally compiled by searching the ISI Web of Science for studies on microphytobenthos (MPB) that collected in situ to estimate MPB biomass and/or primary production. We also updated global MPB biomass and primary production data which previously reported by Cahoon (1999). MPB biomass is often very fluctuated depending on environmental conditions such as air/watertemperature, nutrient input, and meteorological changes even in local scales (Macintyre et al., 1996; Caboon, 1999). We therefore excluded studies in a single period and used data in sequential surveys at regular time intervals over one-year round, for example, monthly, seasonal, or at least the summerand winter surveys were collected. And, we used data that not only surveyed in intertidal areas where bare or low vegetated flats, but also seawater is free-flow among beaches, bays and estuaries. So, halophyte- and seagrass-dominant tidal flats, inner side of lagoon, and freshwater areas (<5 psu) were excluded in this study. In addition, for unification of MPB biomass unit, we only used values expressed in the unit weight of MPB per unit area (mg m^{-2}), except for existing a conversion factor of MPB between unit weight of sediment and unit area at a certain region (Montani et al., 2003). We totally sorted 104 studies (including 103 previous studies and this study, see Table 2.1), and which are averaged the values in a single study over the year. In case for multiple studies surveyed in an overlapping region, we also averaged values within one region for plotting in Fig. 2.1A–C.

To indicate the global tidal range in background of Fig. 2.1, we slightly modified referred from previous studies (Davies & Clayton, 1980; Masselink & Hughes, 2014). We also indicated that tidal ranges dividing into latitudinal intervals of 15 degrees, and then means with standard deviation are presented.

To analyse a global dataset of pelagic chlorophyll-*a* (Chl-*a*) along global intertidal coasts, we used Aqua/Terra MODerate resolution Imaging Spectroradiometer (MODIS) images with a resolution of 4 km × 4 km. The values of pelagic Chl-*a* (mg m^{-3}) through remote sensing is estimated by using the samples

obtained from the field survey or the empirical formula of the reflection ratio by using the indirect survey data through the sufficient verification process. Generally, the OC estimation formulas are using for the estimation of Chl-a from various satellite images such as Coastal Zone Color Scanner (CZCS), Sea-Viewing Wide Field-of-View Sensor (SeaWiFS), and MODIS (O'Reilly et al., 2000). We selected the MPB studies surveyed after 2002 in situ among previous literatures reviewed in Fig. 2.1 because the MODIS images are available from that time. We sorted among the selected studies matched at the condition that of providing precise coordinates or a high-resolution map, and then generated an integrated dataset of MPB Chl-*a* (n = 133) reported from various intertidal regions worldwide. Finally, based on the MODIS images and MPB database, pelagic Chl-*a* in open-sea locations was estimated along YSLME, which are considering of closest and similar spatiotemporal condition as compared with previously reported coordinates of the MPB database.

To compare a trend consistency between the previous data versus in situ data of ours, we additionally conducted in situ MPB sampling along the Yellow Sea coast (see details in Chapter 2.2.2), and then also estimated pelagic Chl-*a* from MODIS images by the same strategy which applied at global data. On average, the locations of pelagic Chl-*a* (Total n = 199 including 133 locations of global data from previous literatures and field-surveyed 66 locations in YSLME) are 10.3 ± 6.3 km away from the MPB sampling locations.

The GOCI (Geostationary Ocean Color Imager), which was firstly launched by South Korea in June 2010, enables researchers to observe the diurnal cycles of ocean in East Asia. The Shorter shooting period of GOCI can produce eight images at one-hour interval during the day time with a higher spatial resolution of 500 m × 500 m compared to prior satellite images (Ryu et al., 2012). The GOCI sensor is based on the OC4 formula, but there is no spectral band image at 510 nm, so that some modified OC3G formula, which is based on the blue-green ratio at 412 nm (band 1), is mainly used (Moon et al., 2012). Therefore, we used GOCI data to analyse the correlation between the MPB Chl-*a* in intertidal flat sediments and the pelagic Chl-*a* in the adjacent coastal waters at higher spatial resolution in the Yellow Sea coasts. The pelagic Chl-a was not only estimated at the closest open-sea

locations (P_{coast}) averagely 7.7 ± 5.6 km away from benthic locations (P_0) where we collected MPB samples, but also further points on transects (n = 67) with 20 km intervals from Pcoast up to 100 km. Altogether, one transect consists of Pcoast and six locations following a distance gradient from coast to open seaward as P_{20}, P_{40}, P_{60}, P_{80}, and P_{100}. In order to determine representative pelagic Chl-*a* in the Yellow Sea coast, additional transect lines have been added to ensure an uniform geographical distribution. Finally, we estimated pelagic Chl-*a* in 552 locations on 92 transects in YSLME.

The present study concomitantly estimated concentrations of total suspended solids (SS) at Pcoast locations by GOCI. The pelagic SS concentrations were estimated using YOC (Yellow Sea Large Marine Ecosystem Ocean Colour Group) algorithm in concern of geographical and oceanographical settings (Siswanto et al., 2011). Consequently, we investigated relationships of pelagic SS versus pelagic Chl-*a* and benthic Chl-*a* versus pelagic SS.

2.2.2 Study area and sampling methodology

Sediment samples were collected from the intertidal regions considering evenly geographical distribution of MPB along YSLME. Sediment samples were collected in ebb tide (during exposure) along coastal areas (68 locations in 21 regions) including brackish (n = 38) and saline areas (n = 30) (Fig. 2.3) within a month between June 27 and July 23, 2018. Three sediment samples were collected using a syringe corer on each sampling site to determine Chl-*a* concentration as a proxy of MPB biomass. In addition, surface sediments (at 0.5 cm depth) were scraped and stored in airtight plastic bags for taxa identification of diatoms and analysis of sediment properties. Before analysis, sediment samples for MPB biomass and sediment properties (total organic carbon, total nitrogen, stable carbon isotopic ratio, and particle size parameters) were frozen in the field and stored at −20 °C in the laboratory, but diatom samples (in surface sediment) were fixed with fixed with formalin to a final concentration of 2% and stored at room temperature.

The following physical seawater parameters were measured at each sampling site using YSI multi-parameter probes (H40d, HACH, Loveland, CO., USA) in subsampled seawater in situ: pH, temperature (°C), dissolved oxygen (mg/l), and salinity (psu). The sediment samples for analyses of total organic carbon (TOC), total nitrogen (TN), and carbon stable isotopic ratio ($\delta^{13}C$) were freeze-dried, homogenized, and powdered using agate mortar. The sediment samples were then decalcified with 10% hydrochloric acid, washed twice with deionized water, and freeze-dried again for determination of TOC and $\delta^{13}C$. TOC, TN, and $\delta^{13}C$ in sediments were measured with an Elemental Analyzer-Isotope Ratio Mass Spectrometer (EA-IRMS) (Elementar, Gmbh, Hanau, Germany). Stable carbon isotopic compositions were expressed as ‰ delta notation, given in equation (1).

$$\delta^{13}C \text{ or } \delta^{15}N\ (‰) = [R_{sam}/R_{ref} - 1] \times 1000 \qquad (1)$$

where, R_{sam} and R_{ref} are the compositions ($^{13}C/^{12}C$ or $^{15}N/^{14}N$) of the sample and reference, respectively. Isotopic compositions were reported relative to conventional reference materials, Vienna Peedee Belemnite (VPDB) for carbon, and atmospheric

N_2 for nitrogen. International isotope standards, IAEA-N-2 and IAEA-CH-3, were used as reference materials to calculate analytical error of carbon and nitrogen, respectively. Measurement precision was approximately 0.04‰ for $\delta^{13}C$ and 0.2‰ for $\delta^{15}N$.

To measure particle size distribution of sediments, subsamples were treated with H_2O_2 to remove organic matter and then analyzed using a laser diffraction method (Mastersizer 3000 grain size analyzer; Malvern Instruments, Ltd., Worcestershire, UK). Sediment Chl-*a* was extracted with 10 ml of 100% acetone for 24 h at 4 ºC. Samples were then centrifuged at 3000 rpm for 5 min. The absorbance of the extracted solution was measured using a spectrophotometry (Jenway 7310 spectrophotometer, UK) by placing 3 ml of the solution in a quartz cuvette. The concentration of Chl-*a* (mg m^{-2}) was calculated by the Lorenzen (1967) equations, data given as mean value.

2.2.3 Data analysis

Benthic primary production (PP) was estimated in YSLME between June 20 and July 20, 2018. We used a MPB PP model which is temperature-based algorithms for the estimation of MPB PP from previous study (Kwon et al., 2018). Based on this empirical MPB PP model, the MPB PP in YSLME is possible to calculate by input of explanatory factors such as temperature, irradiance, tidal height, and chlorophyll-*a* concentration (viz. MPB biomass) (Table 2.4). In brief, both the chlorophyll-specific maximum photosynthetic capacity (P^b_{max}) and the saturated light intensity (I_k) were significantly correlated with temperature ($p < 0.01$), with MPB photosynthesis-irradiance (P-I) equations (2) and (3):

$$P^b_{max} = 0.2156 \times e^{0.0484T} \quad (2)$$

$$I_k = (5.0670 \times T) + 434.5538 \quad (3)$$

where P^b_{max} (mmol O_2 mg Chl-a^{-1} h^{-1}) is the chlorophyll-specific maximum photosynthetic capacity; I_k (μmol photons m^{-2} s^{-1}) is saturated light intensity; and T is temperature (°C). Therefore, the primary production are represented by quantum efficiency derived from P-I model given in equation (4) (Jassby & Platt, 1976):

$$P_G(t) = \text{Chl-}a(t) \times \{[P^b_{max}(t)] \times \tanh [\alpha^b(t) \cdot I(t) / P^b_{max}(t)]\} \quad (4)$$

where P_G is gross primary production (mmol O_2 m^{-2} h^{-1}); Chl-*a* is chlorophyll-*a* concentration (mg Chl-*a* m^{-2}); P^b_{max} (mmol O_2 mg Chl-a^{-1} h^{-1}) is a measure of chlorophyll-specific maximum photosynthetic capacity; α^b (mmol O_2 mg Chl-a^{-1} h^{-1} (μmol photons m^{-2} s^{-1})$^{-1}$) is chlorophyll-specific photosynthetic efficiency, which is an indicator of quantum efficiency of photosynthesis; and I (μmol phothons m^{-2} s^{-1}) is light intensity.

The hourly water temperature and irradiance data were collected from the ocean stations and meteorological stations, respectively, situated close to each study site of China and Korea. The hourly tidal data in Korea were collected from the tidal stations which located close to each study site, while that of Chinese coasts were collected from predicted tide tables presented by the National Marine Data and Information Service, China (NMDIS, 2017). The predicted data error is within 20 to 30 minute in time and 20 to 30 cm in tidal height. The MPB Chl-*a* was used by averaging the values measured in the Yellow Sea field survey. However, there is a possibility that primary production may be over- or under-estimated in areas where Chl-*a* are measured very high or low because Chl-*a* values in the Yellow Sea are showing widely regional variations in MPB biomass are very ranged (0.2−166.2 mg m^{-2}). Thus, we used values in 99% confidence interval for the PP model, namely, top and down of 0.5% of the MPB Chl-*a* of total were excluded.

Altogether, daily production was integrated with gross primary production over exposure periods (hours) which was considered tidal height of sampling location, also assuming that there is little or no primary production by MPB when the tidal flat is submerged (Kwon et al., 2014) (Eq. 5).

$$\int_{ebb}^{flood} P_G(t)dt \qquad (5)$$

where daily PP is integrated with primary production (mmol O_2 m^{-2} d^{-1}) over the period of exposure (viz., after ebb and before flood) to sunlight a day; and PG represents gross primary production given in equation (6). Daily benthic PPs in North Korea were roughly calculated by input of estimated values in benthic Chl-*a* in this study (P-I curve based), irradiance data from closest stations in China and Korea, (air) temperature forecast of Pyongyang, and predicted tidal height (Hwang et al., 2014). The benthic Chl-*a* in North Korea estimated by a regression curve for benthic-pelagic Chl-*a* correlation in this study (see Fig. 2.4B). For irradiance in North Korea, we used irradiance data given in Chinese and Korean regions, which are Dandong (DD) for northern 6 stations; Suncheon (SC, n = 3), Anju (AJ, n = 2), and OC1 station of Oncheon (OC) and Shihwa (SH) for southern 4 stations; OC2 station of OC and Ongjin (OJ, n = 3). As a result, summer benthic PPs (20th

June−20th July) in the Yellow Sea were estimated by the sum of the daily productions (see Fig. 2.6).

Benthic to pelagic ratio. To assess significant environmental factor to benthic-pelagic coupling, we suggested a simplified index in terms of relationship between benthic and pelagic Chl-*a*, expressed as pelagic to benthic (P/B) ratio, given in equation (6):

$$\text{P/B ratio} = (\text{Chl-}a_{\text{pelagic}} \times \text{D}) / \text{Chl-}a_{\text{benthic}} \quad (6)$$

where, Chl-a_{pelagic} is the concentration of chlorophyll-*a* in seawater (mg m^{-3}) at P_{coast} or P_{20} location; D is mean water depth corresponding at P_{coast} or P_{20} locations; Chl-a_{benthic} is MPB biomass (mg m^{-2}) in sediment.

The regression function of SigmaPlot (v10.0, Systat Software, Inc.) was used to confirm significant variation among the data by fitting the curve with 95% confidence interval. Analysis of variance (ANOVA) was perform to evaluate difference of Chl-*a* distribution among groups of pelagic Chl-*a* (P_{coast}, P_{20}, P_{40}, P_{60}, P_{80}, and P_{100}), and correlation analysis (CA) was utilized to assess potential interactions between environmental parameters and benthic/pelagic Chl-*a*. ANOVA, CA, and PCA were performed using SPSS 23.0 (SPSS Inc., Chicago, IL). To evaluate spatial similarity on Chl-*a* distribution among benthic and pelagic locations grouped by distance, cluster analysis and non-metric multidimensional scaling (NMDS) were performed using PRIMER packages (Clarke & Gorley, 2006). The benthic Chl-*a* values were log-transferred before cluster analysis and NMDS.

Table 2.1. Global review on the annual biomass (Benthic Chl-*a*) and primary production (Benthic PP) of microphytobenthos in the present study. Totally, 103 studies were reviewed including this study. Values reported within the same region are presented as regional means. Results given in Fig. 2.1.

Region			Benthic Chl-a (mg m^{-2})	Benthic PP (mg C m^{-2} yr^{-1})	Reference
Europe	Netherlands	Ems-Dollars Estuary	79.0	116.0	Colijn & Dijkema 1981; Van Es 1982; Colijn & de Jonge 1984; de Jonge & Colijin 1994; de Jonge et al. 2012
		Texel, Wadden Sea	122.6	112.0	Cadée & Hegeman 1974; Cadée 1980
		Oosterschelde Estuary	155.0	157.5	de Jonge et al. 1994; Kromkamp et al. 1995
		Westerschelde	113.0	136.0	de Jong & de Jonge 1995
		Molenplaat, Western Scheldt Estuary	15.3	-	Barranguet et al. 1998; Lucas & Holligan 1999
	Germany	Sylt-Rømø Bay	28.8	115.0	Asmus 1982; Agatz et al. 1999; Riethmuller et al. 2000; Billerbeck et al. 2007
		Dornumer Nacken	74.2	-	Andersen et al. 2010
		Meldorfer Bay (Büsum)	65.8	57.8	Riethmuller et al. 2000; Wolfstein et al. 2000
		Hedwigenkoog	-	47.6	Wolfstein et al. 2000
		Solthörn	110.0	-	Scholz & Liebezeit 2012
	UK	Colne Estuary	65.7	257.6	Thornton et al. 2002
		Lynher Estuary	-	143.0	Joint 1978
		Severn Estuary	32.6	35.0	Underwood 2010
	France	Seine Estuary	138.9	135.0	Spilmont et al. 2006
		The Bay of Somme	-	88.5	Migné et al. 2004; Spilmont et al. 2007
		Mont Saint-Michel Bay	113.4	23.0	Davolult et al. 2007; Migné et al. 2009
		Roscoff Aber Bay	24.5	-	Hubas et al. 2006
		Bay of Morlaix	126.9	-	Ouisse et al. 2010
		Marennes-Oléron Bay	-	127.0	Gouleau et al. 1994

Table 2.1. Continued.

Region			Benthic Chl-a (mg m^{-2})	Benthic PP (mg C m^{-2} yr^{-1})	Reference
Europe	Scotland	Loch Ewe	16.1	5.8	Steele & Baird 1968
		Ythan Estuary	-	31.0	Leach 1970
	Portugal	Tagus Estuary	113.3	134.5	Brotas & Catarino 1995; Serôdio & Catarino 2000; Jesus et al. 2009
	Norway	Tautra Island	51.2	-	Cibic et al. 2007
	Spain	Cadiz Bay	210.0	-	García-Robledo et al. 2010
		Vilagarcia de Arousa	61.5	-	Varela & Penas 1985
	Italy	Po River Delta	26.5	67.4	Bartoli et al. 2012
Asia	China	Yueqing Bay	9.8	72.5	Hao et al. 2011
		Rushan Bay	36.7	-	Yin et al. 2006
		Sanggou Bay	18.6	-	Xiuren et al. 2013
		Jiazhou Bay	23.5	-	Xiuren et al. 2013
		Zhujiang Estuary	29.7	-	Liu et al. 2013
		Futian Mangrove Reserve	64.5	-	Liu et al. 2013
		Yellow Sea (this study)	34.2	-	*This study* (only mothly production estimated)
	South Korea	Gteonggi Bay	-	236.0	Kwon et al. 2012
		Ganghwa Island	97.1	75.4	Yoo 2004
		Saemangeum	87.3	-	Oh et al. 2004; Kwon et al. 2016
		Hampyeong Bay	52.5	-	Lee & Jung 2011; Lee 2013
		Song Island	12.8	19.4	Lee 1991
		Geunso	33.9	-	Roh 2008
		Taean	32.7	-	Park et al. 2013; Park et al. 2015
		Daebu Island	61.3	312.0	Kwon et al. 2018
		Yellow Sea (this study)	21.4	-	*This study* (only mothly production estimated)

Table 2.1. Continued.

Region			Benthic Chl-a ($mg\ m^{-2}$)	Benthic PP ($mg\ C\ m^{-2}\ yr^{-1}$)	Reference
Asia	South Korea	Yeoja Bay	30.2	-	Park et al. 2013
		Nakdong Estuary	21.9	498.8	Choy et al. 2008; Du & Chung 2009
	Japan	Seto Inland	32.6	348.5	Magni and Montani 1997; Motani et al. 2003
		Nanaura mudflat, Ariake Sea	41.2	-	Koh et al. 2007
		Hokkaido	-	19.0	Fuji et al. 1991
		Mikawa Bay	-	37.5	Goto et al. 2000
North America	Canada	Greater Vancouver	71.6		Sakamaki & Richardson 2008
		Bay of Fundy	43.0	58.0	Hargrave et al. 1983
		Squamish Estuary	-	106.0	Pomeroy & Stockner 1976
		Nova Scotia	-	19.0	Grant et al. 1986
	USA	False Bay, San Juan Is.	-	108.0	Pamatmat 1968
		Chapman Cove	-	67.0	Thom et al. 1994
		Gray`s Harbor	-	59.0	Thom 1984
		Columbia River Estuary	-	72.0	McIntire & Amspoker 1986
		San Pablo Bay, San Fransico Bay	137.5	15.0	Cohen et al. 2014
		Mugu Lagoon, Ventura County	-	143.0	Shaffer & Onuf 1985
		Bolsa Bay	-	97.0	Riznyk et al. 1978
		Tijuana Bay	-	263.75	Zedler 1980
		Semiahmoo Bay	104.7		Thom et al. 1994
		Chapman Cove	80.6		Thom et al. 1994

Table 2.1. Continued.

Region			Benthic Chl-a (mg m^{-2})	Benthic PP (mg C m^{-2} yr^{-1})	Reference
North America	USA	Savin Hill Cove	164.0	188.0	Gould & Gallagher 1990
		Woods Hole	-	82.5	Van Raalte et al. 1974; Van Raalte & Valiela 1976
		Newport Estuary	-	20.0	Bigelow 1977 (Cahoon 1999)
		Providence River Estuary	84.0		Lake & Brush 2011
		Block Island Sound	100.0	54.0	Marshall et al. 1971
		Long Is.	-	41.0	Baillie 1986
		Galveston Island, Texas	78.3		Thornton & Visser 2009
		Sapelo Is.	30.5	146.3	Pomeroy 1959; Darley et al. 1976; Darley et al. 1981
		Canary creek (Lewes)	-	74.0	Gallagher & Daiber 1974
		South Carolina	-	136.0	Kelly et al. 1986
		North Inlet Estuary	74.6	144.0	Pinckney & Zingmark 1993; Pinckney 1994
		Chesapeake Bay	19.4	154.5	Rizzo & Wetzel 1985; Wendker & Marshall 1993
		Mississippi Sound	92.8	63.0	Sullivan & Moncreiff 1988
		Barataria Bay	-	121.0	Shaffer 1988
Africa	South Africa	St. Lucia Estuary	73.5	-	van der Molen & Perissinotto 2011
		Amanzimtoti Estuary	75.4	-	Anandraj et al. 2008
		Mpenjati Estuary	198.1	-	Perissinotto et al. 2002
		Langebaan Estuary	-	171.0	Fielding et al. 1988
Oceania	Australia	Tamnourine Bay	61.7		Murphy et al. 2009
		Brays Bay	36.7		Murphy et al. 2009
		Brunswick River	65.2		Webb & Eyre 2004
		Manukau Harbour	-	476.0	Wilkinson 1981

2.3. Results

2.3.1. Global distribution of coastal Chl-*a* concentrations

MPB studies mostly have been conducted in the regions of macro- to megatidal regime; our meta-data analysis has shown that the global average values on biomass and annual MPB PP indicated ~80 mg Chl-*a* m^{-2} and ~125 g C m^{-2} yr^{-1}, respectively (Fig. 2.1). Various coastal wetlands are widely characterized in the North America and western Europe, whereas tidal flats are largely developed in East Asia. Interestingly, the very regions are highlighted with enriched MPB biomass being averagely over 100 mg Chl-*a* m^{-2} (Fig. 2.1A−C), on the contrary, that of East Asia showed that relatively depleted MPB biomass (av. 43 mg Chl-*a* m^{-2}). However, annual PP is much greater (Fig. 2.1B), indicating the elevated MPB productivity as biomass-specific PP (viz., higher photosynthetic capability per unit Chl-*a*). This phenomenon is sometimes a result of taxa-specific difference (Hellbust & Lewin, 1977; Underwood et al., 2005) and/or survival strategies supporting metabolic difference of MPB depending on environmental conditions (Sundbäck & Graneli, 1988; Tuchman et al., 2006). The result is also suggesting a possibility of that MPB in East Asia are predominantly adapted to autotrophic (phototrophic) metabolism whereas North America and western Europe MPB are presumably adapted to both of heterotrophic and phototrophic metabolism. These all data and circumstances further suggest the flexibility of MPB to take diverse production strategies upon taxa and various environmental conditions.

We compiled data of benthic Chl-*a* of previous studies (Fig. 2.1A−C), and then estimated the pelagic Chl-*a* in adjacent coastal seawater using satellite images of MODIS (Moderate-Resolution Imaging Spectroradiometer) with a resolution of 4 km × 4 km (Fig. 2.2A). Benthic Chl-*a* is weakly correlated with pelagic Chl-*a* in the global window (R^2 = 0.022, p = 0.089, n = 133), and benthic and pelagic Chl-*a* in the Yellow Sea are not correlated (R^2 = 0.013, p = 0.468, n = 44) (Fig. 2.2B−C).

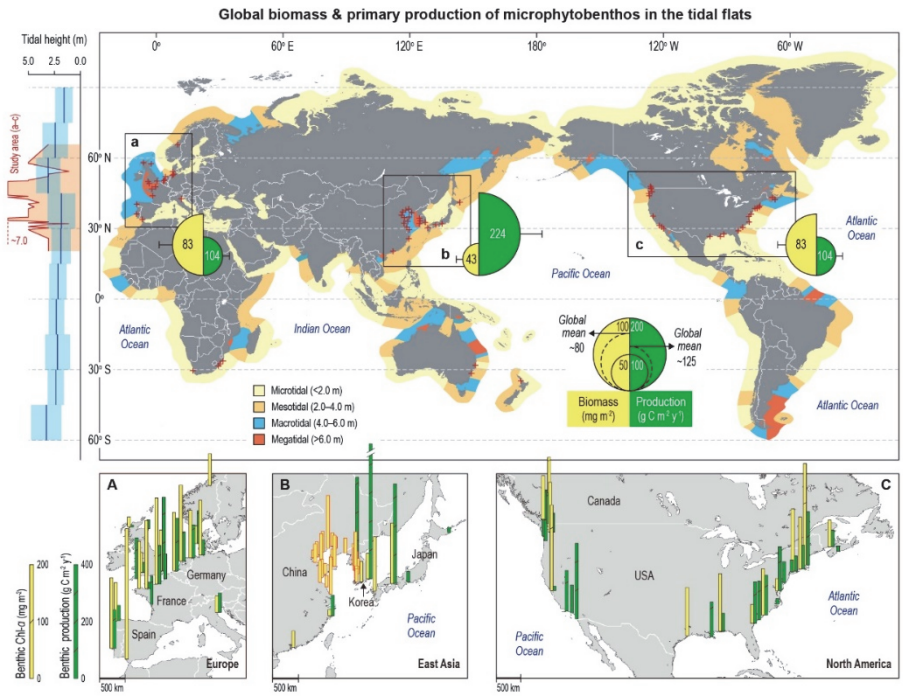

Fig. 2.1. Global biomass and production of microphytobenthos (MPB) in the tidal flats. Map showing the global tidal range (middle) with is slightly modified from previous studies (see Method). Study areas where MPB (viz., benthic) biomass or primary production (PP) reported are presented in red cross. A–C, Yellow and Green circles indicate annual meta-analytic mean of MPB biomass and PP, respectively, and the size of circles represents the magnitude. Solid blue lines and shadings (left) indicate the latitudinal means of tidal height and standard deviations, and red line is indicating mean tidal height in previous studies on MPB biomass and PP. Bottom insets, Yellow and green bars are indicating annual means of MPB biomass and PP in subregions of western Europe (A), East Asia (B), and North America (C). The red outlined bars in East Asia show MPB biomass, which are measured in this study (in situ) from mid-June 2019 to mid-July 2019.

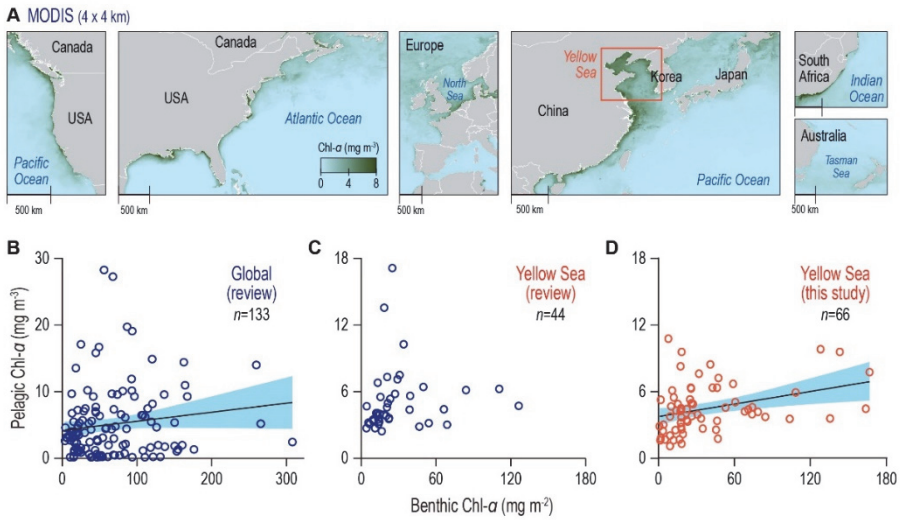

Fig. 2.2. Global-scale distribution of chlorophyll-*a* (Chl-*a*) concentrations between intertidal sediment and coastal seawater. A, Map showing concentration of pelagic Chl-*a* around USA, western Europe, East Asia, South Africa, and Australia. B and C, Distribution of Chl-*a* concentrations data between benthic and pelagic Chl-*a* in global (B) and the Yellow Sea (C) coasts. D, Chl-*a* concentrations were measured in sediments collected from the Yellow Sea coast in this study, and pelagic Chl-*a* concentrations (at the similar time to the in situ sampling) were estimated by MODIS. Solid lines and blue shadings indicate regression fits and the 95% confidence interval, respectively.

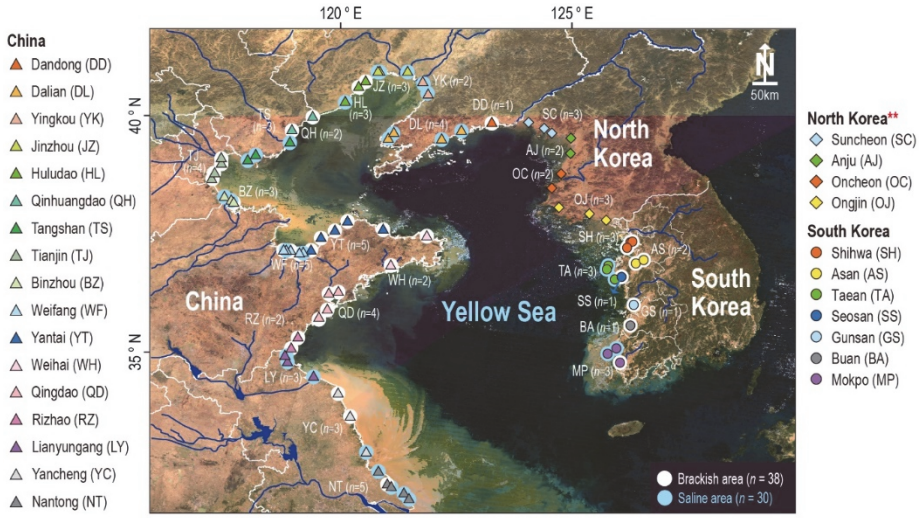

Fig. 2.3. Map showing sediment sampling locations along Yellow Sea coast in China and South Korea. Sediment samples were collected in ebb tide (during exposure) along coastal areas (68 locations in 24 regions) including brackish (n = 38) and saline areas (n = 30) within a month between June 27 and July 23, 2018. **Concentrations of benthic chlorophyll-*a* (viz., microphytobenthos biomass) in North Korean coast were estimated from a regression curve for correlation between benthic and pelagic chlorophyll-*a* in this study.

2.3.2. Benthic-pelagic coupling of Chl-*a* in the Yellow Sea

Satellite image data in higher resolution have addressed stronger correlation between benthic and pelagic Chl-*a*, specifically with the analysis of GOCI (Geostationary Ocean Color Imager) images as well as in situ Chl-*a* data. Namely, spatial linkage on distribution of benthic-pelagic Chl-*a* concentrations at more detailed resolution was of primary interest. As for the concentrations of pelagic Chl-*a* were estimated by us of GOCI-derived images. Finally, correlations between both concentrations of benthic and pelagic Chl-*a* were determined. We also measured environmental parameters to consider significant factors controlling Chl-*a* dynamics (Table 2.2). Overall, spatial distribution of Chl-*a* concentration from benthic to pelagic environment in the Yellow Sea coast is analyzed and depicted (Fig. 2.4 & Table 2.3).

Details for insets of Fig. 2.4, which is showing benthic-pelagic coupling on distribution of Chl-*a* in the Yellow Sea, A, Map showing the sampling sites and each mean concentration of benthic Chl-*a* in sediments (yellow bars) collected from intertidal area, the Yellow Sea. Concentrations of pelagic Chl-*a* on transects are estimated from GOCI images. Basically, a transect line consists of six locations; one closest location (P_{coast}) from a benthic sampling coordinate (P_0), and five locations up to 100 km in 20 km intervals (P_{20}, P_{40}, P_{60}, P_{80}, and P_{100}). In order to ensure a uniform geographical distribution of pelagic Chl-*a*, additional transects have been added along the Yellow Sea coast. In case of benthic Chl-*a* in North Korea (N-KOR), the values were estimated from the best fitting curve of benthic-pelagic correlation. B, Schematic illustration of the MPB and transect locations in the Yellow Sea. B, Frequency of Chl-*a* concentrations in pelagic locations. D, Distribution of Chl-*a* concentrations between adjacent spaces on benthic to pelagic locations. Solid lines and orange shadings indicate a regression fit and the 95% confidence interval, respectively. Outliers (grey circles) are removed to improve accuracy of the regression curve. D, Spatial variability in Chl-*a* concentrations. Solid lines and shadings indicate regression fits and the 95% confidence intervals, respectively. Asterisks indicate statistical significance determined by ANOVA test ($p < 0.005$). F, Dendrogram representing hierarchical clustering based on Euclidean distance. G,

BPC boundary in YSLME, suggested by non-metric multidimensional scaling (NMDS) with respect to the spatial distribution of Chl-*a* concentration. Colors in circles indicate mean concentration of Chl-*a*. (F and G) MPB Chl-*a* (P_0) data were log-transformed before cluster analysis and NMDS.

Locations for pelagic Chl-*a* estimation were conducted on 100 km transects which consists of six locations in a row; a closest location in coast (P_{coast}) and five outer locations allocated in 20 km intervals from P_{coast} (P_{20}, P_{40}, P_{60}, P_{80}, and P_{100}) (Fig. 2.4A−B). Mean concentration of benthic Chl-*a* was relatively greater in the coasts of China (av. 34.2 mg m^{-2}) than that of Korea (av. 21.4 mg m^{-2}), except for estimated values in North Korea. We concomitantly assumed benthic Chl-*a* values in the North Korea, which were based on the correlation curve on relationship between benthic-pelagic Chl-*a* in China and South Korea. On average, the estimated benthic Chl-*a* concentrations in North Korea were relatively higher values than those of South Korea due to enriched pelagic Chl-*a*.

Here, a clear association between benthic Chl-*a* (P_0) and pelagic Chl-*a* (P_{coast}) was demonstrated (Fig. 2.4C−D). It was found that the logarithmic increase of P_{coast} Chl-*a* is in accordance with the benthic Chl-*a* ($R^2 = 0.503$, $p < 0.001$, $n = 67$, one no-data location was removed). Relatively weak association was observed between Chl-*a* concentrations of pelagic locations in P_{coast} and P_{20}, and Chl-*a* concentrations in outer locations were significantly correlated ($p < 0.001$) between two adjacent pelagic locations (viz., P_{20} vs P_{40}, P_{40} vs P_{60}, P_{60} vs P_{80}, and P_{80} vs P_{100}) (Fig. 2.5). Such a trend is also to be confirmed in the frequency of Chl-*a* concentrations by distance gradient (Fig. 2.4C), particularly P_{coast} and P_{20} were markedly distinguished with outer pelagic locations (P_{40}, P_{60}, P_{80}, and P_{100}) (Fig. 2.4E−F). These results imply that MPB was resuspended into seawater column and subsequently transported to offshore, finally mixed with pelagic phytoplankton even in ~10 km away offshore, say active BPC boundary (Fig. 2.4G). The BPC may be related to more direct effects of region-wide and topographical variations by tidal amplitude and current velocity on the local intertidal flats (De Jonge & Beusekom, 1995; Koh et al., 2006) Diurnal cycles of tidal currents have a great influence on the resuspension and transport of sediments in intertidal area, thus MPB in sediments are also suspended. Such a contribution of benthic derived phyto-particles into

overlying water column, in terms of total biomass (or production) in shallow intertidal environment (Park et al., 2014). In our analysis, the relationship between the concentrations of suspended solids (SS) and benthic Chl-*a* were not significant, yet relatively significant correlation was observed between SS and pelagic Chl-*a* (Fig. 2.6).

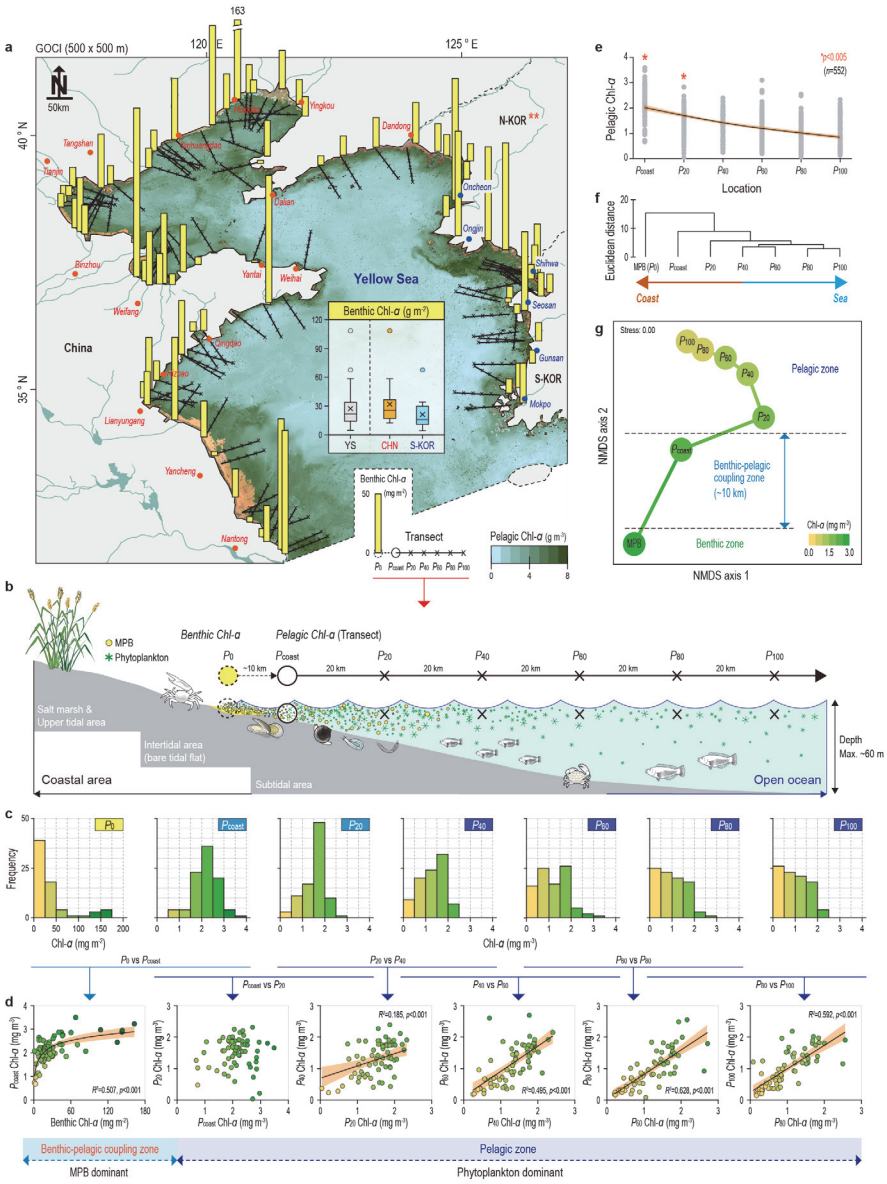

Fig. 2.4. Benthic-pelagic coupling boundary on spatial distribution of chlorophyll-*a* concentration (Chl-*a*) in the Yellow Sea large marine ecosystem scale (see Chapter 2.3.2 for the details of insets).

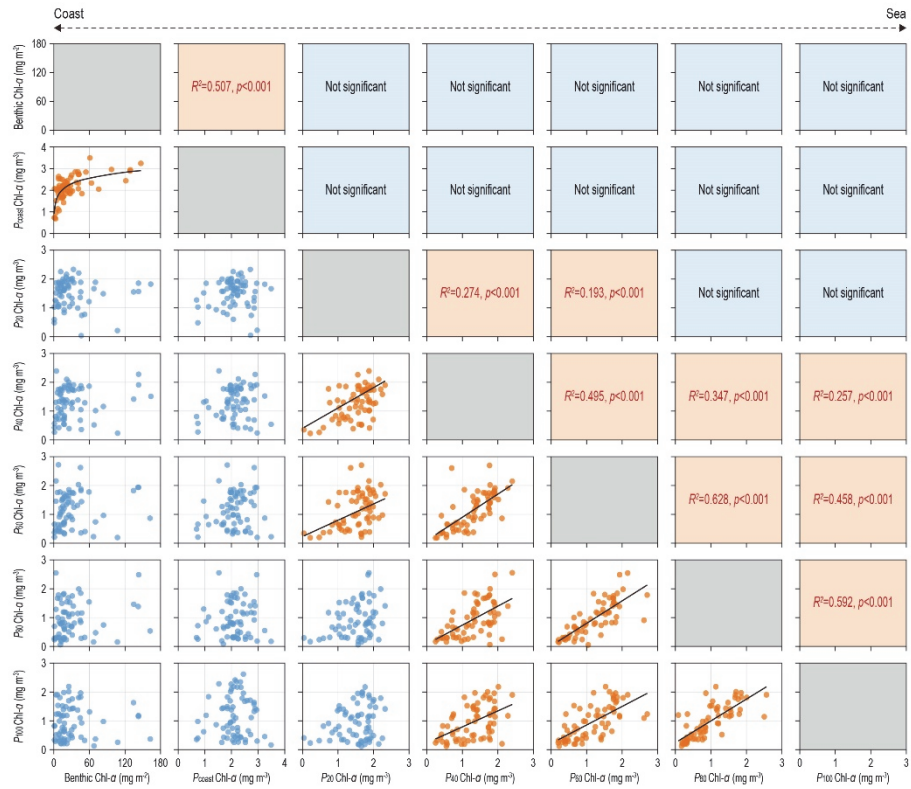

Fig. 2.5. Spatial correlation in concentration variance of chlorophyll-*a* (Chl-*a*) among coastal sediments (benthic Chl-*a*) and pelagic waters ($P_{coast, 20, 40, 60, 80, \& 100}$). Statistical significance was determined at the level of $p<0.005$, and solid line indicates regression fit. The benthic Chl-*a* was measured in sediment collected from the Yellow Sea coast (in situ) and the pelagic Chl-*a* was estimated from satellite images of GOCI (see Chapter 2.2.2).

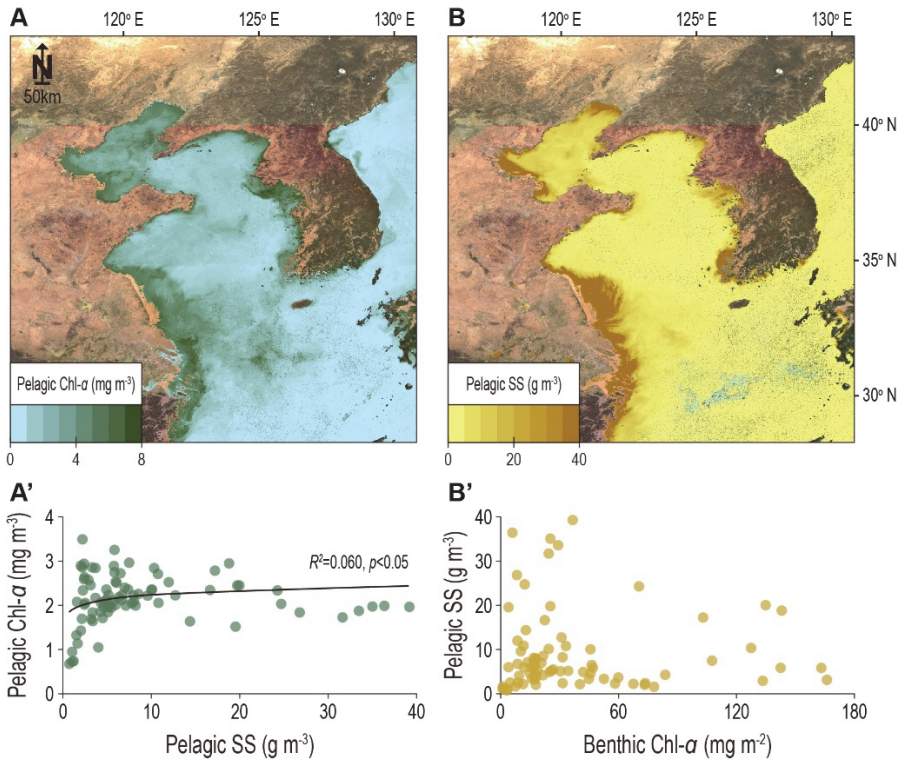

Fig. 2.6. Concentration of chlorophyll-*a* (Chl-*a*) and suspended solids (SS) in pelagic waters of the Yellow Sea. A and B, Map showing pelagic Chl-*a* and SS estimated by GOCI images, respectively. A', Solid line indicate a regression fit between concentrations of pelagic SS and Chl-*a* at P_{coast} locations. B', Correlation was not found between concentrations of pelagic SS (at P_{coast}) and benthic Chl-*a* (in situ).

2.3.3. Primary production and P/B ratio in the Yellow Sea

Temperature-based algorithm (Kwon et al., 2018) allowed us to calculate MPB PPs in the YSLME, which showed that regional variations along the Yellow Sea coast (Fig. 2.7–2.8, Table 2.4). Total mean of PPs was relatively higher in China (~50 g C m^{-2} $month^{-1}$) than that of Korea (~32 g C m^{-2} $month^{-1}$) mainly due to the somehow enriched MPB biomass in Chinese coasts (Fig. 2.4). As a featured trend, the locations with high MPB biomass were adjacent to riverine areas, suggesting that the nutrients input through river play a great role in MPB and pelagic phytoplankton proliferations. Accumulative anthropogenic stresses by long-term coastal developments were major factor to enforce nutritional load in the aquatic environment, for instance, the riverine organic carbon input to the ocean major rivers in China is very outstanding at the moment (Seitzinger et al., 2010).

Globally, the Yellow Sea coast is well known as macrotidal regime (Fig. 2.1), including an extreme megatidal area (max. > 10 m) in the West coasts of Korea (especially South Korea) (Fig. 2.3). Thus, despite of relatively small values of Korean PPs compared to China, more portion of MPB would be resuspended and transported offshore. To test the hypothesis, simplified index of pelagic to benthic Chl-*a* ratio (P/B ratio) was used, which is to provide a qualitative and practical criterion on the degree of BPC. As a result, P/B ratio increases according to tidal height ($R^2 = 0.172$, $p < 0.005$, $n = 48$) (Fig. 2.8A), whereas there was no significance with other physicochemical parameters (Fig. 2.8B–I). Specifically, Korean locations of megatidal regime were clearly distinguishable with Chinese locations of macrotdial regime, reflecting higher tidal energy across the Korean side of the Yellow Sea.

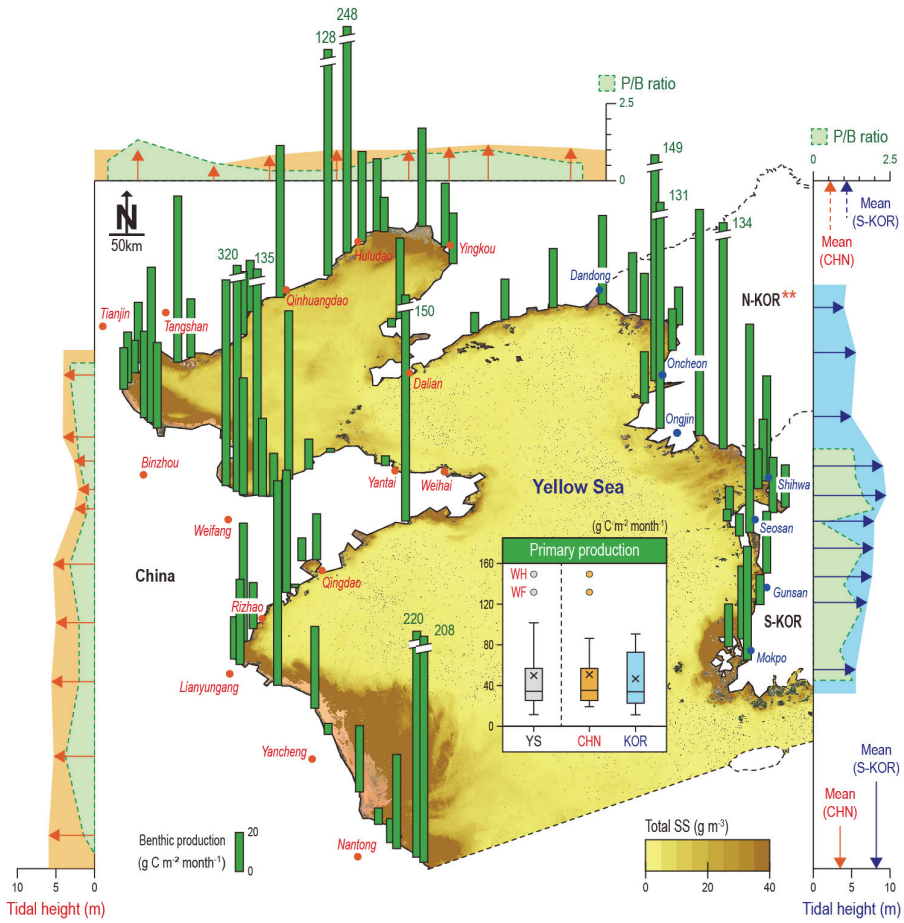

Fig. 2.7. Benthic primary production (PP), pelagic to benthic chlorophyll ratio (P/B ratio), and tidal height along the Yellow Sea coast. Regional benthic PPs during mid-June to mid-July, 2018 calculated from temperature-based PP model (**North Korean PPs were roughly calculated with estimated values; benthic Chl-a, irradiance, temperature, and tidal height). The box plots (center) showing PPs in the Yellow Sea (YS), China (CHN), and North and South Korea (KOR). Total suspended solids (SS) in seawater estimated by GOCI satellite images, and arrows of orange (CHN) and blue (KOR) represent range of tidal height in subregions. Site abbreviations are given in Table 2.2.

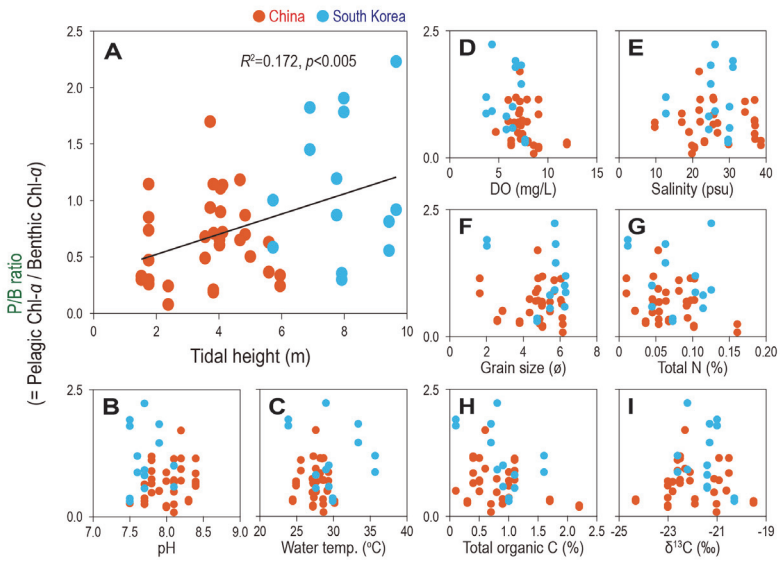

Fig. 2.8. Relationship between P/B ratio and environmental variables including seawater and sediment properties. The tidal height significantly increased P/B ratio (A), however, pH (B), water temperature (C), dissolved oxygen (D), salinity (E), grain size (F), total nitrogen (G), total organic carbon (H), and carbon stable isotopic ratio did not affect to the P/B ratio.

Table 2.2. Environmental parameters in seawater and sediment samples collected from the Yellow Sea coasts.

Site (abb.)	*n**	Sampling date	Seawater					Sediment								
			Tidal height (m)	pH	Temp. (°C)	DO (mg/L)	Salinity (psu)	Grain size (ø)	Sorting (ø)	Gravel (%)	Sand (%)	Silt (%)	Clay (%)	TN (%)	TOC (%)	$\delta^{13}C$ (‰)
China																
Dandong (DD)	1	2 Jul.	4.0	8.4(-)	25.0 (-)	6.6 (-)	9.9 (-)	5.0 (-)	2.0 (-)	0.0 (-)	34.7 (-)	55.9 (-)	9.4 (-)	0.09 (-)	1.0 (-)	-23.0 (-)
Dalian (DL)	4	1 & 2 Jul.	4.0—4.1	7.8 (0.0)	25.6 (0.4)	7.2 (0.4)	34.3 (0.8)	5.7 (0.4)	1.9 (0.1)	0.0 (0.0)	22.6 (9.0)	62.6 (6.6)	14.7 (2.4)	0.08 (0.0)	1.1 (0.3)	-22.6 (0.4)
Yingkou (YK)	2	4 Jul.	4.1	8.1 (0.2)	28.5 (0.4)	6.0 (0.8)	36.9 (1.1)	6.1 (0.4)	1.6 (0.2)	0.0 (0.0)	12.2 (7.6)	73.9 (6.7)	13.8 (0.9)	0.10 (0.0)	1.1 (0.2)	-22.5 (0.7)
Jinzhou (JZ)	3	5 & 6 Jul.	3.8	8.2 (0.3)	28.3 (0.3)	7.9 (0.3)	37.7 (0.6)	5.0 (0.6)	1.7 (0.0)	0.0 (0.0)	29.0 (13.1)	60.7 (10.3)	10.3 (3.2)	0.05 (0.0)	0.5 (0.1)	-20.9 (0.1)
Huludao (HL)	3	6 & 7 Jul.	3.8	8.0 (0.4)	28.4 (1.0)	9.1 (0.9)	16.7 (6.9)	5.5 (0.4)	1.8 (0.1)	0.0 (0.0)	24.1 (6.9)	63.8 (4.2)	12.1 (2.7)	0.18 (0.1)	2.2 (0.5)	-23.0 (0.3)
Qinhuangdao (QH)	2	8 & 9 Jul.	1.5	8.3 (0.2)	24.5 (0.5)	8.0 (0.8)	23.4 (0.6)	2.6 (0.2)	1.5 (0.4)	0.0 (0.0)	81.4 (8.6)	16.4 (7.6)	2.2 (0.9)	0.07 (0.0)	1.7 (1.2)	-24.3 (1.1)
Tangshan (TS)	3	10 Jul.	1.7	7.8 (0.0)	27.2 (0.7)	7.4 (0.5)	36.9 (0.7)	4.4 (0.5)	1.6 (0.1)	0.0 (0.0)	46.4 (11.1)	47.9 (9.0)	5.7 (2.2)	0.05 (0.0)	0.8 (0.1)	-21.1 (0.3)
Qingdao (QD)	4	27—30 Jun.	4.8	8.0 (0.2)	28.9 (0.9)	7.1 (2.0)	18.1 (1.3)	3.8 (1.2)	1.3 (0.2)	2.7 (2.3)	51.8 (21.1)	36.8 (18.4)	8.7 (4.0)	0.05 (0.0)	1.0 (0.4)	-22.1 (0.7)
Rizhao (RZ)	2	27 Jun.	5.0	7.9 (0.1)	29.3 (1.4)	4.7 (0.1)	19.1 (3.7)	1.9 (0.6)	1.3 (0.2)	0.0 (0.0)	78.9 (2.5)	19.4 (2.8)	1.7 (0.3)	0.02 (0.0)	0.1 (0.0)	-20.6 (0.0)
Weihai (WH)	2	1 & 2 Jul.	2.4	8.1 (0.1)	25.6 (2.2)	8.6 (0.5)	23.4 (2.5)	4.1 (1.5)	1.2 (0.5)	0.0 (0.0)	56.2 (30.1)	34.6 (23.6)	9.2 (6.5)	0.08 (0.1)	0.7 (0.5)	-21.0 (0.1)
Yantai (YT)	5	2 & 3 Jul.	1.7—1.8	8.4 (0.0)	28.3 (0.9)	9.1 (0.2)	25.8 (1.9)	1.6 (0.4)	1.0 (0.1)	9.4 (3.8)	82.9 (3.6)	5.1 (3.2)	2.5 (2.0)	0.01 (0.0)	0.4 (0.3)	-20.5 (0.7)
Weifang (WF)	5	4 & 5 Jul.	1.8	7.5 (0.9)	30.2 (0.6)	12.0 (2.3)	29.9 (2.2)	3.8 (0.3)	0.9 (0.2)	0.0 (0.0)	69.1 (9.3)	28.4 (8.1)	2.5 (1.3)	0.04 (0.0)	0.3 (0.1)	-19.5 (1.0)
Binzhou (BZ)	3	8 Jul.	3.6	8.1 (0.2)	27.7 (0.2)	7.0 (0.7)	26.9 (4.6)	5.5 (0.2)	1.6 (0.0)	0.0 (0.0)	15.6 (4.1)	74.6 (2.6)	9.7 (1.6)	0.05 (0.0)	0.5 (0.1)	-22.8 (0.9)
Tianjin (TJ)	4	9 & 10 Jul.	3.7	8.2 (0.1)	27.7 (0.8)	7.2 (0.6)	21.8 (2.5)	4.8 (0.7)	2.0 (0.1)	0.0 (0.0)	41.4 (13.0)	45.7 (10.3)	12.9 (3.5)	0.05 (0.0)	0.6 (0.1)	-22.3 (0.2)
Lianyungang (LY)	3	30 Jun. & 1 Jul.	5.6	7.7 (0.0)	27.4 (0.7)	7.3 (0.1)	37.0 (4.0)	6.1 (0.6)	1.5 (0.1)	0.0 (0.0)	14.6 (10.3)	67.5 (6.1)	17.9 (4.4)	0.09 (0.0)	1.0 (0.3)	-23.0 (0.3)
Yancheng (YC)	3	2 & 3 Jul.	3.2—5.4	7.8 (0.1)	27.3 (0.8)	6.8 (0.5)	25.6 (6.7)	5.0 (0.2)	1.7 (0.2)	0.0 (0.0)	27.6 (3.2)	64.1 (1.5)	8.4 (1.7)	0.05 (0.0)	0.4 (0.1)	-22.5 (0.5)
Nantong (NT)	5	4—6 Jul.	5.4—6.0	7.7 (0.1)	27.9 (0.5)	6.3 (0.6)	36.0 (3.0)	5.5 (0.7)	1.5 (0.2)	0.0 (0.0)	26.2 (16.4)	60.5 (13.4)	13.3 (3.1)	0.06 (0.0)	0.9 (0.2)	-21.9 (0.7)

Table 2.2. Continued.

Site (abb.)	*n**	Sampling date	Seawater					Sediment								
			Tidal height (m)	pH	Temp. (°C)	DO (mg/L)	Salinity (psu)	Grain size (ø)	Sorting (ø)	Gravel (%)	Sand (%)	Silt (%)	Clay (%)	TN (%)	TOC (%)	$\delta^{13}C$ (‰)
Korea																
Shihwa (SH)	3	16 Jul.	9.3—9.4	7.7 (0.0)	27.6 (0.7)	5.8 (0.5)	24.4 (1.7)	5.5 (0.2)	2.0 (0.1)	0.0 (0.0)	25.6 (5.5)	62.9 (4.7)	11.6 (0.8)	0.11 (0.0)	1.1 (0.1)	-21.4 (0.2)
Asan (AS)	2	15 Jul.	9.6	7.7 (0.1)	29.0 (0.3)	4.3 (0.1)	26.1 (0.8)	5.7 (0.2)	2.0 (0.1)	0.0 (0.0)	19.1 (3.7)	67.5 (2.6)	13.4 (1.1)	0.13 (0.0)	0.8 (0.1)	-22.2 (0.4)
Taean (TA)	3	14 & 15 Jul.	8.0	7.5 (0.0)	23.9 (1.3)	6.7 (0.4)	31.0 (0.2)	2.0 (0.2)	0.5 (0.1)	0.0 (0.0)	99.4 (0.5)	32.0 (0.5)	0.6 (0.0)	0.01 (0.0)	0.1 (0.0)	-21.0 (1.6)
Seosan (SS)	1	23 Jul	7.9	7.5 (-)	29.9 (-)	7.7 (-)	29.6 (-)	4.8 (-)	2.3 (-)	0.0 (-)	36.9 (-)	55.0 (-)	8.1 (-)	0.07 (-)	1.0 (-)	-20.3 (-)
Gunsan (GS)	1	14 Jul.	7.7	7.6 (-)	35.7 (-)	3.7 (-)	12.7 (-)	6.3 (-)	1.7 (-)	0.0 (-)	10.6 (-)	72.7 (-)	16.7 (-)	0.10 (-)	1.6 (-)	-22.6 (-)
Buan (BA)	1	14 Jul.	6.9	7.9 (-)	33.4 (-)	7.3 (-)	24.9 (-)	5.8 (-)	1.7 (-)	0.0 (-)	15.0 (-)	72.3 (-)	12.7 (-)	0.06 (-)	0.7 (-)	-21.3 (-)
Mokpo (MP)	3	13 Jul.	5.7	8.1 (0.2)	29.4 (2.3)	6.4 (0.8)	30.1 (1.4)	4.5 (1.4)	1.3 (0.1)	8.2 (6.7)	26.6 (19.4)	55.9 (22.8)	9.3 (3.4)	0.05 (0.0)	0.9 (0.1)	-21.4 (0.8)

**n*, number of sampling locations by site. Values are shown as mean with standard error in parenthesis.

Table 2.3. Concentration of benthic chlorophyll-*a* (Chl-*a*) measured in sediments and pelagic Chl-*a* in open-sea estimated from satellite images (GOCI-derived) along the Yellow Sea coasts.

	Benthic Chl-*a*		Pelagic Chl-a		
Site*	Sampling date	Chl-*a* (mg m^{-2})	Estimating date	Distance (km)	Chl-*a* (mg m^{-3})
China					
DD	2 Jul.	25.7 (-)	2 Jul.	8.0 (-)	2.2
DL	1 & 2 Jul.	15.2 (5.3)	2 Jul.	5.0 (1.1)	2.6
YK	4 Jul.	19.5 (1.5)	4 Jul.	13.7 (1.9)	1.9
JZ	5 & 6 Jul.	23.0 (5.1)	4 & 10 Jul.	14.3 (5.0)	2.4
HL	6 & 7 Jul.	92.5 (31.5)	10 Jul.	5.6 (0.2)	2.1
QH	8 & 9 Jul.	35.1 (12.2)	10 Jul.	8.5 (2.5)	1.4
TS	10 Jul.	26.3 (7.9)	10 Jul.	7.1 (0.9)	1.6
QD	27—30 Jun.	18.5 (8.6)	28—30 Jun.	6.6 (1.7)	2.0
RZ	27 Jun.	31.2 (9.7)	28 & 29 Jun.	4.5 (1.0)	1.7
WH	1 & 2 Jul.	54.3 (37.8)	2 Jul.	6.7 (2.1)	3.0
YT	2 & 3 Jul.	12.4 (6.4)	2 & 3 Jul.	2.6 (0.8)	2.2
WF	4 & 5 Jul.	58.8 (19.9)	3 & 6 Jul.	10.3 (1.4)	2.7
BZ	8 Jul.	32.1 (5.6)	10 Jul.	5.5 (1.2)	2.0
TJ	9 & 10 Jul.	13.4 (1.5)	10 Jul.	9.3 (1.5)	2.2
LY	30 Jun. & 1 Jul.	38.1 (13.6)	1 Jul.	8.2 (2.0)	1.8
YC	2 & 3 Jul.	19.8 (6.6)	3 Jul.	16.0 (2.4)	2.2
NT	4—6 Jul.	64.7 (27.5)	3 Jul.	9.4 (3.1)	2.0
South Korea					
SH	16 Jul.	26.8 (6.8)	16 Jul.	2.1 (1.0)	2.2
AS	15 Jul.	18.3 (1.7)	15 Jul.	3.8 (0.3)	2.5
TA	14 & 15 Jul.	8.2 (1.6)	14 & 15 Jul.	0.9 (0.1)	2.1
SS	23 Jul	67.5 (-)	23 Jul	4.3 (-)	3.5
GS	14 Jul.	16.6 (-)	14 Jul.	14.3 (-)	2.1
BA	14 Jul.	11.9 (-)	14 Jul.	15.8 (-)	2.5
MP	13 Jul.	22.9 (5.1)	14 Jul.	5.6 (1.9)	2.0
North Korea*					
SC	-	25.4 (4.0)	17 & 19 Jul.	-	2.2
AJ	-	14.2 (0.4)	16 & 19 Jul.	-	2.0
OC	-	60.9 (30.3)	17 Jul.	-	2.4
OJ	-	86.6 (2.9)	19 & 20 Jul.	-	2.7

Values are shown as mean with standard error in parenthesis.

*Site names are given in Table 2.2. The distance indicates straight-line distance from sediment sampling location (in situ) to the P_{coast} location (see Method).

**Data in North Korea are estimated by a regression curve for relationship between benthic and pelagic Chl-*a* in this study

Table 2.4. Mean values of water temperature, daily irradiance, and daily primary production (PP) of microphytobenthos (MPB); and total PP of MPB during June 20 to July 20, 2018 in the Yellow Sea coasts.

Site (abb)	Temp. (°C)	Irradiance (MJ m^{-2} d^{-1})	Production (g C m^{-2} d^{-1})	(g C m^{-2} $month^{-1}$)
China				
DD	22.1	20.7	0.98	30.5
DL	23.3	20.7	0.61	19.1
YK	25.3	23.8	0.95	29.5
JZ	24.5	23.8	1.13	34.9
HL	24.4	23.8	2.80	86.8
QH	24.2	17.9	1.68	52.2
TS	26.5	17.9	1.59	49.2
QD	25.2	18.1	1.05	32.6
RZ	24.9	18.1	1.36	42.2
WH	23.0	20.9	4.83	150
YT	26.7	20.9	0.76	23.6
WF	28.0	20.9	4.27	132
BZ	28.2	18.1	1.80	55.9
TJ	28.0	18.1	0.77	23.8
LY	27.2	18.1	1.84	56.9
YC	26.3	18.7	0.88	27.2
NT	27.1	16.7	0.72	22.2
South Korea				
SH	21.9	19.0	1.01	31.2
AS	22.5	19.2	0.80	25.0
TA	21.5	19.6	0.34	10.7
SS	24.3	19.6	3.46	107
GS	29.1	20.0	1.02	31.7
BA	24.3	11.5	0.50	15.4
MP	25.0	20.4	1.27	39.2
North Korea*				
SC	24.0	20.7	1.08	33.4
AJ	24.0	20.7	0.66	20.4
OC	24.0	20.7	2.82	87.5
OJ	24.0	19.0	3.29	102

*Site names are given in Table 2.2.

**PPs in North Korea were roughly calculated by input of estimated values in benthic Chl-*a*, irradiance, air temperature, and tidal height (see Method).

2.4. Discussion

Our broad-scale field surveys highlighted a specific spatial extent of BPC revisited in a large marine ecosystem (LME) scale. A key implication from the BPC boundary in YSLME is that the range of BPC (~10 km) is globally very great among large marine ecosystems. In the same context, in the high tidal regions such as the Yellow Sea, benthic and coastal production will greatly contribute to open-ocean production (Ware & Thomson, 2005). Indeed, high species diversity along with great PP have been acknowledged among global macrotidal regime such as North Sea, Australian Sea, and Yellow Sea (Costello et al., 2010). In local scales, contributions of resuspended MPB have been confirmed through the marine food web. For example, relative MPB proportion (vs. phytoplankton) in water column showed seasonal variations, and contemporarily, similar trends were reflected in stable isotope signatures of filter-feeder (Ubertini et al, 2012). A Korean study also demonstrated a decrease pattern on dietary contribution of MPB to marine invertebrate following a distance gradient from intertidal to open ocean areas (Kang et al., 2014). These trophic linkages are of critical importance, as the biomass of marine benthic primary producers can be highly influential in determining the richness and abundance of upper trophic levels (Ware & Thomson, 2005).

In conclusion, this study synthetically assessed the intertidal benthic production globally, with the first suggestion of the offshore boundary of BPC in the YSLME. The significance of tidal energy on the transport of benthic production to pelagic zone was also highlighted. Of note, the complex cross-ecosystem coupling among the various components of marine ecosystem all starts from the most 'primary' producers of tidal flats in LME; the weakening of benthic productivity could lead to a series of declines in the diversity and proliferation of marine lives. Unfortunately, in the Yellow Sea coasts and elsewhere is subject to the habitat deterioration by means of coastal development e.g. large-scale reclamation. Tremendous degradation of biodiversity with rapid perishment of marine ecosystem has been consequently reported as a result of the demolition of tidal flats which are the basis of benthic production by reclamation (Ryu et al., 2014), implying the fundamental production loss of benthic and pelagic production. In the issue for a worldwide decrease in

fishery catches, such primary production loss by habitat destruction should be addressed in depth, and it has to be concerned if ocean can be to continue its important role in supporting food provisioning. In the end, ‘bottom-up process’ is not only important for the sound implementation of coastal management but also solid sustainability of ocean ecosystem.

CHAPTER 3.

Influences of the estuarine dike on marine food web dynamics

This chapter has been published in Environment International.
Noh, J., Yoon, S.J., Kim, H., Lee, C., Kwon, B.-O., Lee, Y., Hong, S., Kim, J., Ryu, J., Khim, J.S., 2019. Anthropogenic influences on benthic food web dynamics by interrupted freshwater discharge in a closed Geum River estuary, Korea. Environ. Int. 131, 104981.

3.1. Introduction

Estuarine ecosystem represents some of the most highly productive areas globally (Costanza et al., 1997; McLusky & Elliott, 2004). Such high productivity of estuaries is generally explained by a greatly complex environment, whereby the mixing of freshwater and seawater leads to habitats and biodiversity occupying dynamic environmental gradients. Accordingly, the benthic consumers in shallow intertidal zones utilize both autochthonous and allochthonous resources cross terrestrial and marine gradients (Nixon et al., 1986; Yokoyama & Ishihi, 2007; Thottathil et al., 2008; Antonio et al., 2012; McTigue et al., 2015; Dias et al., 2016). Several studies revealed that the relative contributions of these potential food sources would vary depending on the flooding frequency of freshwater (Delong et al., 2001), seasonal abundance of benthic primary producers (Kang et al., 2006), and feeding type or diet preferences of consumers (Davenport et al., 2011; Rossi et al., 2015). In particular, macrobenthos are relatively longlived, lesser mobile, and locality-specific (Diaz-Castaneda & Reish, 2009), and thus could be regarded as ideal medium to elucidate the trophic history through the assimilation of varying food sources.

Natural food sources for consumers in the intertidal areas are diverse from phyto- and zooplankton, microphytobenthos (MPB), detritus, and to organic aggregations formed of exudates and colloidal materials. Those potential food sources are incorporated into the benthic food webs by deposit and/or filter feedings of macrobenthos (Kang et al., 2015). Several studies have reported the ecological significance of MPB in benthic food web, which regularly inhabit bare intertidal flats, as major food sources for many macrobenthos, because they exhibit higher productivity and biomass compared to planktonic organic matter (De Jonge & Van Beuselom, 1992; Lucas & Holligan, 1999; Kang et al., 2003). Further MPB contributes significant proportion, of pelagic organic matters, sometimes over 50% to total, by tide and/or wind driven mixing followed by prolonged resuspension in the shallow water system such as tidal flats (De Jonge & Van Beuselom, 1995; Koh et al., 2006). This periodic process allows deposit feeders, which prey on MPB in the sediment, and filter feeders to prey on resuspended MPB in the water column. Thus, intertidal flats are important because they provide constant sources of food for

various benthic consumers, with locally produced MPB transporting organic carbon into the food web of nearshore marine habitats.

Stable isotope analysis of carbon and nitrogen is widely used to investigate the trophic structure of various ecosystems. It is also used to identify the contribution of potential food sources to upper level consumers. The stable nitrogen isotopic composition ($\delta^{15}N$) is used to determine the trophic levels of organisms in food webs, while the stable carbon isotopic composition ($\delta^{13}C$) is used to assess sources and pathways of organic matter from the dietary source to consumers (Fry & Sherr, 1984; Owens, 1988; Peterson & Fry, 1987). Earlier studies revealed that the relative isotope signatures of potential food sources vary across habitats and/or environments. For instance, vascular plants and mangroves (Lee, 1999; Rossi et al., 2010; Kristensen et al., 2017), terrestrial organic matters (Kasai & Nakata, 2005; Karlsson et al., 2012), macroalgal or seagrass detritus (Vizzini et al., 2002; Karlson et al., 2016), phyto- and zooplankton (Xu & Zhang, 2012; Golubkov et al., 2018), and anthropogenic effluent (McClelland & Valiela, 1998) exhibit distinct ranges in isotope signatures. Therefore, the stable isotopic approach is based on certain assumptions, namely, the consumers integrated in the sum of relative diet contributions and isotopic fractionation between dietary sources and consumers in one trophic level are predictable (Post, 2002).

Freshwater discharge into closed estuaries is artificially controlled by opening and closing of water-gates at low and high water, respectively. A sea dike has closed off natural river flow from 1990 in the Geum River estuary, Korea; consequently, the dietary contribution of freshwater resources to estuarine benthic consumers might be strongly linked to freshwater discharge. Although the food sources available to the consumers may be limited in this anthropogenically altered environment, there are very few studies on the trophic contribution of potential food sources with terrestrial POM introduced by artificial freshwater discharge. Thus, study looking for marine benthic food web in the altered environment of closed estuary in varying perspectives, such as spatiotemporal, organ-specific, and age-related variations for assimilation of nutrition, would be timely necessary and important.

In the present study, we collected macrobenthos and their potential food

sources from four locations along the Geum River estuary, encompassing eight seasons from 2015 to 2017. The clams *Mactra veneriformis* and *Cyclina sinensis* were specifically targeted because they are dominant in the study region and also commercially important along the intertidal flats of the Yellow Sea. The specific objectives were to: 1) evaluate the isotopic signatures of discharged-freshwater POM as potential food sources for intertidal macrobenthos in the closed Geum River estuary; 2) assess the trophic structure of the benthic ecosystem by comparing the stable isotope composition of potential food sources to benthic consumers; 3) determine seasonal variation in the contribution of potential food sources and identify the major food source (s); and (4) highlight organ- and size-specific isotope variations in the two target bivalves. Ultimately, this study supports to better understand benthic food web in the closed estuary and step towards enhanced management of estuarine ecosystem elsewhere.

3.2. Materials and Methods

3.2.1. Study area and data collection

The study area, Geum River estuary, is located on the west coast of South Korea. Freshwater input occurs by irregular discharge through the sea dike. The sampling locations were selected based on the oceanographic settings, following the salinity gradient along the estuary, and included one freshwater area inside the sea dike (Geum River, GR) and three intertidal locations. Of the intertidal zones, two locations were in a coastal area near to the river mouth (Songlim-ri (SL) and Yubu Is. (YB) and one was located offshore (Dasa-ri, DS) far from river mouth (Fig. 3.1). The amount of freshwater discharged to the sea during study period was referenced from a record on freshwater discharge in Geumgang Project Office, Korea Rural Community Corporation (KRCC, 2019). Monthly precipitation rates of Gunsan City in the Geum River estuary was obtained from the open on-line source of the National Climate Data Service System (NCDSS, 2019) of Korea Meteorological Administration. Finally, we overlapped both the amount of daily discharged water and monthly precipitation rate (Fig. 3.2A). In general, 100 to 200 kt water was discharged on five to six occasions per month from the Geum River dike between 2015 and 2017, excluding summer (July to August). During summer, freshwater was discharged up to 30 times per day totaling >800 kilo-tonne water per month, because monthly precipitation is the highest by regular heavy monsoon and typhoon rains.

Sediment, sea/freshwater, and macrobenthos were sampled to analyze stable carbon and nitrogen isotopic compositions in sedimentary organic matter (SOM), particulate organic matter in freshwater (POM_{fw}) and seawater (POM_{sw}), and the soft tissue of biota in eight seasons over October 2015 to November 2017. Sampled macrobenthos were identified and separated into trophic groups followed by Yokoyama et al. (2005b), with diet and feeding type being taken into consideration. Discharged freshwater sample was randomly collected during irregular discharge times from June 2016 to November 2017, because the opening of the floodgate was determined from the amount of precipitation. In total, 22 samples (20 L per sample) were collected (Fig. 3.2A).

MPB samples were collected from two locations (DS and SL) in February and May, 2017, when microalgal mats were visible. The microalgal mats were scraped from the top of the sediment surface (~2 mm) and stored into a clean bottle on ice. The mats were transferred to the laboratory within 4 h. MPB was extracted from sediment following the method of Couch (1989), as described by Riera and Richard (1996). We also collected SOM samples scraped from the top of the sediment surface. POM was size-fractionated in situ by use of nets (mesh sizes of 100–1000 μm and 20–100 μm). For collecting the 0.7–20 μm particle size, 20 L water was filetered through 20–100 μm net by eliminatiing the>20 μm particle size. And then, the 20 L water sample was transported to the laboratory and concentrated by vacuum filtration onto a glass-fiber filter to obtain POM of 0.7–20 μm particle size. Finally, we separated POM into three of size classes: 0.7–20, 20–100, and 100–1000 μm. The size-fractionation reflects the plankton size classification described by Makoto & Tsutomu (1984): nanoplankton (2–20 μm), microplankton (20–100 μm), and macroplankton (100–1000 μm), respectively. MPB, SOM, and POM samples were stored at −20 °C until pretreatment.

Macrobenthos were collected by trap and capturing by hand. In total, >1100 individuals of 19 species belonging to five taxa (Bivalvia, Gastropoda, Crustacea, Holothuroidea, and fishes) were collected in the intertidal area of the Geum River estuary during the study period (Table 3.1). Various size of dominant bivalves, *M. veneriformis* and *C. sinensis* (2.1–4.4 and 2.6–4.5 cm in shell length, respectively), were collected. In addition, two freshwater crustaceans, namely *Palaemon paucidens* and *Eriocheir sinensis* were sampled and analyzed which aids to link terrestrial isotopic signatures of dietary composition to freshwater organisms. All of the captured organisms were stored for 12–24 h in filtered sea/freshwater for evacuation. The hard shell of bivalves and gastropods was removed. The soft tissue was dissected into two sections: gut and remaining parts. For, *M. veneriformis* and *C. sinensis*, the shell length was recorded and individuals were grouped into size classes with a standard error of <0.5 cm in shell length. The soft tissues were dissected into the three sections: adductor, gut, and remaining parts. For crustaceans and holothuroidea, the carapace and gut were removed, and only the remaining parts (in soft tissue) were used for the analysis. For fish, only the fillet was used. The same organs from the

same species were pooled and rinsed with distilled water, homogenized, and stored at −20 ℃ until pretreatment. All of the frozen samples (e.g., macrobenthos, MPB, and POM) were lyophilized before stable isotope analysis. We referred to data of>200 μm pelagic POM for the food web reported in same area of a previous study (Choi et al., 2017).

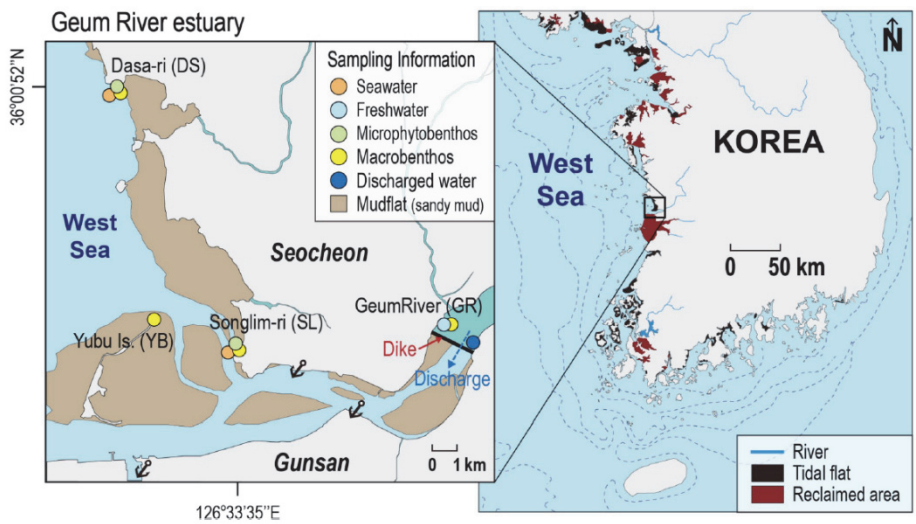

Fig. 3.1. Map of the study area along the Geum River estuary, Korea, showing the sediment types and sampling locations.

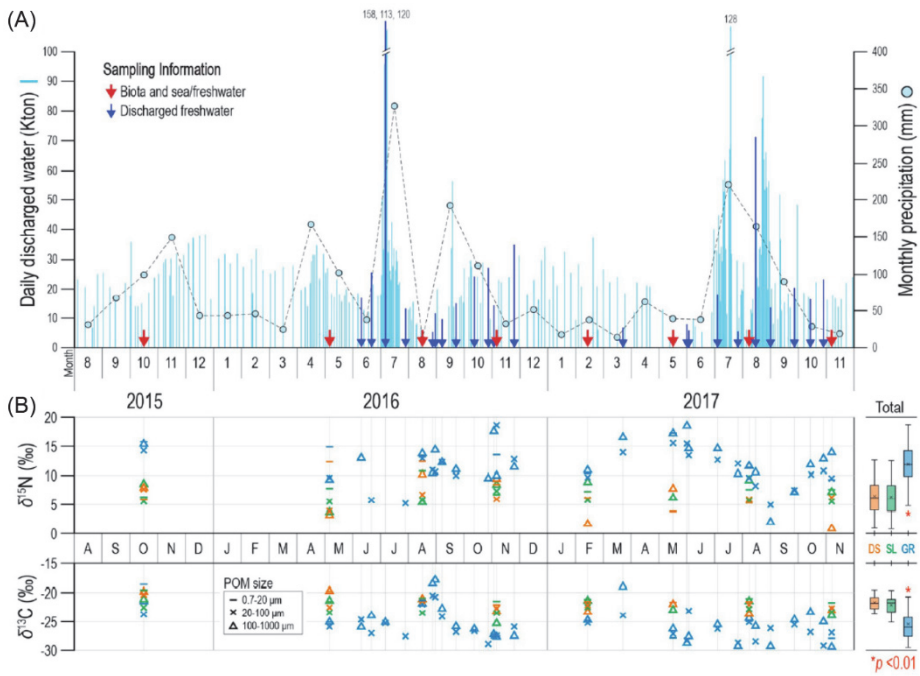

Fig. 3.2. (A) Daily discharge in water mass (kiloton, light blue bar), monthly precipitation rate (mm, light blue circle), and sampling information including seasonal biota and sea/freshwater samples (n = 8, red arrow) and discharge water samples (n = 22, blue arrow) from 2015 to 2017. (B) Stable carbon and nitrogen isotopic compositions ($\delta^{13}C$ and $\delta^{15}N$) of particulate organic matter (POM) in water samples. Water samples were collected from three locations including Dasa (DS, open coast), Yubu (YB, tidal flat on island), and Songlim (SL, river mouth). POM was separated into three size-classes: 0.7–20 μm (dash), 20–100 μm (cross), and 100–1000 μm (triangle).

3.2.2. Laboratory analysis

To determine the stable isotopic compositions of carbon ($\delta^{13}C$) and nitrogen ($\delta^{15}N$) in dried-samples, soft tissues of macrobenthos, MPB, SOM, and POM were used following methods slightly modified from that described previously (Schubert and Nielsen, 2000; Ferrari et al., 2003; Khodse et al., 2007; Svensson et al., 2014). The lipids were removed from a subsample of macrobenthos. In brief, the process involved adding approximately 10 mL dichloromethane (DCM)/methanol (2:1, v/v) to 10–20 mg freeze-dried soft tissues of macrobenthos. The mixture was then sonicated for 10 min and centrifuged at 4000 g for 15 min. Then, organic solvents were pipetted off and discarded. This extraction procedure was repeated three to six times, depending on the lipid content of the sample. Lipid-free samples were evaporated under a gentle stream of N_2 gas at room temperature until fully dry. Before quantifying $\delta^{13}C$ in MPB, SOM, and POM (0.7–20 μm), the samples were decarbonated overnight by fuming them with HCI in a desiccator. A portion of the POM (20–100 and 100–1000 μm) was acidified overnight with 1 N hydrochloric acid (HCl, Sigma Aldrich, St. Louis, MO) to eliminate inorganic carbon. It was then rinsed with distilled water. The acidified samples were repeatedly freeze-dried and subsequent the redried samples were thoroughly mixed, and these samples were then weighed in a tin capsule for isotopic analysis.

The values of $\delta^{13}C$ and $\delta^{15}N$ in MPB, SOM, and POM samples were pre-tested for each sample. Accordingly, the injection amounts of samples were then adjusted to determine the weight; approximately 3–10 mg for MPB and POM and 10–70 mg for SOM. Three replicates were analyzed for $\delta^{13}C$ and $\delta^{15}N$, and the mean of triplicates was used for the data analysis. Very small samples (particularly, POMs) were analyzed without replicates. $\delta^{15}N$ of some POM samples could not be measured due to the low concentration of N. $\delta^{13}C$ and $\delta^{15}N$ were measured with an Elemental Analyzer-Isotope Ratio Mass Spectrometer (EA-IRMS) (Elementar, Gmbh, Hanau, Germany). High purity carbon dioxide and nitrogen gases were used as reference gases, while helium and oxygen gases were used as carrier and combustion gases, respectively. Stable carbon and nitrogen isotopic compositions were expressed as ‰ delta notation refered in Eq. 1.

3.2.3. Data analysis

To estimate the trophic level, we used the trophic enrichment factor (TEF) of $\delta^{15}N$ 3.4‰ estimated in a previous study (Post, 2002). We used the mean $\delta^{15}N$ values of all collected bivalves to represent the second level of the food web, because filter feeders assimilate varying primary producers and organic particles, leading to the assumption that they occupy trophic level 2 (Riccialdelli et al., 2017). The trophic level of each consumer was determined using the equation proposed by Vander Zanden and Rasmussen (1999) (Eq. 7):

$$TL_i = (\delta^{15}N_i - \delta^{15}N_{base})/TEF + TL_{base} \quad (7)$$

where, TL_i is the trophic level of each species evaluated, $\delta^{15}N_i$ is the stable nitrogen isotopic composition of the species i, and $\delta^{15}N_{base}$ and TL_{base} are the mean stable nitrogen isotopic composition and the trophic level, respectively, of all bivalves.

SPSS 23.0 (SPSS INC., Chicago, IL) was used to perform the statistical analyses. The stable carbon and nitrogen compositions of target bivalves (*M. veneriformis* and *C. sinensis*) were analyzed to test for differences between the two species and for different locations (DS, YB, and SL) using a t-test and a one-way analysis of variance (ANOVA) with Bonferroni post-hoc test, respectively. Before analysis, the analysis of variance was determined to be homogeneous between groups by the Levene's homogeneity test, meeting the assumption of variance homogeneity ($p > 0.05$). The same statistical method was used to test differences in $\delta^{13}C$ and $\delta^{15}N$ of the organs (gut, adductor, and remaining parts) of the two bivalves.

Bayesian stable isotope mixing models in R (SIMMR) package (Parnell & Inger, 2016) were used to estimate the proportional contribution of potential food sources (POM and MPB) to the target bivalves as the primary consumers using the data analyzed in February, May, August, and October of 2017. The POM_{fw} and discharged freshwater were excluded for the SIMMR, because it showed that the high enrichment of POM $\delta^{15}N$ (mean 15.9‰) did not fit in model as a diet for primary consumers (e.g., mean 11.7‰ for δ15N in bivalves) in the seawater food web of the Geum River estuary. The isotope values of the adductor and remaining

parts (but not the gut) were used in the mixing model. For the contribution of POM and MPB, each value was pooled and evaluated as a total mean calculated without classifying the size of individuals below 100 μm. The $\delta^{13}C$ and $\delta^{15}N$ values in SIMMR were adjusted for trophic level using previous TEF estimates; 0.4 ± 1.3‰ for $\delta^{13}C$ and 3.4 ± 1.0‰ for $\delta^{15}N$ (Post, 2002).

The nonlinear regression function of SigmaPlot (v10.0, Systat Software, Inc.) was used to fit the curve for isotope signatures of *M. veneriformis* for part-specific variation and size (shell length), but not used for *C. sinensis* because sample size was limited ($n < 20$). The Kolmogorov-Smirnov test was performed, which resulted in data meeting the assumption of normality ($p > 0.05$) (Rosenthal, 1968). The age of *M. veneriformis* was estimated base on the growth curve for shell length by von Bertalanffy's equation following Kim and Ryou (1991). We then separated individuals into, six age-classes: below 1 yr (< 21.7 mm), 1–1.5 yr (21.7–29.0 mm), 1.5–2 yr (29.0–34.6 mm), 2–2.5 yr (34.6–38.8 mm), 2.5–3 yr (38.8–42.0 mm), and above 3 yr (> 42.0 mm) of age. The ages of *C. sinensis* were approximately assumed from a previous study (Lin et al., 2017).

3.3. Results

3.3.1. Variations of $\delta^{13}C$ and $\delta^{15}N$ of POM

$\delta^{13}C$ and $\delta^{15}N$ of the POM in seawater and freshwater (including discharged freshwater) varied both spatially and temporally (Fig. 3.2B & Table 3.1). Over most of the time series in GR, $\delta^{13}C$ and $\delta^{15}N$ of POM were typically between −30 to −25‰, and 10 to 20‰, respectively. The total mean $\delta^{15}N$ of POM in GR was 11.9‰, and it greatly fluctuated across seasons, ranging from 1.9 to 18.5‰. The smallest values for $\delta^{15}N$ of POM were recorded in June and July of 2016, and August and September of 2017 (mean 5.6, 5.2, 3.4, and 7.3‰, respectively), before massive and continuous freshwater discharges. In comparison, $\delta^{13}C$ of POM in GR was relatively consistent (mean: −25.4‰; range: −29.5 to −18.0‰). The highest values for $\delta^{13}C$ POM were observed in August, 2016 and March, 2017 (−19.5‰ and −19.1‰, respectively). While, both of $\delta^{13}C$ and $\delta^{15}N$ of POM_{sw} (DS and SL) were relatively stable between seasons (range: −25 to −20‰ for δ13C and 5 to 10‰ for δ15N). The total mean for $\delta^{13}C$ and $\delta^{15}N$ of POM was −21.7‰ and 6.5‰ in DS, and −22.1‰ and 6.9‰ in SL, respectively. There was no significant difference in the stable isotopic compositions of POM between the two seawater locations (DS and SL); however, there was a significant difference ($p < 0.01$) between the freshwater location (GR and discharged freshwater samples) and the seawater locations (DS and SL) (Fig. 3.2B).

There was no isotopic difference in certain POM size-groups (0.7–20, 20–100, and 100–1000 μm) occupying the same site ($p > 0.05$, Table 3.1). However, for the >200 μm POM size-group, the plausible size for zooplankton, POM values were greater for $\delta^{13}C$ (−19.9 ± 0.1‰) and $\delta^{15}N$ (11.6 ± 0.4‰). The values for $\delta^{13}C$ and $\delta^{15}N$ in >200 μm POM seemed to be the result of feeding on pelagic POM and benthic (MPB) sources of zooplankton. Of note, depleted $\delta^{13}C$ (−22.6 ± 0.2‰) and enriched $\delta^{15}N$ (19.0 ± 1.2‰) isotopic signatures observed in two freshwater crustaceans indicated the separated trophic grouping from distinct intertidal food web. Altogether, we could successfully distinguish three groups of POM (POM_{fw}, POM_{sw}, and > 200 μm sized POM_{fw}), MPB, and macrobenthos in biplot of the estuarine food web (Fig. 3.3).

3.3.2. Benthic food web

There were distinct differences in both $\delta^{13}C$ and $\delta^{15}N$ among potential food sources, including MPB, SOM, and POM for primary consumers (Table 3.1 & Fig. 3.3). As primary producers, MPB had the smallest mean $\delta^{15}N$ (4.7‰), but had relatively enriched mean $\delta^{13}C$ (−17.6‰) compared to those of SOM (−20.9‰), POM_{sw} (−21.9‰), and POM_{fw} (−25.4‰), respectively. Even though irregular freshwater discharge could supply the seawater area with POM, the very enriched-$\delta^{15}N$ and depleted-$\delta^{13}C$ values of freshwater POM were not considered to enter the trophic pathway of the seawater food web in the Geum River estuary. Therefore, three potential food sources for primary consumers were distinguished; POM_{sw} as pelagic sources and MPB and SOM from benthic sources.

Macrobenthos were assigned to its corresponding trophic group, such as filter feeder, deposit feeder, scavenger, carnivore, and omnivore (Fig. 3.3). Based on $\delta^{15}N$ values, the trophic levels of most invertebrate species were estimated to be between two to three. Crustaceans and gastropods occupied slightly higher trophic levels (+0.5 upper) compared to bivalves (TL = 2.0). However, *Upogebia major* and *Macrophthalmus japonicas* occupied similar positions. Carnivorous fish species (*Synechogobius hasta* and *Tridentiger trigonocephalus*) occupied the highest tropic level (3.0–3.2) in this food web. Macrobenthos exhibited taxon-specific variation in $\delta^{13}C$ values.

The mean $\delta^{13}C$ values of bivalve species ranged from −19.2 to −17.7‰, and had more depleted-$\delta^{13}C$ compared to taxa in the upper trophic levels (Table 3.1). Gastropoda were represented by two carnivorous sea-sails (*Neverita didyma* and *Rapana venosa*) and one scavenger sea-snail (*Nassarius livescens*). In particular, *N. didyma* and *R. venosa* had enriched-$\delta^{13}C$ mean values (range: −17.0 to −16.1‰) with much greater $\delta^{15}N$ values (range: 13.3 to 13.7‰, TL: 2.4–2.6) than bivalves which are major prey. Crustacea and fishes had a relatively wide range of mean $\delta^{13}C$ values (range: −18.2 to −13.4‰ and −19.4 to −16.0‰, respectively). The total mean values of stable isotope signatures for *M. veneriformis* were −17.8‰ for $\delta^{13}C$ and 11.2‰ for $\delta^{15}N$, respectively, while those of *C. sinensis* were −18.7‰ for $\delta^{13}C$ and 11.5‰ for $\delta^{15}N$.

Table 3.1. Stable carbon and nitrogen isotopic compositions ($\delta_{13}C$ and $\delta_{15}N$) of microphytobenthos (MPB), sediment organic matter (SOM), particulate organic matter (POM), and macrobenthos collected from four locations (Dasa-ri, DS; Songlim-ri, SL; Geum-River, GR; Yubu Is., YB) along the Geum River estuary in 2015 to 2017, with corresponding trophic level (TL). Isotopic values reported as means with standard deviations (s.d.), and n corresponds to the total number of samples (*Trophic level was not calculated for freshwater crustaceans).

Species	Location	*n*	$\delta^{15}N$		TL	$\delta^{13}C$	
			mean	s.d.		mean	s.d.
MPB	DS & SL	9	4.7	0.5	-	-17.6	0.7
SOM	DS & SL	8	5.9	1.1	-	-20.8	0.2
POM in seawater							
(0.7-20 μm)	DS	7	7.4	3.4	-	-21.5	0.4
(20-100 μm)		7	6.3	1.2	-	-22.0	0.9
(100-200 μm)		8	5.5	3.9	-	-22.0	1.6
Subtotal (DS)		22	6.5	3.2	-	-21.7	1.2
(0.7-20 μm)	SL	7	7.3	1.8	-	-21.1	0.7
(20-100 μm)		7	5.9	0.7	-	-22.9	0.5
(100-200 μm)		8	7.4	2.0	-	-22.1	1.6
Subtotal (SL)		22	6.9	1.7	-	-22.1	1.3
Total (DS & SL)		44	6.7	2.5	-	-21.9	1.2

Table 3.1. Continued.

Species	Location	*n*	$\delta^{15}N$		TL	$\delta^{13}C$	
			mean	s.d.		mean	s.d.
POM in freshwater							
(0.7-20 μm)	GR	8	13.2	2.8	-	-24.7	3.3
(20-100 μm)		30	12.5	3.5	-	-25.4	1.9
(100-200 μm)		28	13.0	2.8	-	-24.9	2.7
Total (GR)		66	11.9	3.4	-	-25.4	2.8
Macrofauna							
Bivalvia							
Mactra veneriformis	DS	229	11.3	0.7	1.8	-17.9	0.8
	YB	193	11.7	0.5	2.0	-17.3	0.6
Cyclina sinensis	SL	37	12.0	0.6	2.1	-18.5	0.7
Dosinorbis japonicus	DS	5	13.0	0.1	2.4	-17.8	0.0
Anadara broughtonii	DS	1	12.0	0.0	2.0	-17.7	0.1
Solen strictus	DS	19	11.8	0.3	2.0	-18.7	0.8
Crassostrea gigas	SL	12	10.2	0.1	1.5	-19.2	0.1
Gastropoda							
Nassarius livescens	DS	147	13.7	0.3	2.6	-15.5	0.4
	SL	226	13.6	0.2	2.5	-15.5	0.1
Neverita didyma	DS	20	13.7	0.5	2.6	-16.1	0.4
Rapana venosa	DS	13	13.3	0.2	2.4	-17.0	1.0

Table 3.1. Continued.

Species	Location	*n*	$\delta^{15}N$		TL	$\delta^{13}C$	
			mean	s.d.		mean	s.d.
Crustacea							
*Palaemon paucidens**	GR	8	20.1	0.3	-	-22.8	0.1
*Eriocheir sinensis**	GR	1	18.0	0.4	-	-22.5	0.0
Squilla oratoria	DS	3	14.6	0.1	2.8	-16.7	0.3
Hemigrapsus penicillatus	SL	26	13.4	0.1	2.5	-16.8	0.4
Callianassa japonica	DS	17	13.2	0.2	2.4	-16.8	0.1
	SL	23	13.2	0.2	2.4	-16.6	0.0
Upogebia major	DS	70	12.1	0.5	2.1	-18.2	0.2
Macrophthalmus japonicus	DS	18	11.9	0.2	2.0	-13.4	0.1
	SL	8	10.1	0.3	1.5	-15.4	0.5
Holothuroidea							
Apostichopus japonicus	DS	1	11.7	0.0	2.0	-16.7	0.1
Fish							
Synechogobius hasta	SL	2	15.9	1.0	3.2	-16.0	1.1
Tridentiger trigonocephalus	DS	3	15.1	1.0	3.0	-16.8	0.2
	SL	6	15.4	0.0	3.1	-19.4	0.2

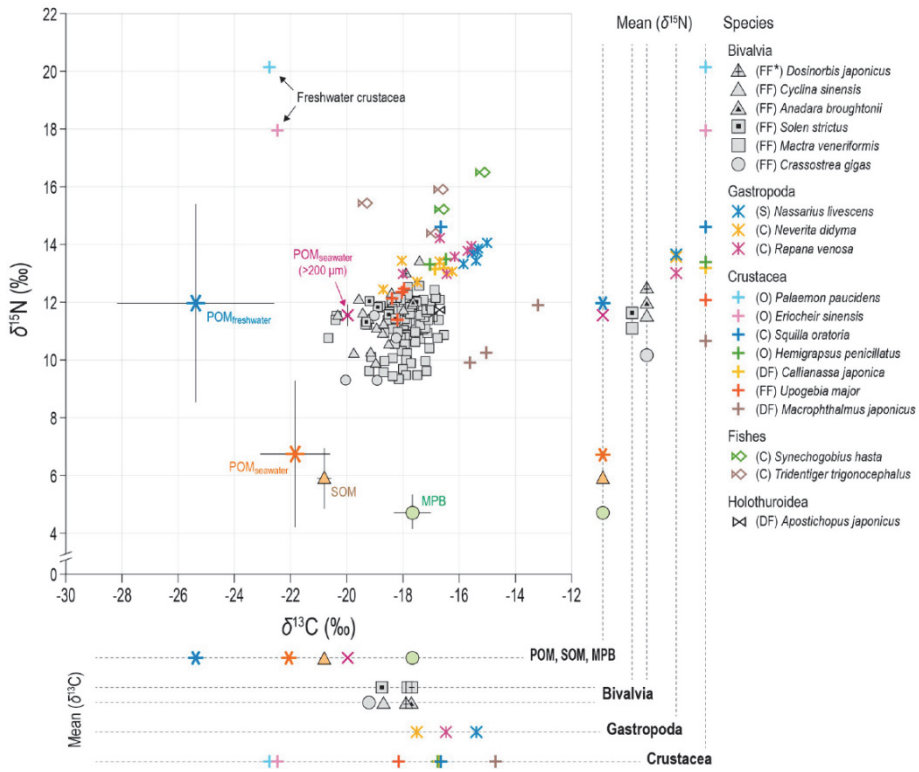

Fig. 3.3. Biplot of stable carbon and nitrogen isotopic compositions ($\delta^{13}C$ and $\delta^{15}N$) of macrobenthos and potential food sources in the Geum River estuary. The values of potential food sources [such as particulate organic matter (POM), sediment organic matter (SOM), and microphytobenthos (MPB)] represent the total means with standard deviations (black line). The values of macrobenthos represent the means of individuals collected at each sampling time. The value of over 200 μm POM in seawater was obtained from Choi et al. (2017) (*Acronyms in parenthesis: (FF) filter feeder, (S) scavenger, (C) carnivore, (O) omnivore, and (DF) deposit feeder).

3.3.3. Variations of $\delta^{13}C$ and $\delta^{15}N$ in target bivalves

The mean $\delta^{15}N$ values of target bivalves did not significantly differ among the three locations where they were collected (*M. veneriformis* in DS and YB, and *C. sinensis* in SL; $p > 0.05$), whereas differences in the mean $\delta^{13}C$ values were spatially significant (Fig. 3.4). Samples collected in winter (February, 2017) had more depleted-$\delta^{13}C$ values compared to other seasons for both *M. veneriformis* and *C. sinensis*. The stable isotope signatures between the target bivalves showed no significant difference in total mean $\delta^{15}N$, but a significant difference for total mean $\delta^{13}C$ ($p < 0.01$) (Fig. 3.5A). *M. veneriformis* and *C. sinensis* of various sizes, as a proxy of age, were collected from the Geum River estuary, ranging from below one-year to above three-years in age (Table 3.2). Seasonal changes to stable isotopic compositions were detected for the two target bivalves. Both species were roughly separated into two groups according to their size: (1) small groups; < 2 yr for *M. veneriformis* and 1–2 yr for *C. sinensis* and (2) large groups; 2–3 yr for *M. veneriformis* and 2–3 yr for *C. sinensis*. The mean $\delta^{13}C$ value of target bivalves in smaller groups was significantly lower (i.e., ~2.3‰ depleted-$\delta^{13}C$) compared to that of large groups in the winter of 2017 ($p < 0.01$). The difference in $\delta^{13}C$ between small and large groups gradually decreased as the season progressed (Fig. 3.5B).

The mixing model for the target bivalves, *M. veneriformis* and *C. sinensis*, indicated seasonal, species-, and size-specific variations in diet contributions (Fig. 3.5B′). Overall, the mean contributions of MPB to target bivalves exceeded that of POM_{sw}, except for the smallest size groups collected in February, 2017 (see Table 3.2). There was a greater contribution of POM_{sw} in these groups (mean 74% and 56% in *M. veneriformis* and *C. sinensis*, respectively). MPB represented a relatively minor component of the diet in winter for small-sized groups of the two target bivalves; however, from spring to fall, MPB formed the main dietary component (mean 49–80%). In comparison, the mean dietary contributions of seawater POM tended to decline from winter to fall in the small-sized groups. MPB represented the main dietary component of large-sized bivalves for both species (mean: 65–88% and 64–78% for *M. veneriformis* and *C. sinensis*, respectively). In comparison, seawater POM was a relatively minor dietary component in large-sized bivalves, with its mean

contribution being about 15% greater in small-sized groups. The mixing model indicated that the diet was the most complex in fall (November, 2017), based on a wide range of credibility intervals between dietary contributions (i.e., 4–7% at the lowest limits and 62–96% at highest limits) (Fig. 3.5B′).

There was a significant difference in organ-specific isotopic enrichment in the target bivalves (Fig. 3.6). Gut tissue had distinctively depleted-$\delta^{15}N$ values compared to those in the adductor and remaining parts for both bivalve species; however, $\delta^{13}C$ was only significantly different in the gut tissue of *M. veneriformis* ($p < 0.01$). The mean $\delta^{15}N$ value of the gut was smaller about 1.0‰ in *M. veneriformis* and 1.4‰ in *C. sinensis*, compared to those in the other tissues (adductor and remaining parts). The mean $\delta^{13}C$ value of *M. veneriformis* was most depleted in gut (−18.2‰), and was significantly different to those in the adductor (−17.5‰) and remaining parts (−17.3‰) (Fig. 3.6A). The mean $\delta^{13}C$ value in the gut (−19.0‰) of *C. sinensis* was also smaller than those in the adductor (−18.6‰) and remaining parts (−18.3‰), but these differences were not significant ($p > 0.05$) (Fig. 3.6B).

The stable isotope values changed with size class (shell length) for *M. veneriformis* (Fig. 3.7). $\delta^{15}N$ values in total soft tissues showed no relationship with shell length; however, $\delta^{15}N$ of adductor and remaining tissues (excluding the gut) increased linearly with shell length ($\delta^{15}N = 10.1 + 0.36 \times$ shell length, $R^2 = 0.14$, $p < 0.001$). On average, the $\delta^{15}N$ value of the largest size class (> 3 yr, n = 74) was slightly higher (+0.44‰) than that of the smallest class (< 1 yr, n = 11). $\delta^{13}C$ values of *M. veneriformis* (excluding gut) increased as a function of shell length, rising exponentially to a maximum, with this relationship being highly correlated ($\delta^{13}C = -1001 + 983.6 \times (1 - 0.064^{\text{shell length}})$, $R^2 = 0.14$, $p < 0.001$). The growth of *M. veneriformis* noticeably changed in relation to $\delta^{13}C$ values during 1–1.5 yr cycle (age) in soft tissues. The mean $\delta^{13}C$ value of the smallest class (< 1 yr, n = 11) was −20.4‰, and noticeably increased until a peak value of −17.2‰ reached (1.5–2 yr, n = 193) when the shell length exceeded 3 cm.

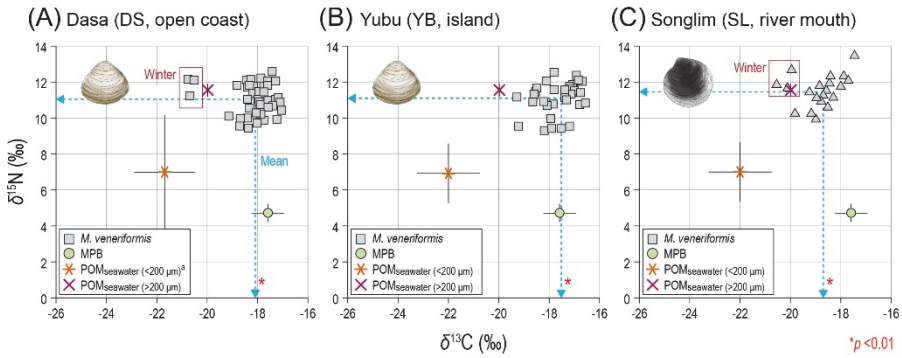

Fig. 3.4. Stable carbon and nitrogen isotopic compositions ($\delta^{13}C$ and $\delta^{15}N$) of *Mactra veneriformis* and *Cyclina sinensis* at three locations: *M. veneriformis* collected from (A) DS, open coast and (B) YB, tidal flat on island; and *C. sinensis* collected from (C) SL, river mouth. The values of potential food sources [such as particulate organic matter (POM) and microphytobenthos (MPB)] represent total means with standard deviations (black line). The values of bivalves represent the means of individuals sampled at different times.

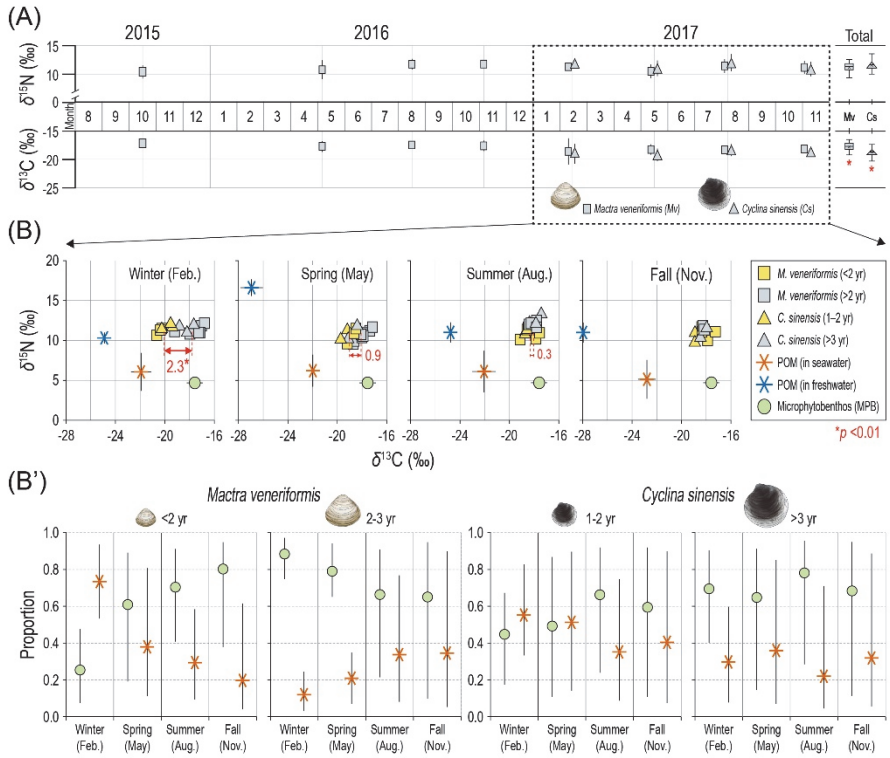

Fig. 3.5. (A) Seasonal values and total means of stable carbon and nitrogen isotopic compositions ($\delta^{13}C$ and $\delta^{15}N$) in target bivalves *Mactra veneriformis* and *Cyclina sinensis* from 2015 to 2017, and (B) seasonal variation in stable isotopes between different size groups among the target bivalves, with potential food sources [such as particulate organic matter (POM) in seawater and freshwater, and microphytobenthos (MPB)] being collected in 2017. (B′) Seasonal proportions of each food source to *M. veneriformis* and *C. sinensis* collected in 2017. The two bivalves were separated into two size groups based on shell length. Each symbol for diet types shows the most likely value with 95% credibility intervals in Bayesian mixing model.

Table 3.2. Shell length and age of Mactra veneriformis and Cyclina sinensis collected from three locations (Dasa-ri, DS; Songlim-ri, SL; Yubu Is., YB) along Geum River estuary in 2015 to 2017. Shell length reported as mean with standard deviation (s.d.), and n corresponds to the number of individuals.

Species	Sampling date	Location	*n*	Shell length (cm)		Age (yr)
				mean	s.d.	
Mactra veneriformis	Oct., 2015	DS	44	3.0	0.2	1.5-2.0
			15	4.3	0.2	3.0-3.5
		YB	10	3.3	0.3	1.5-2.0
			5	4.2	0.2	2.5-3.0
	May, 2016	DS	40	3.1	0.2	1.5-2.0
			20	4.4	0.2	3.0-3.5
		YB	18	3.1	0.2	1.5-2.0
			10	4.3	0.2	3.0-3.5
	Aug., 2016	DS	15	3.6	0.1	2.0-2.5
			11	4.3	0.2	3.0-3.5
		YB	22	3.4	0.1	1.5-2.0
			17	4.1	0.2	2.5-3.0
	Nov., 2016	DS	19	3.7	0.1	2.0-2.5
			12	4.4	0.2	3.0-3.5
		YB	35	3.0	0.4	1.5-2.0
			25	4.0	0.2	2.5-3.0
	Feb., 2017	DS	11	2.1	0.3	<1.0
			9	4.2	0.2	2.5-3.0
		YB	6	4.3	0.1	3.0-3.5

Table 3.2. Continued.

Species	Sampling date	Location	*n*	Shell length (cm)		Age (yr)
				mean	s.d.	
Mactra veneriformis	May, 2017	DS	7	3.5	0.2	2.0-2.5
			5	4.2	0.3	2.5-3.0
		YB	5	2.6	0.2	1.0-1.5
			7	3.9	0.1	2.5-3.0
	Aug., 2017	DS	6	2.7	0.2	1.0-1.5
			4	3.9	0.1	2.5-3.0
		YB	6	2.8	0.1	1.0-1.5
			3	3.9	0.2	2.5-3.0
	Nov., 2017	DS	6	3.8	0.2	2.0-2.5
			5	4.1	0.2	2.5-3.0
		YB	24	3.4	0.3	1.5-2.0
Cyclina sinensis	Feb., 2017	SL	7	2.6	0.3	1.0-2.0
			5	4.4	0.2	>3.0
	May, 2017		9	2.8	0.2	1.0-2.0
			4	4.5	0.3	>3.0
	Aug., 2017		4	2.9	0.1	1.0-2.0
			2	4.3	0.2	>3.0
	Nov., 2017		3	2.7	0.5	1.0-2.0
			3	4.2	0.3	>3.0

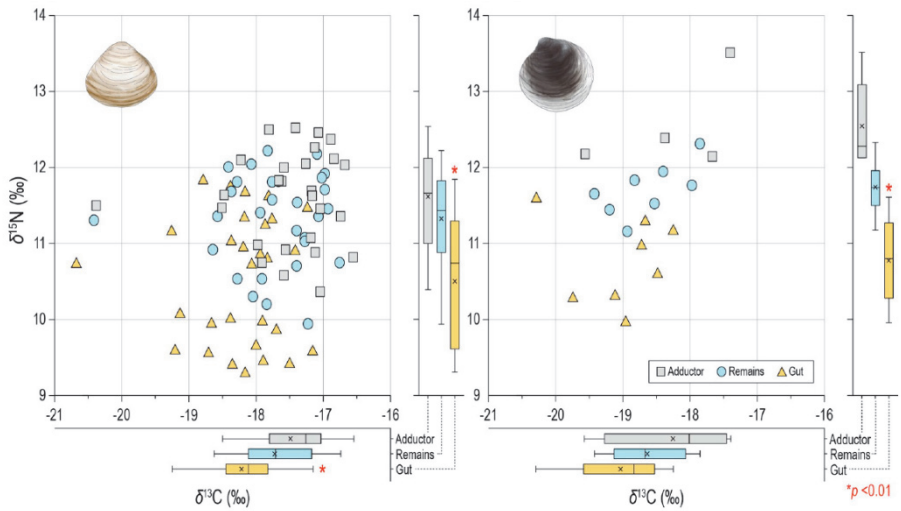

Fig. 3.6. Organ-specific values of stable carbon and nitrogen isotopic compositions ($\delta^{13}C$ and $\delta^{15}N$) in *Mactra veneriformis* (**left**) and *Cyclina sinensis* (**right**). Soft tissues of the bivalves were separated into three organs: adductor (grey square), gut (yellow triangle), and remaining parts (light blue circle). Each value represents the means of individuals sampled at different times.

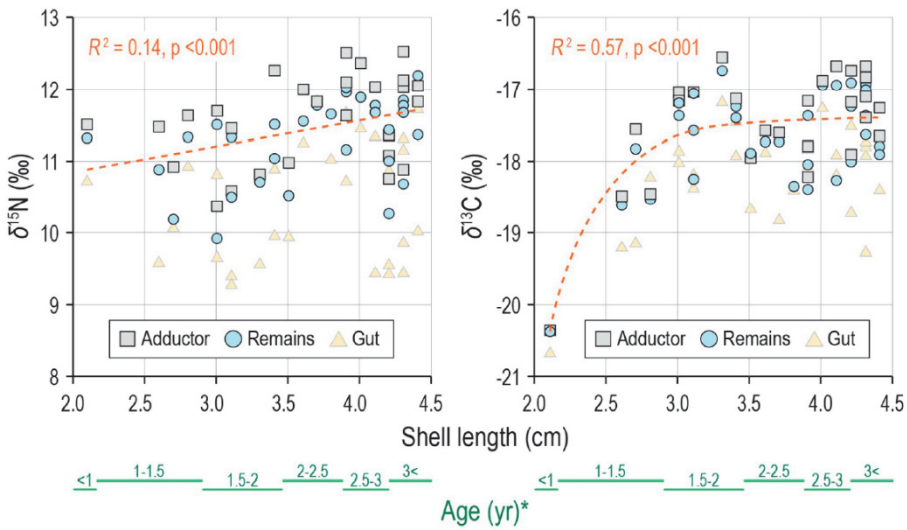

Fig. 3.7. Stable carbon and nitrogen isotopic compositions ($\delta^{13}C$ and $\delta^{15}N$) of *Mactra veneriformis* in relation to shell length as a function of adductor and remaining parts (i.e., organ-specific relationship). Value of gut tissues was excluded for fitting the curve. Each value represents the mean of individuals sampled at different times (*The age of *M. veneriformis* was estimated based on the growth curve for shell length by von Bertalanffy's equation following Kim and Ryou (1991)).

3.4. Discussion

The present study revealed that freshwater POM in the closed Geum River estuary, where freshwater input is artificially controlled by a sea dike, is barely linked to the trophic status of benthic consumers on the outer tidal flats. Large seasonal variation in the isotopic signature of freshwater POM was detected in the Geum River estuary. Thus, different process likely influenced $\delta^{13}C$ and $\delta^{15}N$ values of POM in the freshwater area compared to the seawater area (Fig. 3.2B). The dike has geographically isolated the Geum River from the seawater ecosystem, resulting in the freshwater area being more strongly influenced by terrestrial nutrient input from upstream. High $\delta^{15}N$ enrichment of freshwater POM is mainly influenced by the denitrification process of isotopic fractionation during the microbial transformation and phytoplanktonic assimilation of nitrogen under eutrophic conditions (Owens, 1988; Hadas et al., 2009; Gu, 2009). $\delta^{15}N$ was depleted in freshwater POM during June and July of 2016 and August of 2017, possibly a result of N_2-fixing cyanobacteria blooms under hypereutrophic conditions (Gu et al., 1996). Indeed, during the summer (July to September) of 2016 and 2017, relatively great concentration of Chl-*a* (57.7 ± 26.1 mg/L) and cyanobacteria blooms (up to 50 K cells/mL) were observed in the Geum River upstream (WEIS, 2019). Increased POM $\delta^{13}C$ in August, 2016 might reflect lower isotopic fractionation during carbon fixation when dissolved CO_2 decreased, because of increased temperature and highly photosynthetic conditions (Berman-Frank et al., 1998). The isotopic signatures of marine macrobenthos (especially bivalves as filter feeders) in the Geum River estuary provided no evidence for freshwater POM being a major food source for upper trophic levels, even when intermittent discharges occurred. Ultimately, the discrepancy in the isotopic signature of POM between the areas inside and outside the sea dike indicated that the “closed freshwater area” in the Geum River estuary is now more close to an isolated lake ecosystem, rather than free-flowing river.

The feeding pathway of filter feeders derives from various potential food sources, including SOM, phytogenic detritus, riverine and pelagic suspended matter, and resuspended particulate matter etc. Consequently, this variety could lead to highly complicated dietary contributions as demonstrated by the stable isotopic

compositions. However, the flow of freshwater in the Geum River estuary is almost negligible, with extensive tidal flats being developed without saltmarshes, mangroves, or other vegetation and macroalgal communities. Therefore, the main food sources of filter feeders seemed to be limited with respect to pelagic and benthic sources, resulting two distinct groups existing, i.e., seawater POM and MPB (Table 3.1). The mean $\delta^{13}C$ values of seawater POM and MPB were similar to those obtained by previous studies, ranging from −24 to −18‰ in seawater POM and −20 to −13‰ in MPB (Fig. 3.8). Although seawater POM and MPB had overlapping $\delta^{15}N$ values, $\delta^{13}C$ values were distinct; thus, the isotope biplot of $\delta^{13}C$ and $\delta^{15}N$ distinguished these primary producers (Fig. 3.3).

TEF is generally required to determine the food sources of consumers; however, ideally species-specific values must be applied, even though few studies are available (Post, 2002; Dubois et al., 2007). In the same manner, our results showed that the $\delta^{15}N$ of bivalves, as primary consumers, was ~5‰ greater compared to those of primary producers (seawater POM and MPB). This value exceeded the documented magnitude (3.4 ± 1.0‰, Post, 2002) of isotopic fractionation between consumers and their prey. The isotope signatures of POM of >200 μm in size might be the result of zooplankton preying on seawater POM and/or MPB. The scavenger sea-snail, *N. livescens*, had a relatively enriched isotopic signature, possibly because it consumes the carcasses of benthic animals. Consequently, this species obtained a highly enriched source of carbon and nitrogen (Heinrich, 1988). The carnivorous seasnails, *N. didyma* and *R. venosa*, had TLs of 2.6 and 2.4, respectively. These values indicated that they generally preyed on *M. veneriformis* (TL = 1.8–2.0); thus a TEF of <3‰ was assumed. Crustacea had a wide range of isotope signatures due to a great diversity of feeding types. The carnivorous mantis-shrimp, *Squilla oratoria*, occupied the highest position (14.6‰ in mean $\delta^{15}N$, TL = 2.8) for crustaceans. In comparison, *U. major* was a filter feeder that mainly fed on seawater POM and MPB, and had a similar isotopic signature to the bivalves.

Hemigrapsus penicillatus (an omnivore that incorporates ^{13}C-enriched materials) and *Callianassa japonica* (deposit feeder) had similar isotope signatures, suggesting that both were likely to utilize similar food sources although they employ different feeding strategies (Kang et al., 2015). *M. japonicus* is a consumer that

incorporates ^{13}C-enriched materials and exhibited the widest range of isotope signatures because it used a variety of food sources from the sediment surface (Yokoyama et al., 2005a). The carnivorous Osteichthyes, *S. hasta* and *T. trigonocephalus*, had the greatest $\delta^{15}N$ values among the marine species, representing the top predators in the outside of the dike. While the most enriched $\delta^{15}N$ values were observed for two freshwater crustaceans, *P. paucidens* and *E. sinensis*, in the inside of the dike. Overall, this trophic pathway from primary producers to primary and secondary consumers was well-characterized as a trophic cascade in the benthic food web structure in the Geum River estuary (Fig. 3.3).

Several studies on food webs in tidal flat ecosystems have demonstrated spatiotemporal variations in the $\delta^{13}C$ and $\delta^{15}N$ values of macrobenthos because the pelagic and benthic contributions of potential food sources vary among species and/or habitat (Galvan et al., 2008). Therefore, we initially hypothesized that if the oceanographic setting of the sampling locations followed a salinity gradient (i.e., along the estuary, including locations at a far distance (DS) and near to the river mouth (YB and SL)), the contribution of potential food sources of the target bivalves (*M. veneriformis and C. sinensis*) close to river mouth would be more influenced by riverine organic matter. However, the riverine input did not supply enough dietary items under the closed conditions. Despite this, we detected significant spatial differences in $\delta^{13}C$ values when comparing the three intertidal sites: *M. veneriformis* collected in DS and YB, and *C. sinensis* collected in SL (Fig. 4). Of note, intraspecific variation associated to the feeding sources could be directly influenced by pelagic and/or benthic production, whereas interspecific variation was the result of selective feeding behavior (Kiorboe and Mohlenberg, 1981; Prins et al., 1991; Kang et al., 1999; Cognie et al., 2001; Rossi et al., 2004; Nadon & Himmelman, 2006). Therefore, *M. veneriformis* individuals that were collected near the river mouth (YB) fed on more MPB compared to those collected from more distant coastal location (DS). Furthermore, *C. sinensis* selectively fed on more seawater POM compared to *M. veneriformis* in YB.

The dietary components of *M. veneriformis* and *C. sinensis* collected from the Geum River estuary showed clear seasonal variation over a 1-year period in 2017 (Fig. 3.5). MPB was the most important primary producer on the extensive bare

intertidal flat of the Geum River estuary. In particular, the diurnal production and resuspension of MPB provided a continuous food supply for non-(or lesser) motile invertebrates (De Jonge & Van Beuselom, 1995; Lucas et al., 2000; Page & Lastra, 2003; Koh et al., 2006). Our results showed a seasonal dietary shift in the small-sized groups of both bivalves, associated with selective feeding on seawater POM and/or MPB. Although the smallest group of *M. veneriformis* (< 1 yr individuals collected in 1st winter, Fig. 3.4A) preferentially fed on seawater POM compared to MPB before reaching the next life stage (juvenile), the dietary contribution of MPB continuously accumulated over time (Kang et al., 2003, 2006). Interestingly, the large-sized group of *M. veneriformis* had the highest contribution of MPB during winter, which apparently corresponded to annual blooms of MPB in the intertidal flats from winter to early spring (Kwon et al., 2018). Over 50% to nearly 100% of carbon sources incorporated in the tissues of *M. veneriformis* and *C. sinensis* were derived from MPB. This active utilization was more prominent in the large-sized groups compared to the small-sized groups. The selective feeding strategies for growth (expressed by shell length) across seasons by the filter feeders studied here support previous studies, which demonstrated their ability to utilize nutritionally rich particles in quality or size during critical periods of growth and gamete production (Le Loc'h et al., 2008; Kang et al., 2009; Pernet et al., 2012; Kang et al., 2015).

Further, isotopic variation was detected among organs and size classes, indicating that isotopic shifts between the tissues of consumers and their diets (i.e., TEF) differ between organ types, with temporal variation (Lorrain et al., 2002). The isotope values of *M. veneriformis* in lipid-free tissues exhibited near parity between the adductor and remaining parts (averagely 0.2‰ and 0.3‰ shifts in $\delta^{13}C$ and $\delta^{15}N$, respectively). In comparison, the gut tissues had significantly smaller values of both $\delta^{13}C$ and $\delta^{15}N$; thus, an organ-specific allocation strategy for nutrient storage might exist (Paulet et al., 2006). Available nutritional sources exhibited seasonal variation in pelagic and benthic dietary contributions (Fig. 3.5); thus, variation in δ13C and δ15N values observed in the tissues of each organ (Fig. 3.6) was probably induced from seasonal growth patterns in somatic and reproductive tissues in the Geum River estuary (Strohmeier et al., 2000; Kang et al., 2019).

The positive correlation between the $\delta^{15}N$ values of soft tissues and the shell

length (i.e., age) of *M. veneriformis* (Fig. 3.7) indicated shifts in diet through feeding of enriched-$\delta^{15}N$ sources, possibly due to differences in foraging ability such as selective feeding, metabolic process, and discrimination factor. Nevertheless, for better understanding of the enriched-$\delta^{15}N$ in bivalves, the $\delta^{15}N$ of bulk tissue was corrected using $\delta^{15}N$ of the source amino acid based trophic level removing variations of nitrogen trophic baseline, which is able to provide more accurate trophic information (Won et al., 2018). Juvenile bivalves have a small inhalant siphon that restricts their ability to consume fine particles, whereas adult individuals have larger siphons and can feed on a wider range of prey (Aya and Kudo, 2017). Our data supported this assumption, in that large-sized groups had a wider range of dietary contributions (for *M. veneriformis* and *C. sinensis*) compared to small-sized groups of *M. veneriformis* (Fig. 3.5B).

In contrast to the linear relationship for $\delta^{15}N$ enrichment, the relationship between the $\delta^{13}C$ values of soft tissues and the shell length of *M. veneriformis* showed an exponential increase that peaked at 1.5 years old (Fig. 3.7). Ryou and Chung (1995) reported that, after recruitment in June to July, spats (mean size: 250–350 μm) of *M. veneriformis* could reach to ~2.4 cm shell length after 160 d; however, there was no growth during winter (December to March). Therefore, the relatively depleted-$\delta^{13}C$ values of the <1 yr group (mean 2.1 cm shell length) of *M. veneriformis* reflected rapid growth from summer to winter and the dietary contributions of the items that they fed on at that time. This phenomenon was followed by the subsequent enrichment of $\delta^{13}C$ values during the growing season. This finding clearly showed an age-related dietary shift from seawater POM to MPB, further supporting previous studies in that the seasonality of MPB determines the growth and reproduction of intertidal invertebrates (Fry & Sherr, 1984; Herman et al., 2000; Page & Lasta 2003; Kang et al., 2006; Grippo et al., 2011; Kang et al., 2015; Christianen et al., 2017).

The present study investigated the structure of benthic food web in the Geum River estuary and identified the main food sources for two dominant bivalves of *M. veneriformis* and *C. sinensis*, which are major fishery resources in the local area. In general, our results confirmed that prolonged geographical isolation of the Geum River estuary by a sea dike might have hindered natural distributions of dietary

organic matters to intertidal marine organisms inhabiting outer open coastal tidal flats. The results showed that MPB was found to be the most important food source for primary consumers, with the riverine input of organic sources to the seawater ecosystem being interrupted by the dike. Thus, the irregular (or lagged) terrestrial input of riverine POM was found to be lesser associated with trophic status of benthic consumers on tidal flats. Further our results provided isotopic evidence for the organ-specific allocation of nutrients, as well as growth-related dietary shifts by bivalves. Overall, the stable isotopic analysis was powerful to address natural and/or anthropogenic influences of altered environmental condition towards understanding trophic structure and pathways.

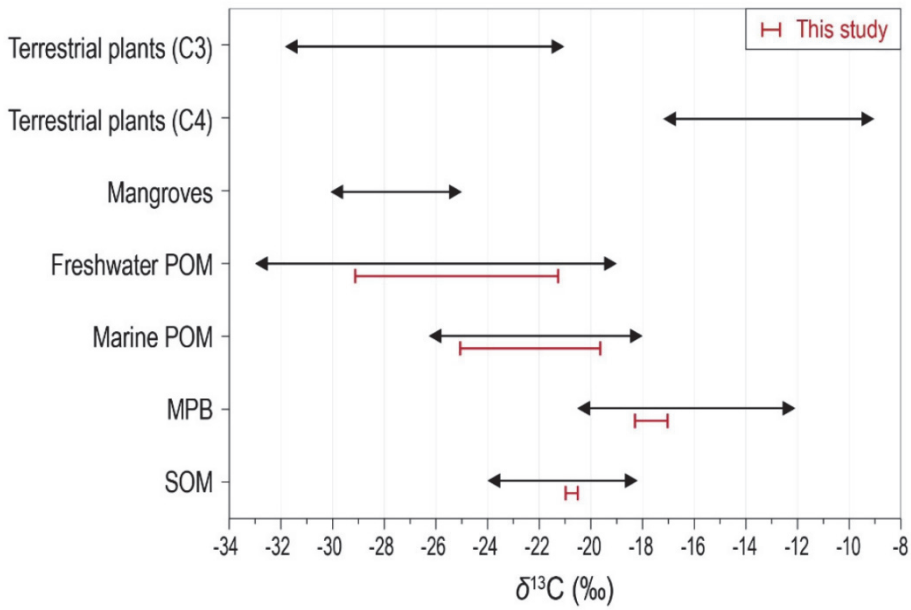

Fig. 3.8. Range of stable carbon isotopic compositions ($\delta^{13}C$) for organic inputs to coastal environments; terrestrial plants, mangroves, particulate organic matter (POM), microphytobenthos (MPB), and sediment organic matter (SOM) (data compiled from this study; Page 1997; Kang et al. 2003; Lamb et al. 2006; Finlay & Kendall 2007; Kristensen et al. 2017; and references therein).

CHAPTER 4.

Influence of the artificial reef installation on fish assemblages

This chapter has been published in Marine Pollution Bulletin.
Noh, J., Ryu, J., Lee, D., Khim, J.S., 2017. Distribution characteristics of the fish assemblages to varying environmental conditions in artificial reefs of the Jeju Island, Korea. Mar. Pollut. Bull. 118, 388–396.

4.1. Introduction

Globally, coastal ecosystems are being destroyed by various natural and anthropogenic threats, including habitat destruction, climate change, over exploitation, pollution, waterfront development, erosion, natural disaster, eutrophication, invasive species, tourism, and marine litter. In turn, these issues are causing the loss of economically important fisheries resources (Lundin and Linden, 1993; Jackson et al., 2001; Goudie, 2006; Worm et al., 2006; Lebata-Ramos and Doyola-Solis, 2016). As part of efforts to restore fishery resources and recover damaged coastal ecosystems, artificial reefs are often deployed on the sea floor to provide new habitats for marine organisms (Collins et al., 1990; Jensen et al., 1994; Steimle et al., 2002; Fang et al., 2013; Leitão, 2013; Lowry et al., 2014). Since 1972, artificial reefs have been gradually deployed along the coastal area of Korea, with the areas covered by such reefs expanding in the 1990s (Fig. 4.1). In 2004, an annual monitoring program was officially launched to manage these reefs effectively by the Korean government.

The positive effects of artificial reefs on the fish community are well documented in coastal areas (Bohnsack and Sutherland, 1985; Bombace et al., 1994; dosSantos et al., 2010). A number of studies have conducted post-deployment observations of the marine ecosystem surrounding artificial reefs. However, the effects of artificial reefs, considering also negative influences, on specific fish assemblages have been rarely studied. Furthermore, science-based policy studies on the management of such reefs are also limited (Pratt, 1994; Jensen, 2002; Claudet et al., 2004). Artificial reefs do not warrant the direct enhancement of fish community at all times, and thus it is necessary to delve into finding the specific responses of fish species to artificial reefs deployment. Most studies assessing how the fish community interacts with the material that forms artificial reefs a wide spectrum of species in various scales (Sherman et al., 2002; Jordan et al., 2005; Hackradt et al., 2011). Nevertheless, studies at the regional scale remain limited due to a lack of long-term monitoring data.

Many statistical techniques have been proposed and applied to interpret the relationship between environments and organisms. For example, non-metric

multidimensional scaling (NMDS) produces ordinations of objects from any matrix, and it is a frequently used approach to understand how marine organisms are associated with environmental conditions (Mueter and Norcross, 2002; Nobriga et al., 2005; Habit et al., 2007; Bennett and Kozak, 2015). Another technique is indicator value (IndVal) analysis, which was proposed by Dufrêne and Legendre (1997), and is considered to be a simple and intuitive method for assessing indicator species within a certain group (Table 4.1). Several studies have successfully applied IndVal analysis to select representative fish species in marine environments (Penczak, 2009; Lasne et al., 2007; Sirot et al., 2015).

In the present study, we collected meta-data on environmental parameters and the fish community at control sites and artificial reefs along the coastal area of the Jeju Island, Korea. We then used both statistical techniques (NMDS and IndVal analyses) to characterize the relationship between artificial reef environments and fish community responses. We also used these methods to identify indicator fish species of specific habitat conditions at the regional scale. In brief, we 1) compared fish species and individuals between control sites and artificial reefs with different spatial environmental conditions to characterize the environmental conditions that contribute to establishing the fish community in artificial reefs, 2) identified relevant indicator species for the specific environmental conditions of artificial reefs, 3) assessed potential negative impacts following installation of artificial reefs, and 4) suggested how to improve ecosystem based management with respect to artificial reef fisheries.

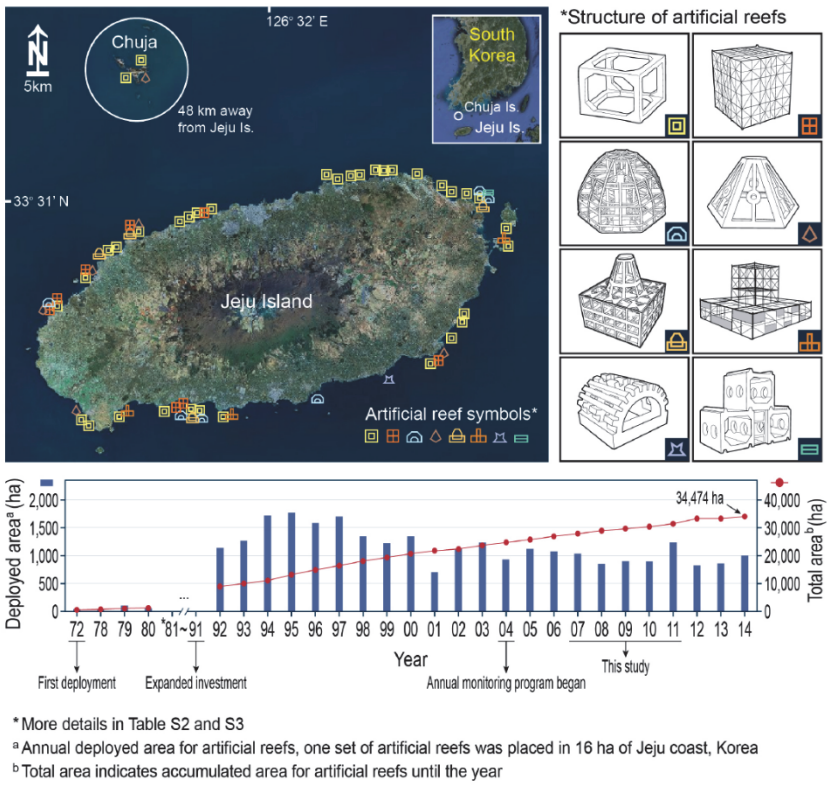

Fig. 4.1. Map of the study area around Jeju Island, Korea showing the sampling sites, artificial reef structure, and a brief history and of artificial reef deployment, since 1972. The meta-data analyzed in this study were collected from 5 years of monitoring surveys extending from 2007 to 2011.

Table 4.1. Definition or description of selected terms and abbreviation used in this study.

Terms or abbreviation	Definition or description	Reference
Representative species	Species reflecting habitat preference in the targeted environmental conditions	In this study
Indicator species (and species assemblages)	Representative species and/or species assemblages calculated by IndVal analysis	Dufréne and Legendre, 1997
IndVal (indicator value) analysis	To find indicator species and species assemblages characterizing groups of sites according to combine a species relative abundance with its relative frequency of occurrence in the various groups of sites	Dufréne and Legendre, 1997
Trophic group	Species assemblages in the similar feeding types	Micheli and Halpern, 2005; Halpern and Floeter, 2008; Hackrdt and Félix-Hackradt, 2009
MCAR	Macrocarnivores	
BINV	Benthic invertivores and/or cleaners	
SAND	Invertivores mainly feeding on sandy seafloor	
PLAN	Planktivores	
OMNI	General omnivores	
PISC	Piscivores	

4.2. Materials and Methods

4.2.1. Study area

Jeju Island is located about 100 km off the southwest of the Korean peninsula (126° 08′ ~ 58′ E; 33° 06′~ 34° 00′ N), while Chuja Island is located about 48 km north of Jeju Island (126° 19′ E; 33° 56′ N) (Fig. 1). A total of 231,000 modules of artificial reefs, mostly made of concrete and steel, have been deployed along 34,474 ha coastal area around the Jeju and Chuja islands from 1972 to 2014 (FIRA, 2014). These reefs were deployed at seafloor depth ranges of 10 to 50 m at Jeju Island and 5 to 48 m at Chuja Island (averaging 25 m). Several reef blocks were deployed at once to form a community set. Various shapes of blocks were used, such as quadrilateral, box, cylinder, cone, and pyramid types. The number of quadrilateral and box types were predominant. This study used a set of environmental and fish sampling data collected from annual surveys (2007-2011) around the Jeju Island, which formed part of the artificial reef management program (Fig. 4.1).

4.2.2. Data collection and sampling methodology

Since the mid-2000s, annual monitoring surveys have been conducted in the artificial reefs along the coasts of Jeju and Chuja islands by the Korea Fisheries Resources Agency. Collectively, a total of 110 artificial reefs and 81 control sites were analyzed between 2007 and 2011 (5 annual reports) in this study; 16 reefs in March of 2007, 11 reefs from March to August of 2008, eight reefs in October of 2009, 13 reefs from May to September of 2010, and 14 artificial reefs from July to October of 2011 (refer to Supplementary Information in Noh et al., 2017). The control sites were located adjacent to artificial reefs with comparable conditions except for the absence of reefs. The locations of the artificial reefs and control sites were recorded using a global positioning system with a WGS84 of coordinate system.

Dissolved oxygen, pH, salinity, and water temperature, were measured in situ using a YSI 650 multi-Parameter Display System (YSI Inc., Yellow Springs, OH, USA) at each site. Fish sampling was conducted using four trammel nets that were 25 min length and 3 m in high from 2007 to 2010, and three gill nets that were 50 m in length and 3 m in height during 2011. The nets were set once at each site for 12 h after sunset. Fifty fish traps were also used in 2011. These traps were placed at 2 m intervals in each site. Sampled fishes were identified and counted to the species level. The fishes were then, classified and counted into designated trophic groups.

4.2.3. Data analysis

Environmental variables included seafloor depth, pH, dissolved oxygen, salinity, water temperature, artificial reef material, and habitat type on which artificial reefs were deployed. Three environmental variables (water temperature, artificial reef materials, and bottom habitat) were compared to the fish community (species, individuals, and dominant species) and ecological indices at the control sites (n = 81) and artificial reefs (n = 110). Control sites and artificial reefs were sub-classified with seven independent environmental sub-groups; specifically: two water temperature groups (low temperature from March to May and high temperature from July to October), two artificial reef material groups (steel and concrete artificial reefs), and three bottom habitat groups (sandy, sand-rocky, and rocky seafloor).

The fish species and individuals present in artificial reefs were classified in relation to the various combinations of water temperature, artificial reef material and bottom habitat, producing 11 combinations. Three ecological indices of the fish community were calculated, including Shannon-Weaver diversity (H′, Shannon and Weaver, 1949), Pielou's evenness (J, Pielou, 1966), and Margalef's richness (R, Margalef, 1958). These indices were separated into the seven environmental sub-groups. The fish community data were used to designate trophic groups, with diet being taken into consideration (Micheli and Halpern, 2005; Halpern and Floeter, 2008; Hackrdt and Félix-Hackradt, 2009). Each species was assigned to one of six designated trophic groups; namely 1) macrocanivores (MCAR), 2) benthic invertivores/cleaners (BINV), 3) sand invertivores (SAND), 4) planktivores (PLAN), 5) general omnivores (OMNI), and 6) piscivores (PISC) (Table 4.1). However, the PISC group was excluded from fish community analysis because of lack of their occurrence.

NMDS was used to explore the similarities in trophic group composition between the control sites and artificial reefs. The similarity matrix for NMDS was calculated using the Bray-Curtis coefficient, based on fourth-root transformed abundance data (Field et al., 1982) using PRIMER software (Clarke and Gorley, 2006). To find indicator species of different habitats under the specific environmental conditions of the artificial reefs, indicator value (IndVal) analysis (Dufrêne and

Legendre, 1997) was conducted. The IndVal index was calculated as (Eq. 8):

$$IndVal_{ij} = A_{ij} \times B_{ij} \times 100 \quad (8)$$

where, A_{ij} was specificity (i.e., the proportion of individuals of species i that were in class j), and B_{ij} was fidelity (i.e. the proportion of sites in class j that contained species i). The ecological indices and IndVal index were calculated using free-downloaded software RStudio version 0.96.316 (www.rstudio.com).

4.3. Results

4.3.1. Control sites vs. artificial reefs in the fish community

The fish community was categorized in relation to three major environmental conditions for control sites and artificial reefs. Interestingly, more fish species were consistently found at artificial reefs compared to control sites for all three cases, including seven sub-groups (Table 4.2). In addition, more individuals were detected in artificial reefs compared to control sites, with twice as many more individuals being detected in the rocky bottom habitat. There were no significant differences in overall environmental characteristics between control sites and artificial reefs across the seven sub-groups, except for water temperature. Small variation was detected in the number of species among sub-groups, artificial reef materials (steel vs. concrete), and bottom habitats (sandy vs. sand-rocky vs. rocky). In contrast, major significant differences were detected for the mean number of species between low and high temperature sub-groups.

A total of 136 fish species and 2,985 individuals were recorded at control sites (90 species, 1011 individuals) and artificial reefs (122 species, 1974 individuals) combined. Out of these, 18 dominant species (>2% occurrence) were listed (Table 4.2). Four fish species represented >10% of total individuals in the community; namely, *Scyliorhinus torazame* (Cloudy catshark), *Stephanolepis cirrhifer* (Threadsail filefish), *Sebastiscus marmoratus* (False kelpfish), and *Pseudolabrus sieboldi* (Bambooleaf wrasse). It was difficult to identify certain dominant species under certain habitat conditions. However, dominant species were detected with respect to trophic characteristics. For example, macrocarnivores and benthic invertivores/cleaners primarily assembled in artificial reefs compared to control sites. Sand invertivores were more frequently observed in sandy bottoms compared to rocky bottoms (Fig. 4.2).

The occurrence frequency of species across the artificial reefs showed that, six dominant species were detected at all sites around Jeju Island; namely, *S. marmoratus*, *S. cirrhifer*, *Chaetodontoplus septentrionalis* (Blueline angelfish), *Choerodon azurio* (Scarbreast tuskfish), *Zeus faber* (John Dory), and *Microcanthus*

strigatus (Stripey fish). The most common species were S. marmoratus and *S. cirrhifer*, accounting for>50% (sum of both species) individuals of all dominant fishes (Fig. 4.3). These dominant species occurred more frequently in artificial reefs compared to control sites, except for steel reefs (Fig. 4.3B). NMDS showed that the trophic group composition of the fish community was clearly segregated with respect to variation in water temperature. The trophic groups in the artificial reefs were separated into two clear groups (bottom insets of Fig. 4.4A) in comparison to a mixed pattern at control sites. Yet, there were no significant differences between control sites and artificial reefs for any of the other environmental conditions (viz., reef material and bottom habitats) (Fig. 4).

Table 4.2. Overview of the environmental conditions and fish community at the control sites and artificial reefs of the Jeju Island; all values for, water temperature, artificial reefmaterial, and bottom habitat, given as mean within the corresponding classes.

	Water temperature				Artificial reef material				Bottom habitat					
	Low		High		Steel		Concrete		Sandy		Sand rocky		Rocky	
	Cont.[a]	AR[b]	Cont.	AR	Cont.	AR	Cont.	AR	Cont.	AR	Cont.	AR	Cont.	AR
Number of sites	33	40	48	70	29	38	52	72	36	48	39	50	6	12
Environmental conditions (Mean ± SD)														
Water temperature (°C)	15±1.5	16±1.6	22±1.9	22±2.0	21±2.4	21±2.5	19±4.2	19±3.9	19±4.2	19±3.8	19±3.6	20±3.5	22±2.3	21±2.7
Dissolved oxygen (mg/L)	8.6±0.6	8.7±0.5	8.0±0.6	8.1±0.6	8.1±0.5	8.1±0.5	8.4±0.7	8.3±0.7	8.4±0.8	8.3±0.9	8.2±0.5	8.1±0.5	8.3±0.3	8.4±0.2
pH	8.3±0.2	8.3±0.2	8.0±0.5	8.0±0.5	8.0±0.5	8.0±0.5	8.1±0.3	8.1±0.4	8.1±0.4	8.2±0.3	8.1±0.4	8.1±0.5	7.9±0.5	8.1±0.5
Salinity (psu)	35±0.6	35±0.5	34±1.2	34±1.1	34±0.7	34±0.7	34±1.2	34±1.1	34±1.1	34±1.0	34±1.1	34±1.0	35±0.5	35±0.6
Depth (m)	28±7.3	29±7.1	30±6.5	31±6.6	34±4.6	34±4.1	26±6.5	28±6.9	29±5.8	30±6.2	29±7.7	30±7.5	28±7.2	30±5.7
Fish community														
Total mean species (sp./site)	3.9	5.6	7.0	8.7	6.8	7.5	5.1	7.6	5.9	8.1	5.7	7.3	4.5	6.6
Total mean individuals (indiv./site)	7.6	10	16	22	13	16	12	19	14	20	12	17	7.5	14
Dominant fish species* (%)														
(B) *Scyliorhinus torazame*	**17**	7.5	7.1	1.2	3.1	0.8	**14**	3.2	7.9	0.9	**12**	4.8	-	-
(O) *Stephanolepis cirrhifer*	**16**	**17**	7.4	7.6	**10**	8.9	9.2	9.9	**14**	9.9	5.6	9.3	6.7	9.8
(M) *Sebastiscus marmoratus*	5.2	6.8	10	**16**	**12**	**16**	7.1	**13**	4.2	**14**	**12**	**12**	**36**	**21**
(S) *Okamejei acutispina*	4.4	3.9	4.2	3.2	4.4	4.4	4.2	2.8	6.9	5.8	1.9	1.1	-	-
(S) *Paraplagusia japonica*	3.2	0.2	2.2	0.8	-	0.2	4.0	0.9	3.8	0.4	1.3	1.2	-	-
(O) *Chaetodontoplus septentrionalis*	2.8	3.9	4.2	3.5	5.4	4.7	2.9	3.1	2.8	2.3	4.9	5.0	4.4	4.3
(M) *Pagrus major*	2.4	1.0	3.4	3.7	2.3	2.2	3.7	3.5	4.0	5.7	2.6	0.7	-	-
(M) *Scorpaenodes littoralis*	2.0	3.4	1.7	1.8	0.5	1.3	2.6	2.5	1.2	2.0	2.6	2.1	-	3.0
(M) *Zeus faber*	1.6	3.2	2.1	1.7	3.6	2.9	1.0	1.7	2.6	1.9	1.3	2.4	2.2	1.2

Table 4.2. Continued.

	Water temperature				Artificial reef material				Bottom habitat					
	Low		High		Steel		Concrete		Sandy		Sand rocky		Rocky	
	Cont.[a]	AR[b]	Cont.	AR	Cont.	AR	Cont.	AR	Cont.	AR	Cont.	AR	Cont.	AR
(O) *Thamnaconus modestus*	1.2	5.6	1.1	1.7	2.3	2.9	0.3	2.4	1.0	1.8	1.3	3.1	-	4.3
(B) *Microcanthus strigatus*	1.2	1.7	1.4	2.3	2.1	2.9	1.0	1.8	0.2	0.8	2.4	3.8	4.4	1.2
(S) *Urolophus aurantiacus*	1.2	-	2.8	0.7	-	1.2	3.9	0.3	3.8	0.4	1.1	0.8	-	-
(P) *Engraulis japonicus*	0.4	10	0.7	0.3	-	-	1.0	3.3	0.6	4.6	0.6	0.1	-	-
(M) *Parapristipoma trilineatum*	0.4	1.7	2.9	3.6	1.8	1.3	2.6	4.0	-	1.1	4.7	5.4	2.2	4.3
(B) *Choerodon azurio*	0.4	1.5	5.7	4.1	5.7	3.9	3.5	3.4	4.0	4.1	4.7	3.3	4.4	1.2
(M) *Sebastes thompsoni*	-	1.7	-	3.1	-	0.2	-	3.9	-	3.6	-	2.4	-	-
(B) *Pseudolabrus sieboldi*	-	-	7.4	**11**	**11**	**14**	2.4	6.2	6.0	5.9	4.1	8.5	**16**	**24**
(M) *Conger myriaster*	-	-	2.2	4.6	1.8	2.7	1.6	4.0	1.2	5.7	2.4	1.8	-	0.6

[a]Control sites, [b]Artificial reefs

*Species in bold indicate >10% individuals in each corresponding class. Acronyms: (M) macrocarnivores, (B) benthic invertivores/cleaners, (S) sand invertivores, (O) general omnivores, and (P) planktivores.

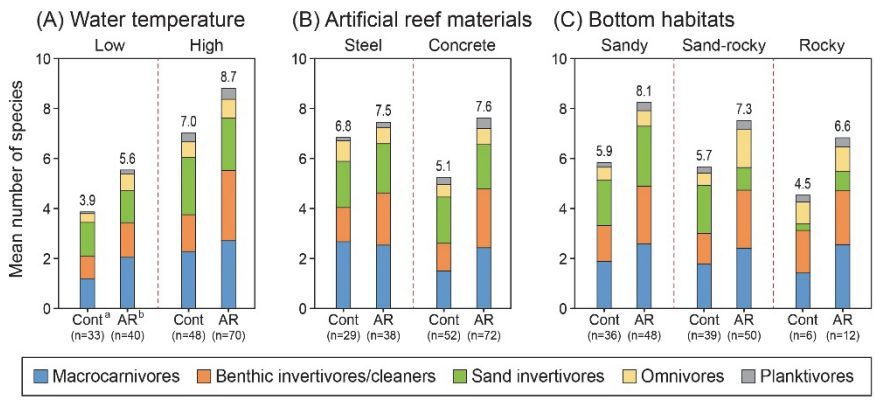

[a] Control site, was determined 1-2 km away from AR (there was no existence of natural reef and/or AR)
[b] Artificial reef

Fig. 4.2. Number of fish species found at control sites (n = 81) and artificial reefs (n = 110), on average, with respect to three major environmental condition groups (A) water temperature, (B) artificial reef material, and (C) bottom habitat. The water temperature was sub-classified according to two seasons: low temperature from March to May and high temperature from July to October. The artificial reef material was sub-classified into two materials: concrete and steel. The bottom habitats ware sub-classified into three sediment types: sandy, sand-rocky, and rocky. Fish communities were classified into five trophic groups reflecting feeding and settlement behaviors (macrocarnivores, benthic invertivores/cleaners, sand invertivores, omnivores, and planktivores).

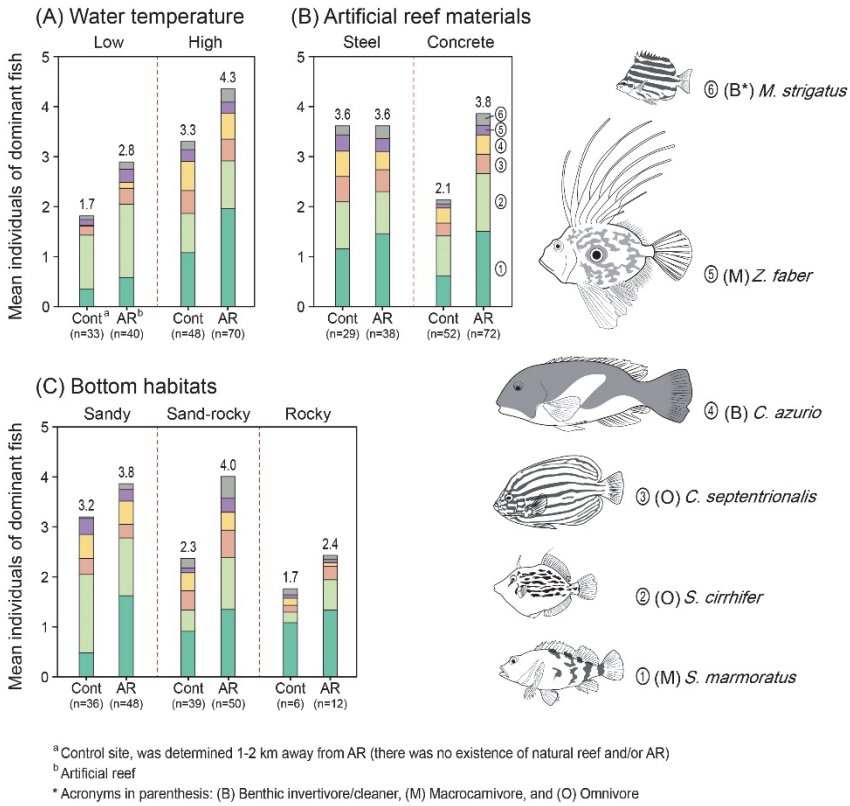

Fig. 4.3. Number of individuals of dominant fish that were recorded at all sites, on average, control sites (n = 81) and artificial reefs (n = 110) in relation to the three major environmental condition groups (A) water temperature, (B) artificial reef materials, and (C) bottom habitats. Six dominant fishes were detected at all sites. The water temperature was sub-classified according to two seasons: low temperature from March to May and high temperature from July to October. The artificial reef material was sub-classified into two materials: concrete and steel. The bottom habitat was sub-classified into three sediment types: sandy, sand-rocky, and rocky.

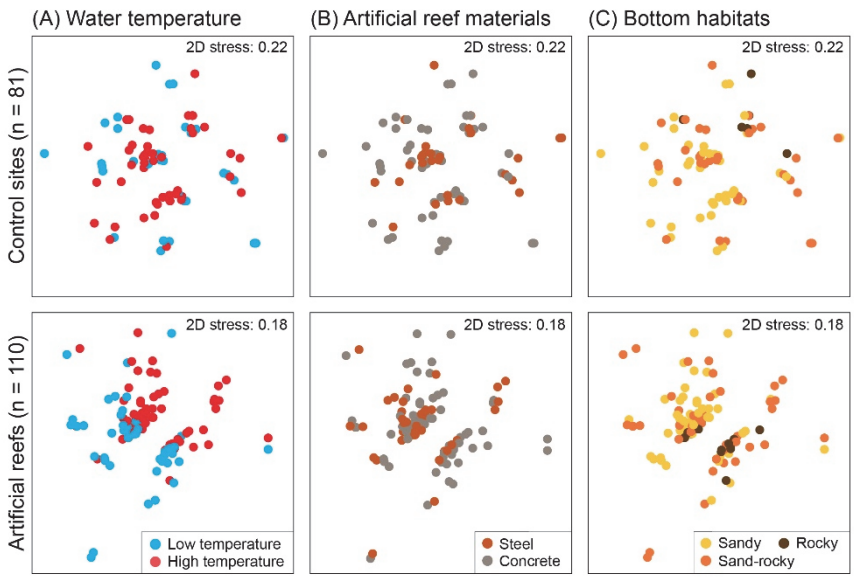

Fig. 4.4. Non-metric multidimensional scaling (NMDS) ordination with respect to the trophic group composition of fishes at the control sites and artificial reefs. The colored dots in plots represent the three major environmental condition groups: (A) water temperature, (B) artificial reef material, and (C) bottom habitat on which artificial reefs were deployed. The water temperature was sub-classified according to two seasons: low temperature from March to May and high temperature from July to October. The artificial reef material was subclassified into two materials: concrete and steel. The bottom habitat was sub-classified into three sediment types: sandy, sand-rocky, and rocky.

4.3.2. Habitat preferences of the fish community

Artificial reefs were classified by environmental condition groups (viz., water temperature, artificial reef material, and bottom habitat), producing 11 sub-groups. These 11 groups were assessed with respect to the environmental parameters and fish community data (including the number of species, number of individuals, and composition of dominant species) (Table 4.3). To determine the habitat preference of the fish community in artificial reefs, the environmental condition groups were rearranged in relation to the mean number of individuals (Fig. 4.5). This grouping successfully separated the associated environmental conditions, with water temperature being the dominant condition, supporting NMDS result. The next separation was attributed to reef material, with the fish community preferring concrete over steel, in general. The final associated condition was bottom habitat type, with the number of individuals decreasing from sandy to rocky bottoms. Overall, when excluding the effect of seasonal temperature, concrete artificial reefs deployed on sandy or sand-rocky bottom were more attractive to fish, particularly macrocarnivores, around Jeju Island.

The IndVal analysis identified a total of eight indicator species ($p < 0.1$) that corresponded to the specific environmental condition groups in artificial reefs (Table 4.4). Indicator species representing specific environments with low water temperature were *Dasyatis akajei* (Red stingray) for steel reefs on sandy bottoms, *Sebastes schlegelii* (Korean rockfish) for concrete reefs on sandy bottoms, and *Parupeneus spilurus* (Blackspot goatfish) for concrete reefs on rocky bottoms. At high water temperatures, *Okamejei acutispina* (Sharpspine skate) and *Narke japonica* (Japanese sleeper ray) represented steel reefs on sandy bottoms, *P. sieboldifor* for steel concrete on rocky bottoms, and *Pagrus major* (Red seabream) and *Conger myriaster* (Whitespotted conger) for concrete reefs on sandy bottoms.

Furthermore, the association between the environmental condition groups and the fish community was characterized by the degree of similarity in the composition of dominant species. NMDS ordination was used to calculate the geometric mean (set as max. of 1.0) of Bray-Curtis similarities for each environmental condition group, which produced two distinct patterns; namely, a congregated pattern (pattern 1: mean Bray-Curtis similarity ≥ 0.7) and a scattered pattern (pattern 2: mean Bray-Curtis similarity < 0.7). Six environmental condition groups belonging to the congregated group (pattern 1) were further grouped into three typical habitats; namely, 1) high-concrete-sandy, 2) steel-sandy, and 3) rocky bottom (Fig. 4.6). The Bray-Curtis similarity analysis indicated that the rocky bottom habitat was the most important environmental condition, with indicator species including *P. sieboldi* and *P. spilurus*, regardless of water temperature and reef material. Next, steel and sandy conditions also contained a typical fish community, with the composition not being primarily influenced by water temperature. However, the similarity of the fish community under concrete and sandy condition might have been influenced by water temperature to a certain degree. There were two species (*S. cirrhifer* and *S. marmoratus*) common to artificial reefs, regardless of environmental conditions; thus, these species could not be considered as indicator species, but were considered as typical artificial reef species.

Table 4.3. Fish community data showing the number of fish species and individuals occurring in the artificial reefs of the Jeju Island, in relation to the environmental conditions; the relative values also given within the dataset.

Environmental conditions			Number of sites	Number of species					Number of individuals					
Water temperature	Artificial reef material	Bottom habitat		Mean (sp./site)	Relative abundance* (%)					Mean (ind./site)	Relative abundance (%)				
					M	B	S	O	P		M	B	S	O	P
Low	Steel	Sandy	3	4.7	57	14	14	14	-	9.0	33	7.4	26	33	-
Low	Steel	Sand-rocky	5	3.2	19	50	13	19	-	6.2	19	26	9.7	45	-
Low	Concrete	Sandy	15	2.6	39	18	23	15	5.1	12	29	7.2	16	25	23
Low	Concrete	Sand-rocky	14	2.6	36	25	19	17	2.8	10	30	32	7.5	30	0.7
Low	Concrete	Rocky	3	5.0	40	33	6.7	20	-	9.0	44	26	3.7	26	-
High	Steel	Sandy	11	3.8	31	21	31	12	4.8	22	38	21	25	15	0.8
High	Steel	Sand-rocky	15	3.6	37	26	24	11	1.9	15	31	33	15	20	0.9
High	Steel	Rocky	4	3.0	33	33	8.3	25	-	16	33	47	1.6	19	-
High	Concrete	Sandy	19	3.5	35	32	21	9.1	3.0	27	53	20	11	15	1.0
High	Concrete	Sand-rocky	16	3.8	31	34	16	13	4.9	27	44	32	7.2	15	1.6
High	Concrete	Rocky	5	4.6	35	26	8.7	22	8.7	15	41	32	2.7	22	2.7

[a]Control sites, [b]Artificial reefs

*Species in bold indicate >10% individuals in each corresponding class. Acronyms: (M) macrocarnivores, (B) benthic invertivores/cleaners, (S) sand invertivores, (O) general omnivores, and (P) planktivores.

Table 4.4. IndVal analysis listing the indicator fish species under the specific environmental condition sub-groups within the three major environmental groups for artificial reefs of the Jeju Island (viz., water temperature, artificial reef material, and bottom habitat).

Water temperature	Low					High					
Artificial reef materials	Steel		Concrete			Steel			Concrete		
Bottom habitats	Sandy	Sand-rocky	Sandy	Sand-rocky	Rocky	Sandy	Sand-rocky	Rocky	Sandy	Sand-rocky	Rocky
Number of sites	3	5	15	14	3	11	15	4	19	16	5
Indicator species[a]											
(S) *Dasyatis akajei*	**0.26****	-	-	0.02	-	0.11	-	-	-	-	-
(M) *Sebastes schlegelii*	-	-	**0.27****	0.01	-	-	-	-	0.05	-	-
(B) *Parupeneus spilurus*	-	0.02	-	-	**0.31****	-	-	-	-	-	0.06
(S) *Okamejei acutispina*	0.06	-	0.07	-	-	**0.28****	0.02	-	0.13	0.01	-
(S) *Narke japonica*	-	-	0.01	-	-	**0.20***	0.01	-	-	-	-
(B) *Pseudolabrus sieboldi*	-	-	-	-	-	0.05	0.05	**0.35****	0.03	0.06	0.06
(M) *Pagrus major*	0.03	-	0.01	-	-	0.12	-	-	**0.43****	0.02	-
(M) *Conger myriaster*	-	-	-	-	-	0.05	0.02	0.01	**0.25***	0.03	-

*p <0.1, **p <0.05

[a]Species in bold indicate the greatest value among the artificial reef groups. Only species that were present in at least >5 sites were used for IndVal analysis. Acronyms: (M) macrocarnivore, (B) benthic invertivore/cleaner, and (S) sand invertivore.

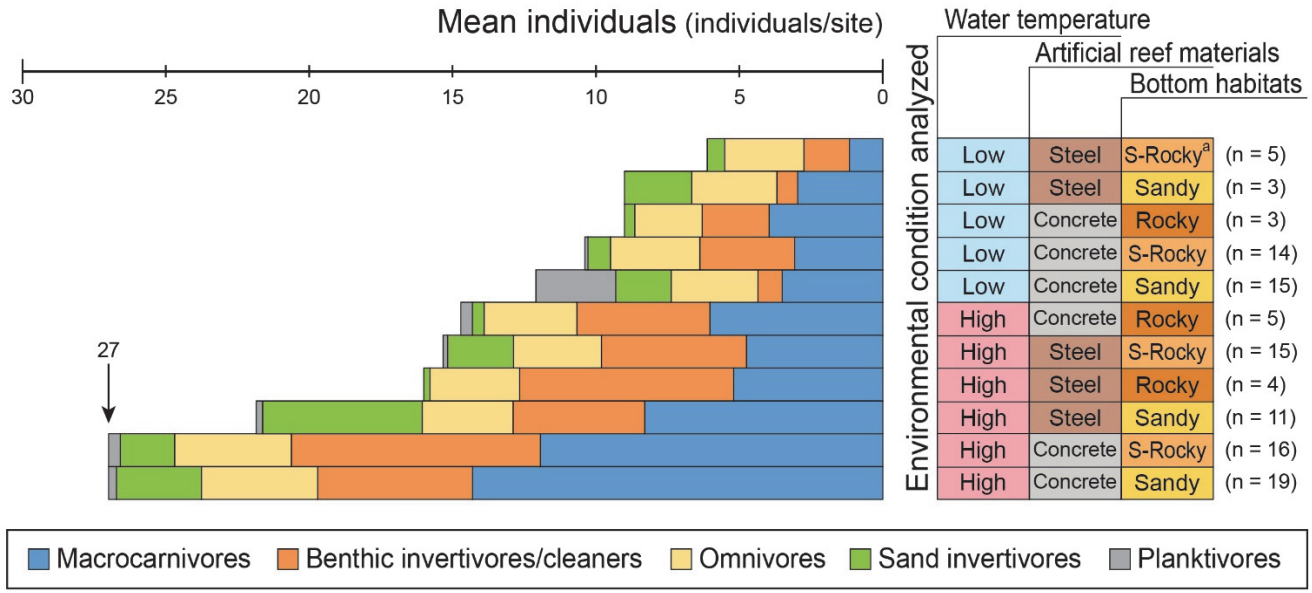

Fig. 4.5. Number of fish individuals, on average, showing the proportion of the five trophic groups in association with the environmental condition groups in the artificial reefs (n = 110). Fish communities were classified into five trophic groups reflecting feeding and settlement behaviors (macrocarnivores, benthic invertivores/cleaners, omnivores, sand invertivores, and planktivores).

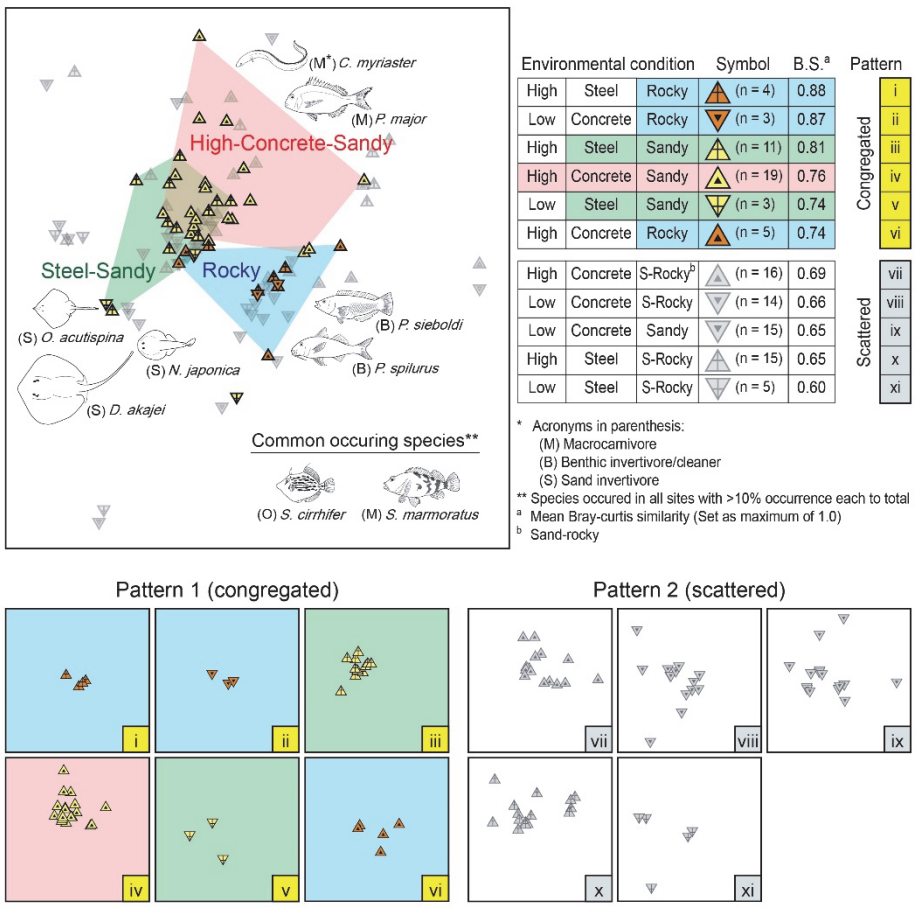

Fig. 4.6. Illustration of the fish community in the artificial reefs of Jeju Island based on non-metric multidimensional scaling (NMDS) and Bray-Curtis similarity (given as geometric mean) of the environmental condition groups. Indicator fish species were selected for each specific habitat from IndVal analysis and were overlapped on the NMDS plot. The commonly occurring species were the most prevalent, accounting for >50% individuals of dominant fishes at all control sites and artificial reefs. The environmental condition groups were classified according to two distributional patterns in the mean Bray-Curtis similarities (B.S.): congregated (pattern 1, B.S. > 0.7) and scattered (pattern 2, B.S. ≤ 0.7).

4.3.3. Potential impacts driven by artificial reef installation

ARs are usually deployed on bottom habitat where natural reefs are limited, and expected to enhance secondary production (Bohnsack and Sutherland, 1985; Derbyshire, 2006). Out of the various combinations of ARs conditions, the concrete reefs deployed on sandy bottom were found to be more efficient at attracting fish compared to steel or rocky bottom reefs (Fig. 4.5). This difference might be due to the structural similarity between concrete reefs and natural reefs. Previous studies showed that sessile organisms colonized concrete reefs in a similar way to natural reefs (Fitzhardinge and Bailey-Brock, 1989). However, introducing artificial elements on the seafloor, it has to be careful because of adverse environmental effects such as secondary pollution and possible invasion of neobiota (London Convention and Protocol/ UNEP, 2009).

Although positive effects on the installation of artificial reefs as recruitment of fish assemblages, potential negative effects were observed in the results of this study (Fig. 4.7). For example, the shifting of fish community on dominant groups was the most remarkable impact because of the introduction of artificial reefs. In particular, fish assemblages in natural habitat with sandy and/or sand-rock bottom showed that consist of predominant groups of rays (*O. acutispina*, *N. japonica*, *D. akajei*) and subdominant groups of snapper (*P. major*), eel (*C. myriaster*). However, after the installation of concrete reefs, the assemblages were changed into the snapper-dominant structure (Fig. 4.2 & Table 4.2). Moreover, some cases showed that relatively low effectiveness of artificial reef installation in the recruitment of fish assemblages. In general, steel reefs were relatively low-effective attraction to not only rocky-bottom-preferred fishes such as *P. sieboldi* and *P. spilurus*, but also rays. Such a trend observed in the case of concrete reefs installed on the rocky bottom. Thus, the installation of artificial reefs on rocky bottom habitat is seemed to be inefficient.

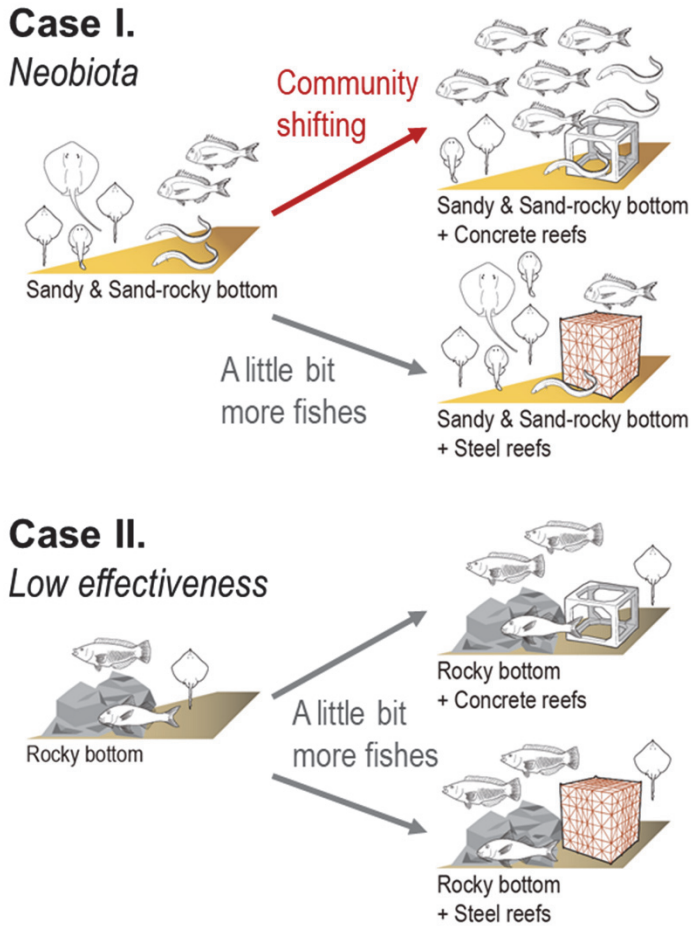

Fig. 4.7. Schematic illustration showing potential impacts of artificial reef installation observed in this study.

4.4. Discussion

The ecological effect of artificial reefs has been previously evaluated by comparing the species occurrence and abundance between artificial reefs and adjacent control sites (Bohnsack & Sutherland, 1985; Bombace et al., 1994; dos Santos et al., 2010; Lowry et al., 2014). This study is the first to provide scientific evidence supporting the effectiveness of the Jeju artificial reefs, following their construction and management since the mid-2000s. Our analyses showed that water temperature condition is a key factor controlling fish assemblages in artificial reefs (Fig. 4.2 & Fig. 4.3). Indeed, water temperature would be the key factor allowing artificial reefs to provide seasonal benefits to the fish community in terms of shelter, food resources, spawning habitat, and facilitating recruitment (Kojima, 1956; Yoshimuda & Fujii, 1982; Bohnsack & Sutherland, 1985; Johnson et al., 1994). Other environmental conditions (such as avoidance space, structural complexity, and surface traits etc.) are also important factors for creating sustainable fish communities in artificial reefs (Anderson et al., 1989; Charbonnel et al., 2002; Sherman et al., 2002; Jordan et al., 2005). The biological coverage of sessile organisms or invertebrates on the surface of artificial reefs might also provide potential food resources for fish assemblages (Relini et al., 1994; Perkol-Finkel & Benayahu, 2005).

Previous studies on the fish community in artificial reefs were primarily limited to reporting species occurrence and taxonomic composition (Rooker et al., 1997; Rilov & Benayahu, 1998; Gratwicke & Speight, 2005; Brotto et al., 2006). These limitations were due to the complexity of the fish community and a paucity of data linking habitat preference to controlling environmental factor(s). In the present study, we analyzed both the occurrence and abundance of fish community data, as well as trophic characteristics, to include feeding and settlement behaviors (Table 4.2 and Table 4.3). The analysis of multiple indices of the fish community using the combined analyses of NMDS and IndVal allowed us to find spatial variations

between control sites and artificial reefs (Table 4.3, Fig. 4.4, & Fig. 4.5). The very strategy also aided to determine the habitat preferences of specific fish and trophic groups (Fig. 4.6).

Artificial reefs are usually deployed on bottom habitat where natural reefs are limited, and expected to enhance secondary production (Bohnsack et al., 1985; Derbyshire, 2006). Out of the various combinations of artificial reefs conditions, the concrete reefs deployed on sandy bottom were found to be more efficient at attracting fish compared to steel or rocky bottom reefs (Table 4.2 and Fig. 4.5). This difference might be due to the structural similarity between concrete reefs and natural reefs. Previous studies showed that sessile organisms colonized concrete reefs in a similar way to natural reefs (Fitzhardinge & Bailey-Brock, 1989).

Trophic group analysis provided a concise understanding of the huge number of fish species occupying the artificial reefs of the Jeju Island. This analysis showed the habitat preference of artificial reef fishes. It also helped us to understand the feeding- and settlement-associated behaviors of certain fish species. For example, macrocarnivores and benthic invertivores/cleaners showed greater abundance and more stable populations in artificial reefs compared to control sites (Fig. 4.2). These groups appeared to aggregate successfully with existing scattered individuals, or promoted secondary biomass production, due to increased food sources. However, it should be noted that the proportion of trophic groups between control sites and artificial reefs did not greatly differ from each other, which indicated that artificial reefs well recovered the natural habitat conditions as a whole. Specific habitat preference of the trophic groups to environmental conditions surrounding artificial reefs would not be necessarily warranted in situ, thus providing of combined environmental conditions facilitating fish diversity and abundance would be recommended.

The integrated analysis of IndVal with NMDS ordination generated spatial occupation patterns of specific indicator species in the artificial reefs. Although, some species (such as *S. marmoratus* and *S. cirrhifer*) were widely distributed

species cross all control sites and artificial reefs (Fig. 4.3), some species represented characteristics of distinct indicator species, particularly with respect to the way in which they congregated. Interestingly, three representative environmental groups of artificial reefs (rocky bottoms, steel reefs on sandy bottoms, and concrete reefs on sandy bottoms with high temperature) provided similar habitat for specific trophic fish groups; namely, macrocarnivores, sand invertivores, and benthic invertivores/cleaners, respectively (Fig. 4.6). Two trophic groups had the potential to obtain food sources from sessile organisms and invertebrates on and around artificial reefs. Sand invertivores (such as *O. acutispina*, *N. japonica* and *D. akajei*) were indicator species for steel reefs on sandy bottoms. These species are relatively flat, like stingrays, and burrowing into the sandy bottom to escape from predators or to hunt prey. Thus, the softness of the bottom habitat (viz., sandy) attracts this community more than reef material.

For sustainable artificial reef management, the side effects of artificial reef facilities should also not be overlooked. The side effects of the artificial reefs in this study were the change of fish community structure and the low effectiveness (Fig. 4.7). In particular, artificial reefs in sandy habitats (if there are rich in stingray fish populations), need to take special care because the installation of artificial reef significantly could be altered the fish community composition. In addition, the facilities of artificial reefs in the rock area have been relatively ineffective on fishery enhancement because the artificial reefs are also hard structures like the natural rocky bottom. Therefore, for a more sustainable and efficient artificial reef management, it is important to consider the qualitative aspects of the ecosystem rather than just the logic of quantity.

Overall, the spatial variation in fish species found in artificial reefs strongly reflected their habitat preferences with respect to available prey sources and/or settlement suitability. This type of direct association between the fish community and artificial reefs conditions should be carefully considered when designing and managing the artificial reefs of the Jeju Island, and elsewhere, promoting science-

based policy implementation. Post-monitoring efforts on the management of artificial reefs should be conducted in a targeted manner, because fish species exhibit both general and specific habitat preferences, depending on the varying environmental conditions in given areas.

CHAPTER 5.

Influences of the OSA formation in marine environment: PAHs bioaccumulation and biodegradation

This chapter has been published in Environmental Science and Technology.
Noh, J., Kim, H., Lee, C., Yoon, S. J., Chu, S., Kwon, B.-O., Ryu, J., Kim, J.-J., Lee, H., Yim, U.-H., Giesy, J.P., 2018. Bioaccumulation of polycyclic aromatic hydrocarbons (PAHs) by the marine clam, *Mactra veneriformis*, chronically exposed to oil-suspended particulate matter aggregates. Environ. Sci. Technol. 52, 7910–7920.

5.1. Introduction

In December 2007, the Hebei Spirit Oil Spill (HSOS) that occurred 10 km off the coast of Taean in Korea, released approximately 10,800 tonnes of crude oil into the sea and eventually damaged entire marine ecosystems (KCG, 2008; Kim et al., 2010). Recovery of the marine environment from this oil spill took over five years to return to baseline conditions of water and sediment quality (Hong et al.,2014). To date, it is still debatable whether recovery of the benthic community in the area is complete.

PAHs are omnipresent contaminants in marine environments. In fact, pyrogenic PAHs are commonly found in marine organisms. Petrogenic PAHs, which originate from crude oil, contain a wide range of alkylated derivatives. Thus, it is not surprising that marine organisms exposed to oil spills contain significant concentrations of both PAHs and alkylated PAHs (Soriano et al., 2006; Uno et al., 2010; Sammarco et al., 2013). Lower molecular mass (LMM) PAHs, such as naphthalene and its alkylated groups dominate the PAHs of Iranian heavy crude (IHC) oil, followed by the another group of LMM PAHs including dibenzothiophene, phenanthrene, and fluorene, and then by relatively minor components representing higher molecular mass (HMM) PAHs, such as chrysene and other HMM PAHs (Hong et al., 2015). HMM PAHs are particularly hazardous because they have greater toxic potencies and are also carcinogenic to humans and wildlife and often degrade quite slowly.

PAHs are transformed primarily by microbes, which play an essential role in degrading spilled oils and/or residues. In fact, a number of bacterial taxa can decompose a wide variety of hydrocarbons and those taxa can reproduce rapidly in oiled environments (Röling et al., 2004; Hazen et al, 2010; Redmond & Valentine, 2012; Valentine et al., 2012; Hazen et al., 2016). Thus, microbial communities could be used to effectively and economically bioremediate environments contaminated by oil (Duran & Cravo-Laureau, 2016).

Suspended particulate matters (SPM) have been recognized as vectors for transport of oil from one environment to another and to affect accumulation by marine organisms. Oil and a variety of SPMs bind together in seawater, to form oil−SPM aggregate (OSA), which is known to affect dispersions of spilled oil and degradation of petroleum hydrocarbons (Muschenheim & Lee, 2002; Owens & Lee, 2003; Gong et al., 2014; Boglaienko & Tansel, 2016). In addition to being called OSAs, previous studies have referred to these aggregates of oil and SPM as oil−mineral aggregates, or oil−particle aggregates (Stoffyn-Egli & Lee, 2002; Ajijolaiya et al., 2006; Sun & Zheng, 2009; Sun et al, 2014; Gustitus & Clement, 2017). In areas where SPMs are prevalent, OSAs form naturally (Sun et al, 2014). Due to their lesser viscosities, OSAs are not as adhesive to seashore habitats as is crude oil. This is because oil droplets originating from spills usually become coated with fine, nonsticky organic particles as oil disperses. This type of aggregation enhances biodegradation because aggregates significantly increase oil−water contact areas, which maximizes accessibility of hydrocarbon-degrading bacteria and fungi to oil (Lee et al., 1996; Weise et al., 1999; Silva et al, 2015). Furthermore, by being nearly neutrally buoyant, OSAs can be easily dispersed away from the oil-contaminated sites by tides and/or currents (Rios et al., 2017). Although characteristics of OSAs formed under various environmental conditions have been well studied (Stoffyn-Egli & Lee, 2002; Sun et al., 2010; Khelifa, 2012; Loh et al, 2014), there have been few studies examining bioaccumulation and/or biodegradation of oil in the form of the OSAs, by microbial communities. In the present chapter, a laboratory mesocosm experiment was used to simulate a shallow, subtidal environment contaminated by chronic exposure to OSAs. Since this shellfish is commercially important worldwide and the very species prefer to inhabit in muddy tidal flat (Ryu et al., 2011) which has greater potential in OSAs formation compared to that in sandy areas, when exposed to the oil contaminated environment, the filter feeding bivalve, clam *Mactra veneriformis* was studied. Concentrations of PAHs in exposed animals, microbial communities, and other parameters were

monitored for 50 d because the spilled oil could last >30 days (KCG, 2008; Kim et al., 2010) and possibly OSAs could be formed and persist for longer periods of time. Specific objectives were to 1) evaluate bioaccumulation of PAHs into soft tissues of *M. veneriformis* chronically exposed to OSAs in the water column, 2) examine compound-specific patterns of bioaccumulation in clams targeting parent PAHs and alkylated PAHs, 3) identify specific constituents of microbial communities dominating an OSA-contaminated environment, and 4) assess how bioaccumulation of PAHs into clams influences microbial mediated biodegradation.

5.2. Materials and Methods

5.2.1. Experimental design

OSAs were prepared by previously described methods (Gustitus & Clement, 2017), with a slight modification (see details in Table 5.1). In brief, OSAs were prepared using 1 L (1000 g) of filtered seawater in a glass carboy, with 0.6 g of IHC oil, and 0.2 g of ground and sieved sediment (Φ < 20 μm). Sediments used were relatively enriched with greater organic matter (>6% loss on ignition). This enriched, dried sediment was mixed with seawater, and then IHC was added by use of precalibrated pipettes. A reciprocating shaker (set up at 170 rpm) in a temperature-controlled room (18 ± 0.5 °C) was used to simulate mixing of the crude oil, sediment, and seawater. After 24 h, the carboy was allowed to stabilize for about 5 min, and then 700 mL of a mixture of OSAs and seawater was extracted using a faucet located at the bottom. The mixture was used for feeding materials of 300 and 600 mL, respectively, in OSA_{low} and OSA_{high} treatments (Fig. 5.1).

Individuals of the test organism, *M. veneriformis* (mollusks) were collected in June of 2016, from an intertidal mudflat off the west coast of Korea (36.095°N, 126.613°E). After collection clams were immediately (within 4 h) transported to laboratory aquariums where they were acclimated to lab conditions for one month. For each OSA feeding experiment (described below), 40 clams (3.5 ± 0.5 mm shell length) were placed in experimental aquariums (40 × 40 × 30 cm), which were filled with sandy sediment (3 cm deep) and seawater (40 L). Clams were acclimated in aquariums for 2 days before the beginning of experiments. Seawater was filtered through 0.7 μm glass-fiber filters. Movement of water inside aquariums was maintained by use of a continuous-flow pipe attached to an air pump. During the experiment, salinity was maintained at 34 (±1.0) psu. To minimize the influence of organic carbon from exogenous sources, a sediment composed of cleaned and dried

sandy loam (<1 mm diameter; Samhangang INC., Incheon, KOR) was used; the details of sediment properties are given in Table 5.2 and Fig. 5.2. A water bath and cooler were used to maintain water temperature at 15 °C (Fig. 5.1A).

The experiment consisted of three treatments with two replicates per treatment (Fig. 5.1B). Foods were chosen to cover two OSA concentrations reflecting that typical for marine water columns: 1) no OSA (Control), 2) moderate concentration OSA (OSA_{low}), and 3) high-concentration OSA (OSA_{high}). Clams in the Control were fed 3.0 mL clam feed only, which consisted of mixed algae (dry weight 8%, Shellfish Diet 1800, Reed Mariculture Inc.) every 3 days. Clams in the OSA_{high} treatment were fed 600 mL mixture of OSA and seawater every 3 days, while clams in the OSA_{low} were fed a combination of 300 mL mixture of OSA and seawater with 1.5 mL clam feed every 3 days to provide sufficient food. Just before feeding or water renewal, clams (n = 4) and about 3 g of sediment were sampled each day (Days 1, 2, 4, 7, 14, 30, 40, and 50). Seawater was renewed every 6 days until Day 30 and then every 12 days thereafter, when less than on half ($n \leq 20$) clams remained.

After clams (n = 4) were collected, their shells and guts were removed and only soft tissues were pooled and analyzed for PAHs. This was done to avoid bias of possible overestimation due to accumulated or preassimilated OSAs in shells or guts, respectively. Soft tissues were rinsed with distilled water, homogenized, and stored frozen at −20 °C until PAHs analysis. Samples of sediments were also stored frozen at −20 °C until the microbial community in sediments were analyzed. Subsamples of OSAs were sieved through a glass-fiber filter and then stored at −20 °C until PAHs were analyzed.

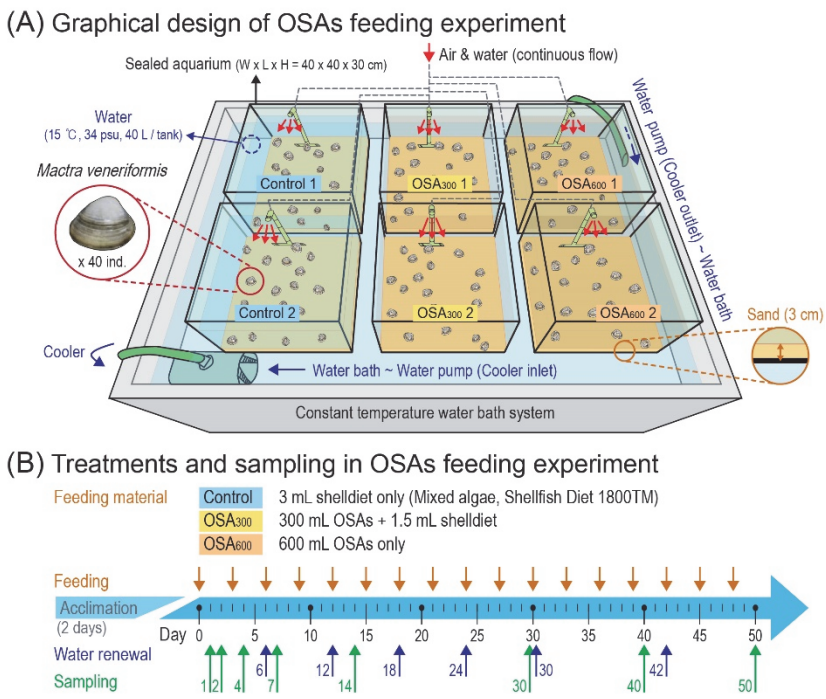

Fig. 5.1. Schematic overview showing the study design of the OSAs feeding experiment. (A) Control and OSAs feeding treatments in constant temperature water bath. (B) Experimental flowchart with information on the feeding materials and interval, water renewal, and sampling time. Seawater, Iranian Heavy Crude oil, and fine sediment particles (<20 μm) were used for the preparation of OSAs mixture, the mixing ratio of 1000:0.6:0.2 in weight. The details of preparation of OSAs in feeding materials were described in Table 5.1.

Table 5.1. Details for the preparation of OSAs.

Schematic description of OSA preparation		
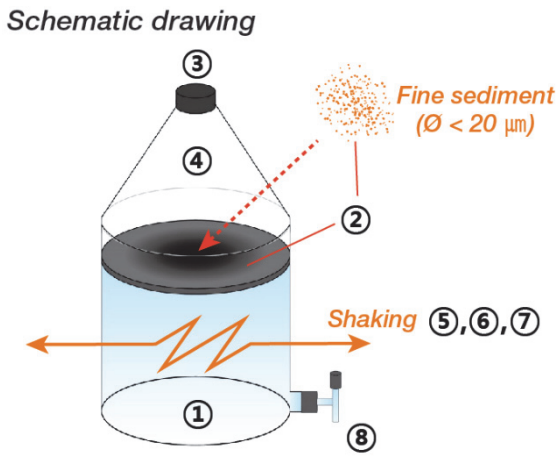		
Water (①)	**Seawater/crude oil/sediment (②)**	**Vessel volume (③)**
GF/F-filtrated seawater	Weight ratio of 0.2:0.6:1000	>2 L carboy (volume for app. 700 mL of OSAs)
Head space (④)	**Mixing speed (⑤)**	**Mixing time (⑥)**
>10% by volume	170 rpm (reciprocating shaker)	24 h
Mixing condition (⑦)	**Extraction (⑧)**	**Reference**
Sealed vessel, mixing in the dark, and at test temperature	70% by volume from carboy (app. >80% of total OSAs)	Sun et al., 2010

Table 5.2. Baseline information of sediment properties. Sandy loam was used for bottom sediment in experimental tank.

Experimental treatment	Organic contents* (%)	Mud contents (%)	Grain size	Sediment source
Control	0.92 ± 0.25	0.79 ± 0.25	< 1 mm	Samhangang INC., Incheon, KOR
OSA_{low}	0.98 ± 0.20			
OSA_{high}	0.81 ± 0.08			

*Mean values during the whole treatment period (Day 1, 2, 4, 7, 14, 30, 40, and 50).

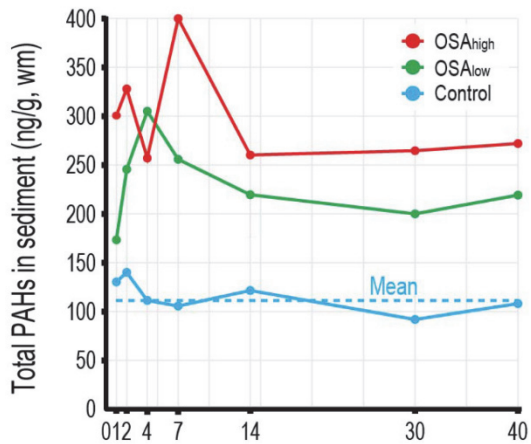

Fig. 5.2. Total PAHs concentration in sediments. Blue line denotes Control treatment, green line denotes the OSA_{low} treatment, and red line denotes the OSA_{high} treatment, the PAHs concentrations are found to be fairly consistent after the 14 days and maintained at certain levels for the last period of experiments cross the treatments.

5.2.2. Laboratory analysis

An aliquot of 1 g of thawed, soft tissues was extracted three times with 6 mL of DCM with sodium sulfate in a polypropylene tube. Four surrogate standards acenaphthene-d10, phenanthrene-d10, chrysene-d12, and perylene-d12 were added before extraction. Extracts were concentrated to 1 mL under a gentle stream of N_2, then purified by passing it through ~8 g silica gel (70−230 mesh size), and then eluted with 50 mL hexane/DCM mixture (80:20, v/v). Eluents were concentrated to 1 mL with hexane using a rotary evaporator and a gentle stream of N_2. It was then transferred into a GC vial for analysis. The OSA particles (~25 mg obtained by glass-fiber filtering 1 mL of OSAs) and crude oil sample (0.2 g) were also extracted using the above methods.

Concentrations of PAHs and alkylated PAHs were determined by use of an Agilent 7890A gas chromatograph equipped with a mass selective detector (Agilent Technologies, Santa Clara, CA) and analyzed in selected ion mode (GC/MSD-SIM) as described previously (Jonsson et al., 2004). 35 target analytes of PAHs were analyzed by GC/MSD and their acronyms were listed in Table 5.3 and details of instrument conditions for the analyses of PAHs and alkyl-PAHs are provided in Table 5.4. Concentrations and compositions of the 35 PAHs and alkyl-PAHs in the OSAs are given in Fig. 5.3. However, it should be noted that only 25 PAHs were detected and quantified in soft tissue of clams (Fig. 5.4 & Table 5.5). In order to characterize accumulation of specific PAHs by clams, observations for which (1) no apparent temporal accumulation over 50 days or (2) detectable concentrations of <30 ng/g wet mass for LMM PAHs (Fluorene, Dibenzothiophene, and Phenenthrene) or <10 ng/g wm for HMM PAHs (Fluoranthene and Pyrene) were removed for further statistical analyses to discern the trends. Finally, 20 target PAHs were selected for quantification (Table 5.5).

Microbial communities in sediments were characterized by extracting total genomic DNA by use of a PowerSoil DNA Isolation Kit (MoBio Laboratories, Solana Beach, CA). Libraries were constructed using the Illumina MiSeq Platform, with 16S, rRNA gene amplicons. The bacterial V3 and V4 regions of the 16S ribosomal gene were amplified by using Illumina primers and barcoded adapters. The sequence data were analyzed by using Quantitative Insights into Microbial Ecology (QIIME). Sequences were clustered into operational taxonomic units (OTUs) at a 97% identity threshold by use of the UCLUST algorithm (Edgar, 2010). Taxonomic information was assigned by aligning reads against data from the Ribosomal Database Project (RDP) (Cole et al., 2014).

Table 5.3. List of target PAHs compounds measured by gas chromatograph equipped with a mass selective detector (GC/MSD) in OSAs experiment; Full chemical name, acronym, molecular mass grouping, carbon ring number, and Log K_{ow} values with references given.

Full chemical name	Acronym	MMG*	Ring number	Log K_{ow}**
Naphthalene	Nap	LMM	2	3.33[b],3.35[a]
Acenaphthylene	Acl	LMM	3	3.67[a],4.2[b]
Acenaphthene	Ace	LMM	3	3.92[a],4.0[b]
Fluorene	Flu	LMM	3	4.18[a],4.32[b]
Dibenzothiophene	Dbt	LMM	3	4.38[a],4.52[c]
Phenanthrene	Phe	LMM	3	4.52[b],4.57[a],4.90[c]
Anthracene	Ant	LMM	3	4.50[b],4.68[a]
1-Methylnaphthalene	C1-Nap	LMM	2	3.89[d]
2-Methylnaphthalene	C2-Nap	LMM	2	3.88[a],3.96[d]
1,4,5-Trimethylnaphthalene	C3-Nap	LMM	2	4.48[d]
1,2,5,6-Tetramethylnaphthalene	C4-Nap	LMM	2	4.95[d],5.53[a]
9-Methylfluorene	C1-Flu	LMM	3	4.66[e]
1,7-Dimethylfluorene	C2-Flu	LMM	3	5.08[e]
9-n-Propylfluorene	C3-Flu	LMM	3	5.85[a]
2-Methyldibenzothiophene	C1-Dbt	LMM	3	4.93[a],5.04[c]
2,4-Dimethyldibenzothiophene	C2-Dbt	LMM	3	5.47[c]
2,4,7-Trimethyldibenzothiophene	C3-Dbt	LMM	3	6.03[a,c]
3-Methylphenanthrene	C1-Phe	LMM	3	5.34[c]
1,6-Dimethylphenanthrene	C2-Phe	LMM	3	5.64[c]
1,2,9-Trimethylphenanthrene	C3-Phe	LMM	3	6.03[c]
1,2,6,9-Tetramethylphenanthrene	C4-Phe	LMM	3	6.48[c]

Table 5.3. Continued.

Full chemical name	Acronym	MMG*	Ring number	Log K_{ow}**
Fluoranthene	Fl	HMM	4	5.20[b],5.23[a]
Pyrene	Py	HMM	4	5.00[b],5.13[a]
Benzo[*a*]anthracene	BaA	HMM	4	5.91[a,b]
Chrysene	Chr	HMM	4	5.81[a],5.86[b]
Benzo[*b*]fluoranthene	BbF	HMM	5	5.78[a],5.8[b]
Benzo[*k*]fluoranthene	BkF	HMM	5	6.11[b]
Benzo[*a*]pyrene	BaP	HMM	5	6.13[a],6.35[b]
Perylene	Pery	HMM	5	6.25[a]
Indeno[*1,2,3-cd*]pyrene	IcdP	HMM	6	6.58[a],6.72[b]
Dibenzo[*a,h*]anthracene	DbahA	HMM	5	6.75[a,b]
Benzo[*g,h,i*]perylene	BghiP	HMM	6	6.5[a],6.9[b]
3-Methylchrysene	C1-Chr	HMM	4	6.42[c]
6-Ethylchrysene	C2-Chr	HMM	4	6.88[c]
1,3,6-Trimethylchrysene	C3-Chr	HMM	4	7.44[c]

*Molecular mass groups (MMGs) were categorized based on ring number class as either lower molecular mass (LMM, 2-3 rings) or higher molecular mass (HMM, 3-4 rings).

**Data for Log K_{ow} values obtained from studies by: (a) Ma et al., 2009; (b) Kang et al., 2014; (c) Lee et al., 2015; (d) Dimitriou-Christidis et al., 2003; and (e) ChemSpider, 2017.

Table 5.4. GC/MSD conditions for the analyses of PAHs and alkylated PAHs.

GC/MSD system	Agilent 7890A GC and 5975C MSD
Column	DB-5MS (30 m long, 0.25 mm i.d., 0.25 μm film thickness)
Gas flow	1 mL/min He
Injection mode	Splitless
Injection volume	2 μL
MS temperature	180 °C
Detector temperature	230 °C
Oven temperature	60 °C hold 2 min
	Increase 6 °C/min to 300 °C
	300 °C hold 13 min

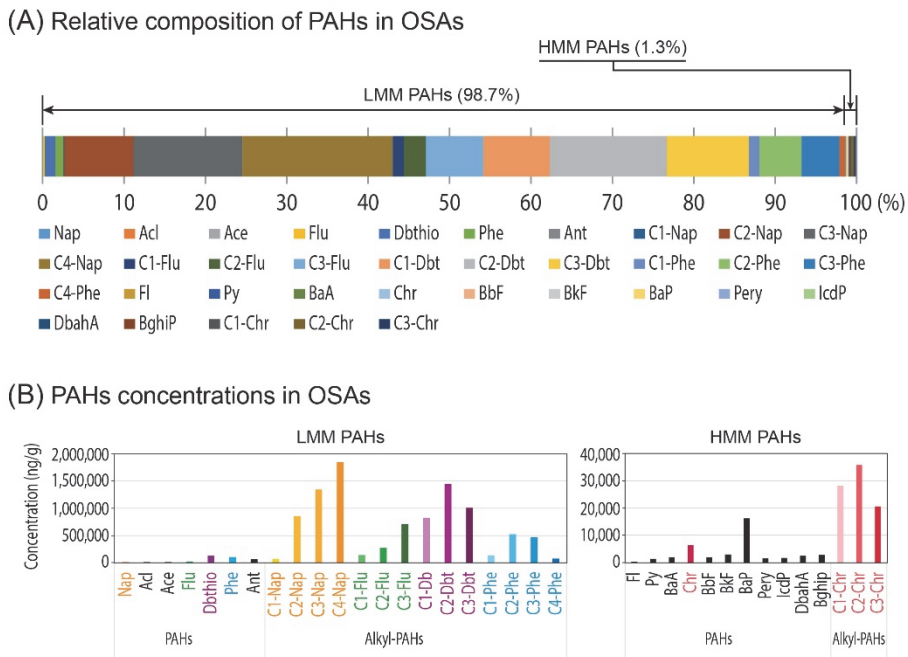

Fig. 5.3. PAHs and alkylated PAHs in OSAs. (A) Relative composition of PAHs compounds in OSAs and (B) Concentrations of PAHs and alkylated PAHs in OSAs. Acronyms for the target PAHs given in Table 5.3.

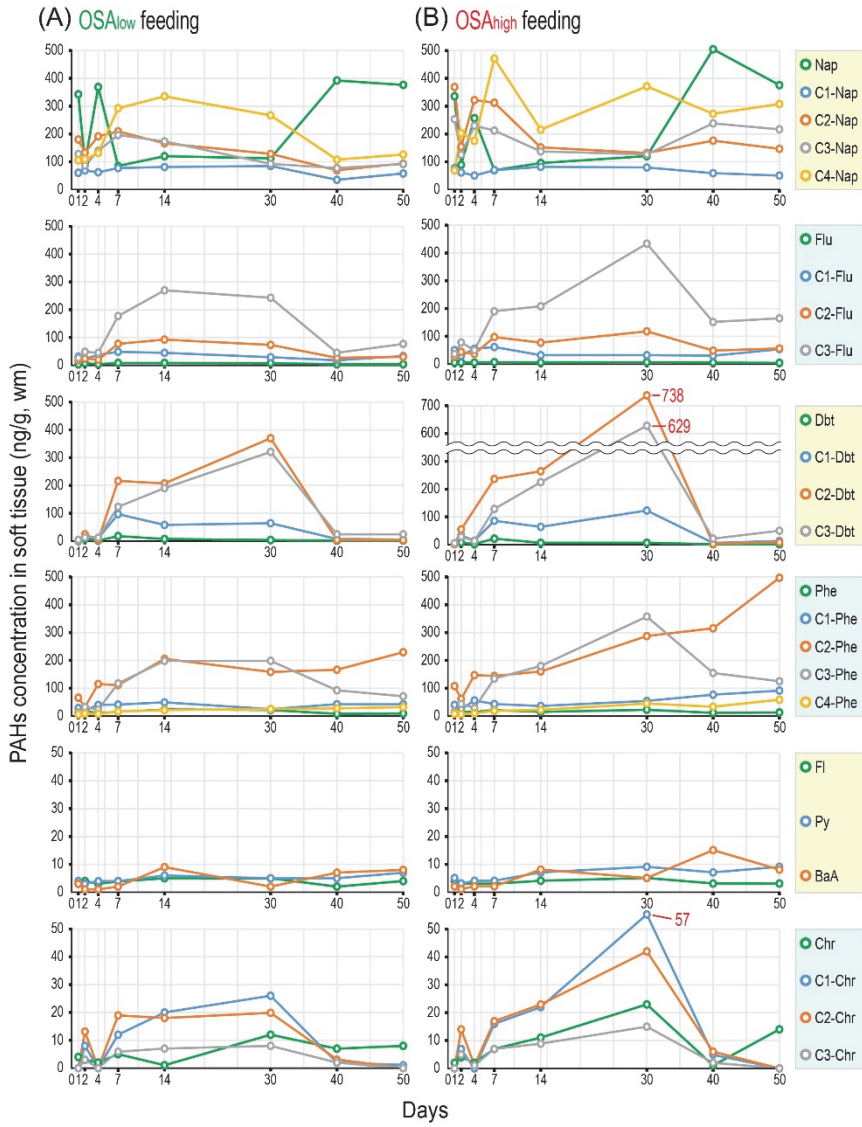

Fig. 5.4. Concentrations of 25 PAHs in soft tissue of clams, *Mactra veneriformis*, under (A) OSA_{low} feeding treatment and (B) OSA_{high} feeding treatment. Acronyms for PAHs given in Table 5.3.

Table 5.5. Mean concentrations of PAHs (ng/g, wm) in soft tissue of clams, *Mactra veneriformis*, under OSAs feeding experiments. Acronyms for PAHs given in Table 5.3.

Treatment		OSA_{low}								OSA_{high}							
Sampling day		1	2	4	7	14	30	40	50	1	2	4	7	14	30	40	50
LMM PAHs	Nap*	341.9	97.1	365.9	79.0	120.1	114.5	389.5	375.9	336.1	87.8	255.6	69.5	94.8	120.3	506.1	376.0
	C1-Nap	57.8	67.3	58.9	69.6	74.4	78.0	32.2	47.8	78.1	62.0	50.3	70.5	81.4	78.7	59.3	49.9
	C2-Nap	177.4	127.0	185.9	206.4	162.1	124.6	60.7	94.2	369.5	153.7	320.8	311.8	151.8	131.9	176.0	146.8
	C3-Nap	129.1	77.0	147.4	196.1	177.9	96.1	78.1	90.0	252.6	125.7	228.6	213.0	138.0	125.6	237.4	215.5
	C4-Nap	106.2	108.7	138.3	290.8	330.2	264.1	106.9	128.9	68.1	203.2	174.6	471.5	214.8	370.7	273.5	307.6
	Flu	3.0	5.7	3.4	6.6	7.1	6.1	2.8	2.9	4.6	5.5	4.7	6.9	5.2	7.1	4.8	3.6
	C1-Flu	30.1	21.5	35.1	48.7	44.0	25.1	16.4	31.5	50.5	30.1	56.0	60.9	31.5	32.4	29.6	54.0
	C2-Flu	16.1	27.5	23.5	79.2	93.8	72.8	23.9	26.7	25.8	43.3	36.1	96.7	77.7	118.3	48.6	56.4
	C3-Flu	24.4	45.2	39.8	176.0	262.7	238.4	42.6	74.4	36.1	79.3	50.2	189.8	209.3	433.8	152.7	164.4
	Dbt	0.4	3.6	1.3	16.1	5.8	3.4	0.7	0.5	0.6	8.1	2.2	20.6	6.8	6.8	1.1	1.0
	C1-Dbt	2.8	16.2	8.1	98.0	52.0	63.9	5.5	5.2	4.2	32.8	13.3	85.9	64.4	122.6	5.8	12.3
	C2-Dbt	0.9	21.1	3.1	217.8	207.1	360.0	4.1	2.9	1.4	54.9	4.1	235.8	264.4	738.1	3.5	8.0
	C3-Dbt	3.7	11.3	10.2	126.1	190.2	317.7	19.4	18.8	5.3	27.8	12.8	128.4	223.9	629.2	21.1	50.0
	Phe	7.0	13.3	9.5	21.8	19.6	18.0	6.2	7.5	11.2	15.9	13.9	20.9	14.6	21.6	11.4	12.4
	C1-Phe	23.8	15.2	37.1	37.9	46.0	21.0	34.7	40.7	40.5	25.0	56.4	42.4	35.6	53.7	77.1	90.8
	C2-Phe	68.0	29.6	118.0	114.4	205.1	158.5	169.1	230.3	109.0	61.2	147.5	143.4	159.9	287.0	315.3	495.9
	C3-Phe	13.4	33.6	22.8	117.0	197.7	198.2	91.7	71.6	17.2	43.1	28.7	134.2	179.8	367.9	154.1	125.3
	C4-Phe	5.9	8.6	8.1	17.0	22.5	25.1	28.0	32.0	8.0	7.5	10.3	18.9	21.7	45.2	32.5	58.8

Table 5.5. Continued.

Treatment		OSA_{low}								OSA_{high}							
Sampling day		1	2	4	7	14	30	40	50	1	2	4	7	14	30	40	50
HMM PAHs	Fl	2.9	4.1	3.3	3.8	4.7	4.6	1.8	3.5	3.7	3.3	3.1	3.1	4.3	5.3	2.9	3.0
	Py	3.5	3.3	4.0	4.1	5.7	5.5	4.5	7.2	4.6	3.3	4.1	4.3	6.6	8.7	6.8	9.4
	B*a*A	2.8	1.2	1.4	1.6	9.3	1.9	6.7	7.5	1.7	1.3	1.7	2.0	7.9	5.3	15.1	8.1
	Chr	3.6	3.1	2.2	4.8	1.1	12.4	6.7	7.9	2.4	3.6	2.0	6.6	8.8	23.0	1.1	14.4
	C1-Chr	0.4	8.4	0.4	12.4	20.2	26.5	2.4	0.7	0.5	7.2	0.5	16.2	22.5	57.1	5.3	0.3
	C2-Chr	0.3	13.2	0.3	18.8	17.7	20.0	3.1	0.3	0.2	13.6	1.1	17.3	23.0	42.4	6.2	0.4
	C3-Chr	0.2	3.3	0.3	6.2	6.9	7.8	1.7	0.4	0.3	4.7	0.7	6.6	8.9	14.6	2.0	0.4

*20 PAHs in bold indicate that accumulated PAHs concentrations higher than 30 ng/g wm for LMM PAHs and 10 ng/g wm for HMM PAHs over the period of 50 days.

5.2.3. Data analysis

SPSS 23.0 (SPSS INC., Chicago, IL) and PRIMER software packages were used to perform statistical analyses (Clarke & Gorley, 2006). The Mann−Whitney U-test was used for comparison of replicates (n = 2) per treatment and results indicated that, there were no significant differences in total concentrations of PAHs among treatments of Control, OSA_{low}, and OSA_{high} treatment (at $p < 0.05$) (Table 5.6). Spearman rank correlation coefficient analysis (r) was used to investigate relationships among concentrations of the primary 20 PAHs in soft clam tissues (Table 5.7). Concentrations of selected PAHs were standardized to total concentrations of PAHs, then transformed by taking the square root, which resulted in data meeting the assumption of normality (Kolmogorov−Smirnov test; $p > 0.05$) because the combined data of OSA_{low} and OSA_{high} treatments were used for following statistics, the assumption of homogeneity was not needed (Table 5.8). Subsequently, to evaluate bioaccumulation patterns, cluster analysis was performed by use of the Bray−Curtis similarity matrix (BCS). Next, the principal component analysis (PCA) was utilized to assess potential interactions between specific PAHs and bacterial communities at the level of phyla. Finally, the Shannon−Weaver index was calculated for bacterial species diversity at the taxonomic level of class.

Table 5.6. Result of Mann-Whitney U-test for comparison of replicates (n = 2) per treatment in total PAHs. The replications of Control, OSA_{low}, and OSA_{high} were tested.

	Experimental treatment		
	Control	OSA_{low}	OSA_{high}
Mann-Whitney U	18.0	29.0	28.0
p value	.491	.798	1.00

Table 5.7. Spearman rank correlation results for concentrations of 20 PAHs in soft tissue of marine clam, *Mactra veneriformis*. Values in bold indicate correlation significance at the p <0.0l level (matched with ++). Acronyms for PAHs given in Table 5.3.

Compounds		Lower molecular mass (LMM) PAHs															Higher molecular mass (HMM) PAHs				
		Nap	C1-Nap	C2-Nap	C3-Nap	C4-Nap	C1-Flu	C2-Flu	C3-Flu	C1-Dbt	C2-Dbt	C3-Dbt	C1-Phe	C2-Phe	C3-Phe	C4-Phe	B*a*A	Chr	C1-Chr	C2-Chr	C3-Chr
LMM PAHs	Nap		**-.624**	-.229	.085	-.362	-.221	-.556	-.435	**-.753**	**-.659**	-432	.335	.521	-.206	.379	.476	-.112	**-.624**	**-.624**	-.618
	C1-Nap	++		.194	.115	.365	.144	.609	.562	**.624**	**.624**	.544	-.106	-.129	.476	-.076	-.082	.115	**.747**	**.641**	**.688**
	C2-Nap				**.815**	.041	**.703**	.003	-.224	-.018	-.259	-.306	.297	-.371	-.394	-.544	-.268	-.571	-.268	-.244	-.256
	C3-Nap			++		.247	**.724**	.159	-.012	-.071	-.224	-.097	**.668**	.138	-.091	-.056	.186	-.421	-.309	-.229	-.200
	C4-Nap						.403	**.918**	**.879**	**.776**	**.726**	**.824**	.535	.491	**.794**	.535	.356	.250	.532	**.691**	**.688**
	C1-Flu			++	++			.341	.159	.224	.024	.068	**.632**	.085	-.053	-.047	.018	-.088	-.191	-.097	-.068
	C2-Flu	+	+			++			**.947**	**.882**	**.859**	**.903**	.388	.374	**.844**	.471	.279	.318	**.759**	**.835**	**.868**
	C3-Flu		+			++		++		**.832**	**.874**	**.971**	.312	.503	**.941**	.585	.391	.400	**.791**	**.865**	**.891**
	C1-Dbt	++	++			++		++	++		**.944**	**.832**	.062	.062	**.691**	.215	-.100	.344	**.788**	**.921**	**.888**
	C2-Dbt	++	++			++		++	++	++		**.918**	-.038	.168	**.809**	.347	.026	.497	**.859**	**.959**	**.953**
	C3-Dbt		+			++		++	++	++	++		.203	.482	**.947**	.585	.362	.526	**.806**	**.894**	**.912**
	C1-Phe				++	+	++							**.703**	.288	.559	.562	-.085	-.168	-.059	-.006
	C2-Phe	+							+				++		**.647**	**.932**	**.859**	.321	.088	.168	.212
	C3-Phe					++		++	++	++	++	++		++		**.741**	.544	.438	**.774**	.821	**.853**
	C4-Phe			+		+			+			+	+	++	++		**.726**	.488	.253	.321	.362
HMM PAHs	B*a*A												+	++	+	++		.144	.079	.082	.147
	Chr			+								+							.300	.356	.356
	C1-Chr	++	++			+		++	++	++	++	++			++					**.912**	**.947**
	C2-Chr	++	++			++		++	++	++	++	++			++				++		**.976**
	C3-Chr	+	++			++		++	++	++	++	++			++				++	++	

++ Significantly correlated at the p< 0.01 level (2-tailed).

+ Significantly correlated at the p< 0.05 level (2-tailed).

Table 5.8. Result of Kolmogorov-Smirnov normality test for concentrations of PAHs in soft tissue of clams, *Mactra veneriformis*, over the period of 50 days in OSAs feeding treatments (OSA_{low} and OSA_{high}). The concentrations of 20 PAHs (refer to Table 5.5) were standardized by total, and root transformed before these test.

Statistic	degree of freedom	p value
.048	3.20	.072

5.3. Results

5.3.1. Bioaccumulation of total PAHs by clams

Bioaccumulation of total PAHs (TPAH) in soft tissues of clam after 50 days of exposure, including LMM and HMM PAHs, was found to be similar between treatments of OSA_{low} and OSA_{high} (Fig. 5.5A). For both treatments, concentrations of PAHs increased rapidly for 7 days, peaked at Day 30, and then declined until the end of the experiment on Day 50. Under OSA_{high} treatment conditions, the peak of LMM PAHs (3.7 × 103 ng/g, wm) was observed on Day 30 and its concentration almost doubled compared to that on Day 14 (2.0 × 103 ng/g wm). In contrast, although the peak concentration of LMM PAHs in the OSA_{low} treatment on Day 14 was 2.2 × 103 ng/g wm its concentration was similar to that on Day 30 (2.2 × 103 ng/g, wm). Of note, peak concentrations of both LMM and HMM PAHs in the OSA_{high} treatment were nearly twice compared to those of the corresponding PAHs concentrations in the OSA_{low} treatment. By the end of the experiment (Day 50), the concentration of LMM PAHs remaining in soft clam tissue under both OSA treatments had diminished to about half of their peak values. In contrast, in both treatments, concentrations of HMM PAHs had diminished by 90% relative to their peak concentrations.

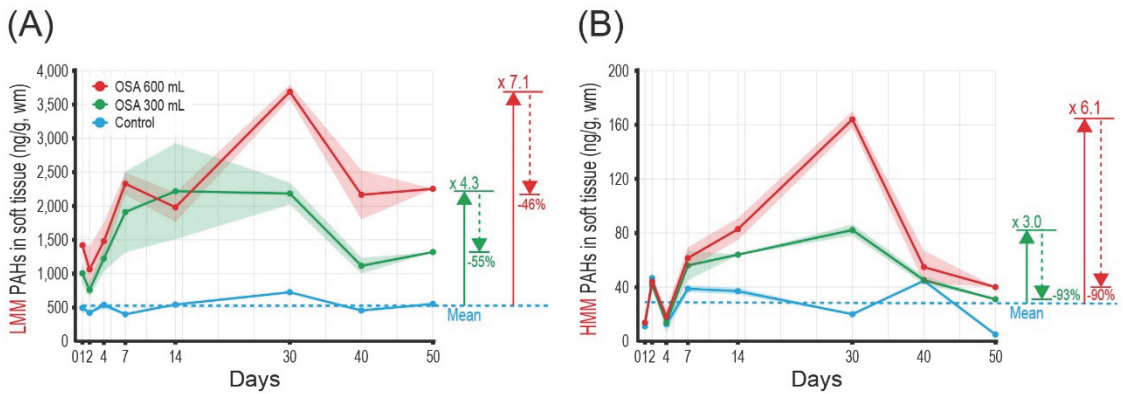

Fig. 5.5. Concentration of (A) lower and (B) higher molecular mass PAHs in soft tissues of *Mactra veneriformis* during the OSAs experiment for 50 days. Blue, green, and red lines denote Control, OSA_{low}, and OSA_{high} treatment, respectively.

5.3.2. Bioaccumulation characteristics of PAHs in clams

In general, during the 50 days experiment, PAHs were accumulated to concentrations approximately twice those observed in the OSA_{high} treatment than those observed in the OSA_{low} treatment (Fig. 5.5). Concentrations of 9-n-propylfluorene (C3-Flu), 2-methyldibenzothiophene (C1-Dbt), 2,4-dimethyldibenzothiophene (C2-Dbt), 2,4,7-trimethyldibenzothiophene (C3-Dbt), 1,2,9-trimethylphenanthrene (C3-Phe), chrysene (Chr), 3-methylchrysene (C1-Chr), 6-ethylchrysene (C2-Chr), and 1,3,6-trimethylchrysene (C3-Chr) all peaked on Day 30, and then decreased by >50% by the end of the experiment (Table 5.5). Among the measured PAHs, concentrations of C2- and C3-Dbt in the OSA_{high} treatment were the two greatest PAHs in clam tissues (738 and 629 ng/g, respectively). The concentration of 1,6-dimethylphenanthrene (C2-Phe) in the OSAhigh treatment was accumulated continuously from Day 1 to 50 with the peak on Day 50 (496 ng/g) (Fig. 5.4).

Spearman rank correlation analysis provided a more detailed signature relating to the pattern of accumulation among groups and/or individual PAHs (Table 5.7). First, concentrations of all PAHs were positively correlated, except for naphthalene (Nap) (negative correlations prevailed). Second, C1-Dbt and C2-Chr were most widely correlated among unsubstituted PAHs. Third, within PAHs homologue groups, Chr was most strongly correlated among derivatives of alkylated PAHs ($p < 0.01$ for all cases). Fourth, in general, correlations of alkylated PAHs to other PAHs exhibited more significant relationships compared to their corresponding unsubstituted PAHs. Finally, there was a clear trend in correlations between LMM and HMM PAHs such as among alkylated-Dbt and alkylated-Chr compounds.

Further cluster analyses were performed to simplify such complex correlations, and to discern specific accumulation patterns for the individual 20 PAHs and alkylated PAHs in clams. Degree of similarity in cluster analysis was used to characterize associations among PAHs. Square roots of standardized values of PAHs concentrations were used to calculate the BCS. The result indicated two specific patterns for 10 PAHs and alkylated PAHs in >85% of BCS indices (Fig.

5.6A); specifically, a progressive bioaccumulation of PAHs for Group I and a rapid bioaccumulation of six PAHs with peaks and then declined until the end of the experiment (a bell-shaped pattern) for Group II (Fig. 5.6B). Of note, other PAHs grouped apart from these two groups of typical patterns showed relatively low BCS values (Fig. 5.7). Benzo[*a*]anthracene (B*a*A) and 3-methylphenanthrene (C1-Phe), C2-Phe, and 1,2,6,9-tetramethylphenanthrene (C4-Phe) belonged to the Group I, while C1-, C2-, and C3-Dbt, C1-, C2-, and C3-Chr belonged to Group II (Fig. 5.6A). Group IPAHs exhibited moderate cross-correlations, while all Group II PAHs included the most widely correlated chemicals (Fig. 5.6). Overall, bioaccumulation of PAHs by clams could be categorized by cross-correlations, which were according to physicochemical properties of PAHs, such as molecular mass, octanol/water partition coefficient, and their degradation or metabolic half-lives (Baumard et al., 1998; Zakaria et al., 2001; Wan et al., 2007).

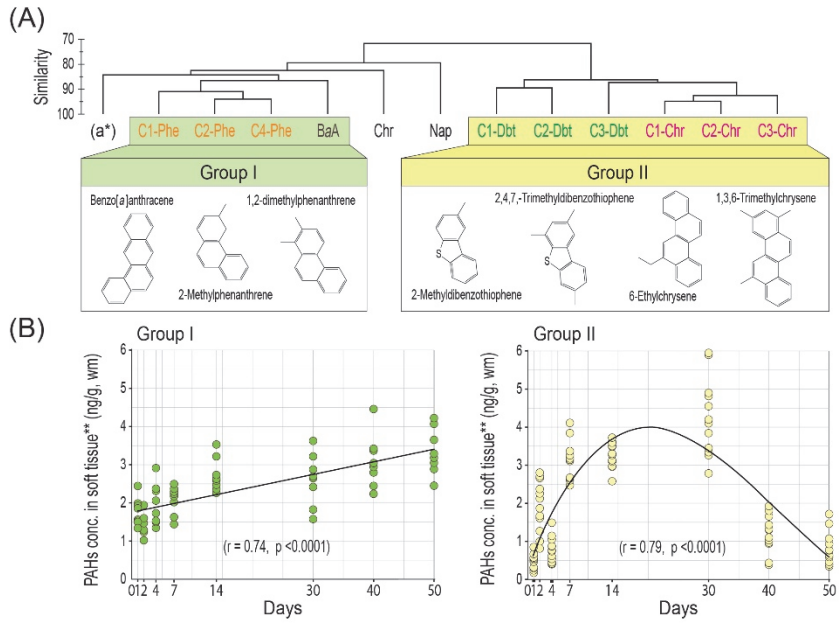

Fig. 5.6. Bioaccumulation patterns of PAHs revealed by the OSAs feeding experiments. (A) Dendrogram representing hierarchical clustering based on Bray−Curtis similarities (BCS) (*(a) PAHs compounds described in Fig. 5.7). (B) Concentrations of PAHs for Group I & II (BCS ≥ 85%). Groups were classified based on response patterns of BCS scores: Group I represents concentrations of PAHs that continually increase over time, Group II represents PAHs for which maximum concentrations reached then declined with time (**Concentrations of PAHs in soft tissue were standardized by total, and square root transformed for normality). Acronyms for corresponding PAHs compounds refer to Table 5.3.

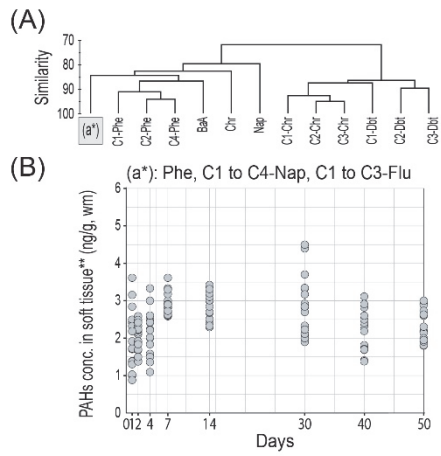

Fig. 5.7. PAHs compounds in soft tissue of clams, Mactra veneriformis, by the bioaccumulation of OSAs feeding experiments; (A) Dendrogram representing hierarchical clustering based on Bray-Curtis similarities (BCS) by group means, (B) Group (a*) indicated group of PAHs in BCS <85% including Phe, C3-Phe, C1 to C4-Nap, and C1 to C3-Flu (**Concentrations of PAHs in soft tissue were standardized by total, and square root transformed for normality). Acronyms for PAHs given in Table 5.3.

5.3.3. Structure of microbial communities

Abundances of bacterial 16S rRNA gene sequences discriminatively revealed differences among absolute and relative compositions of microbial communities in sediments; dried sandy loam (Source) and in the following treatments such as control and OSAs feeding treatments (Control, OSA_{low}, and OSA_{high}) (Fig. 5.8 & 5.9). Seven phyla which occurred at all sampling times, included Proteobacteria, Bacteroidetes, Actinobacteria, Firmicutes, Planctomycetes, Acidobacteria, and others, which encompassed additional unresolved taxa. Each of these phyla constituted >0.01% of the entire bacterial community for at least one treatment type at any sample point. These phyla represented >95% of the population in samples, except dried sediment. In particular, Proteobacteria and Bacteroidetes represented >92% of the microbial populations, while in the source sample (dried sediment) represented <69%.

Results of PCA conducted on the correlation matrix of 10 PAHs, represented by Group I and II (those shown in the Figure 3A cluster analysis) and on relative abundances of microbial phyla, demonstrated possible interaction(s) between selected PAHs and relative abundance of microbial communities. PCA revealed that the two principal components collectively accounted for 81.1% of the total variance (Fig. 5.8A). The first principal component axis (PC1) exhibited significant, positive loadings on PAHs and Bacteroidetes and negative loadings on Proteobacteria. In contrast, the second principal component axis (PC2) exhibited significant, positive loadings on Pattern I PAHs and negative loadings on Pattern II PAHs. Such groupings indicated taxa-specific associations of microbial populations in bioaccumulation of PAHs in clams.

To further clarity such association(s), abundances of 12 classes and 3 additional (unidentifiable) taxa were examined relative to PAH concentrations in soft tissue as functions of treatments, for Day 1 (first sampling), Day 30 (peak PAH), and Day 50 (end of experiment) (Fig. 5.8B & 5.8B′). Relative abundances of classes in phyla Actinobacteria, Planctomycetes (unresolved taxa), Betaproteobacteria, Deltaproteobacteria, and Verrucomicrobiae declined during exposure, even after 1 day, compared to the source sediment, before the exposure. Overall, there were more classes present in experimental tanks than in the initial source sediments. The core

microbial community, representing >5% of members, were identified in all three temporal sampling times of the experiment, including representatives of Bacteroidetes (unresolved taxa) and Proteobacteria (Alphaproteobacteria and Gammaproteobacteria) (Fig. 5.8B′). The Shannon-Weaver index of the core communities ranged from 2.5 to 3.8, which suggested that the number of species and evenness indicated relatively more diverse bacterial communities in each class compared with that of other classes in phyla. Gammaproteobacteria was the most prevalent class in all samples. It was abundant in the OSA of all feeding tanks and the Shannon-Weaver index of Gammaproteobacteria increased over the experimental period.

Two dominant genera (>10%) in initial source sediment were Hydrogenophaga and Panacagrimonas, however, the dominant genera in treatments with OSA indicated changes during experimental periods (Fig. 5.9A). Communities of Proteobacteria bloomed during the beginning of the experiment (at Day 1), representing over 85% dominated by anaerobic and halophilic species, then the proportion of Proteobacteria sharply declined until Day 14 (Fig. 5.9B). After Day 14, there was still a large proportion of Proteobacteria which predominated, with relative abundance of ca. 70% to the total. The sum of Proteobacteria and Bacteroidetes were maintained collectively at greater than 90% in relative abundance during the experiment.

Comparisons of three phylogenetic representations at Day 1, Day 30, and Day 50 showed that specific genera of Gammaproteobacteria were remarkably changed and more abundant in the OSA treatments compared to Control. The corresponding genera included Pseudomonas, Methylophaga, Rheinheimera, Porticoccus, Cyclosticus, Methylophaga, and Alcanivorax (Fig. 5.9A). At species level, nine Gammaproteobacteria taxa were found to be abundant in the OSA treatments, including Porticoccus litoralis, Pseudomonas guineae, Pseudomonas taeanensis, Porticoccus hydrocarbonoclasticus, Cycloclasticus spirillensus, Thioprofundum lithotrophicum, Alcanivorax borkumensis, Alcanivorax dieselolei, and Alkalimarinus sediminis (Fig. 5.9C). In general, Pseudomonas was found to be the predominant genus, particularly peaked during early exposure (until Day 7 or 14) among treatments. However, its relative abundance gradually decreased over the last

period of time. Alternatively, the relative abundance of Porticoccus increased consistently, ultimately to become the most prevalent taxa, representing over 20% of the total microbial abundances (Fig. 5.9C). Relative abundances of Porticoccus and Pseudomonas seemed to indicate a competitive interaction, which might be influenced by temporal changes in PAHs concentrations and/or compositions apparently related to the degree of PAHs degradation.

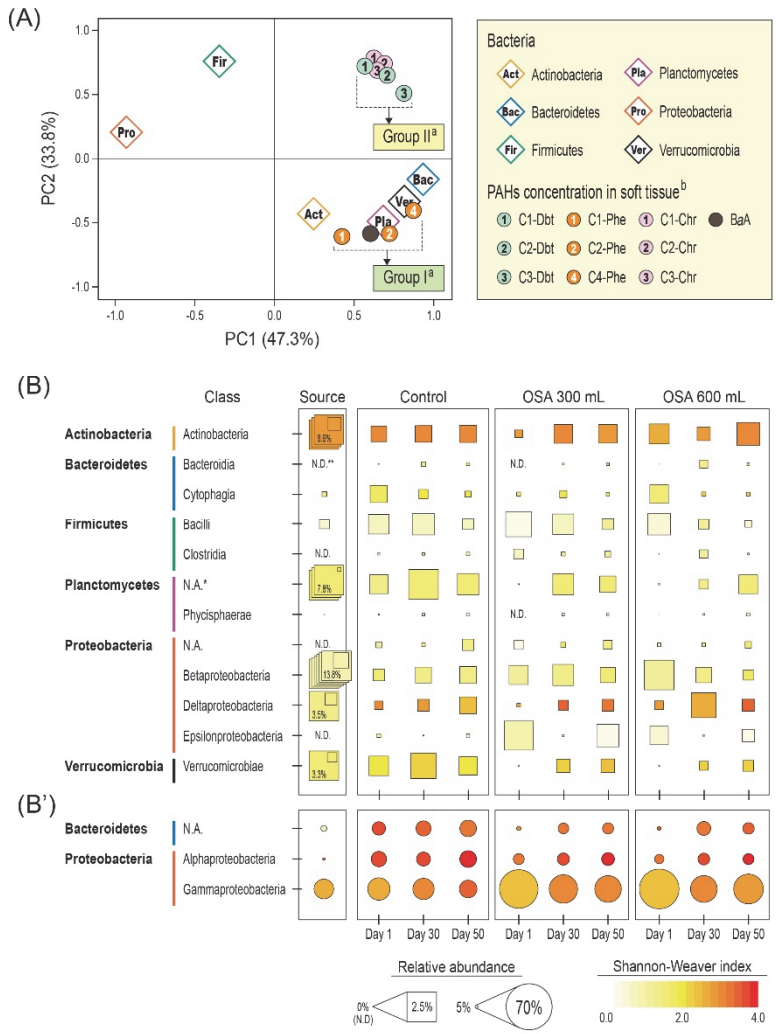

Fig. 5.8. (A) Principal component analysis (PCA) ordination between selected PAHs representative of Group I or II ([a]see Fig. 5.6) and relative abundances of microbial community, at the phylum level. [b]Acronyms for PAHs compounds refer to Table 5.3. (B) Relative abundances (square and circle sizes) of the most prevalent classes (y-axis) in sediments (x-axis) at Day 1, 30, and 50 are plotted for sediment source and experimental treatments (Control, OSA_{low}, and OSA_{high}). Shannon-Weaver diversity index is related to red-scale color intensity of symbols (i.e., redder is higher diversity). N.A.* = "not available" for unidentifiable taxa; N.D.** = "not detected".

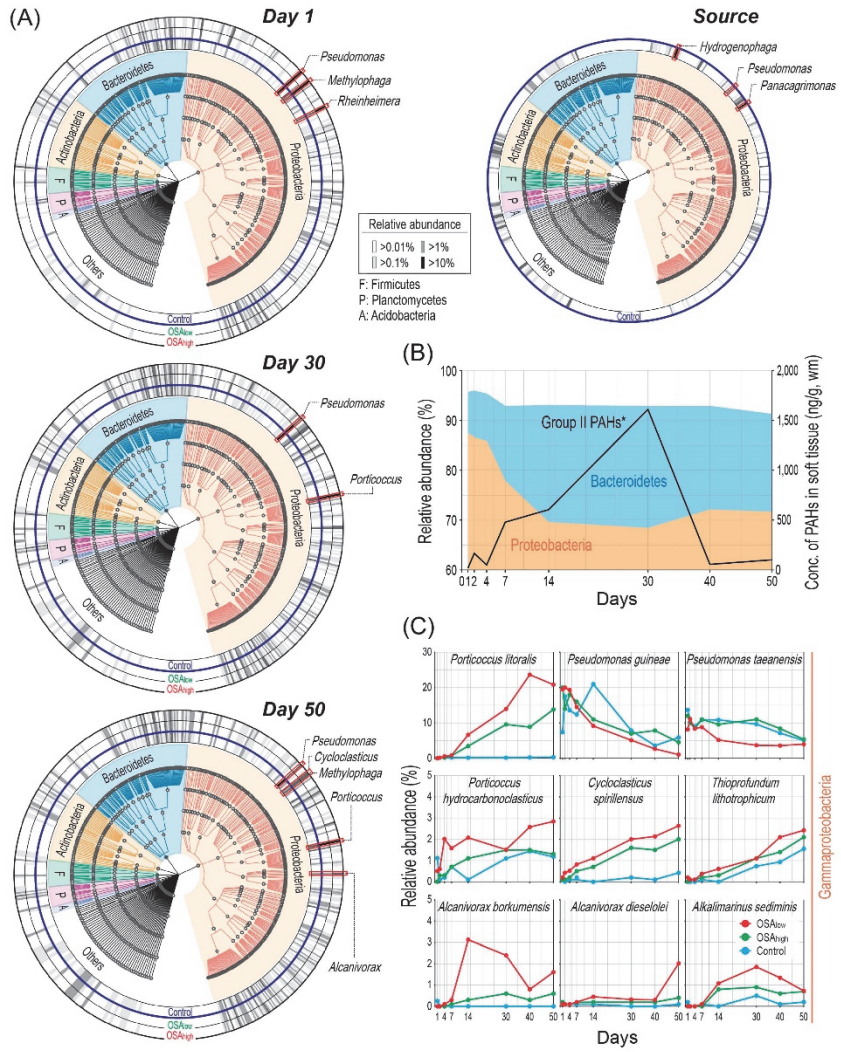

Fig. 5.9. (A) Taxonomic profiles of microbial communities, based on genera (n = 489) relative to sediment source and experimental treatments over time. A phylogenetic representation of the taxonomic composition in experimental treatments (at Day 1, 30, and 50), including Control (inner ring), OSA_{low} (middle ring), and OSA_{high} (outer ring). The average relative abundance of each genus is plotted within the concentric rings, represented by the shaded cells, with higher relative abundance indicated by darker shades. The phylum to which each taxa belongs is indicated by the phylogenetic tree. Abundant taxa in Proteobacteria are labeled by the red outline. (B) Relative abundances of two dominant phyla, Proteobacteria (orange) and Bacteroidetes (blue), with total concentrations of Group II PAHs of OSA_{high} treatments (black line) (*refer to Fig 5.6.) (C) The most abundant nine species belonging to class Gammaproteobacteria. Blue lines and dots denote Control treatments, green lines and dots denote OSA_{low} treatments, and red lines and dots denote OSA_{high} treatments.

5.4. Discussion

Relative compositions of PAHs in OSAs were a function of the process used to prepare OSAs. Naphthalene (Nap), 1-methylnaphthalene (C1-Nap), 2-methylnaphthalene (C2-Nap), 1,4,5-trimethylnaphthalene (C3-Nap), 1,2,5,6-tetramethylnaphthalene (C4-Nap), fluorene (Flu), 9-methylfluorene (C1-Flu), 1,7-dimethylfluorene (C2-Flu), 9-n-propylfluorene (C3-Flu), Phe, C1 to C4-Phe in the OSAs of this study, had relative compositions of PAHs as did weathered oil in situ sediments, while relative proportions of other PAHs, including Dbt, C1 to C3-Dbt, Chr, and C1 to C3-Chr resembled that of IHC, supporting lesser weathering at the beginning stage of oil exposure in the environment (Hong et al., 2015, refer to Fig. 5.10). Characteristics that typically occur after weathering of HMM PAHs were not observed during preparation of OSAs. Shaking was performed to form OSAs, thus, the weathering of Nap, Flu, Phe, and their alky derivatives proceeded as the input of energy and microbial activities were experienced during formation of OSAs.

Results of several previous studies indicated that some marine mollusks possess detoxification enzymes, especially with cytochrome P450 catalyzed enzymatic reactions such as by benzo[*a*]pyrene-hydroxylase, ethoxycoumarin O-deethylase, and N,N-dimethylaniline N-demethylase, which can biotransform PAHs (Rewitz et al., 2006; Bebianno et al., 2007; Zanette et al., 2010). Nevertheless, due to high hydrophobicity in stable lipid-rich tissues, bivalves usually have been reported to be a media as retaining xenobiotic contaminants (Baussant et al., 2001).

In general, the major route of exposure for LMM PAHs is via water, while GMM PAHs generally accumulate via an intake of particulate materials from sediments (Meador et al., 1995; Lee et al., 2014). In this study, LMM PAHs were more abundant than HMM PAHs in OSAs. The concentration of Nap fluctuated among LMM PAHs, of which accumulation was seemingly controlled by osmotic uptake, such that slight variations in rates of filtration and elimination by *M. veneriformis* resulted in differences in rates of accumulation. This is because relatively greater hydrophilicity (i.e., the log octanol−water partition coefficient, log K_{ow}) of Nap was less (3.3) than those of other targeted PAHs (Table 5.3). Among alkylated PAHs during 30 days, bioaccumulation was proportional to log Kow of

PAHs, such that PAHs with greater log K_{ow} were more accumulated by clams (Fig. 5.11). The TPAH in Group I gradually increased until the end of the 50 day experiment without any inflections, with C2-Phe accounting for >75% of the total concentration of PAHs. In spite of the regular and lasting intake of OSAs, the TPAH in Group II included not only LMM PAHs (C1- to C3-Dbt) but also HMM PAHs such as alkylated chrysene (C1- to C3-Chr) reported to exhibit greater log K_{ow} (refer to Table 5.3). Therefore, PAHs of Group II did not follow predictions based on log K_{ow}, although substituted, chrysene compounds have been reported to exhibit greater log K_{ow} (Chr = 5.81, C1-Chr = 6.42, C2-Chr = 6.88, and C3-Chr = 7.44).

Theoretically, by exposing a much greater surface area of oil to microbial communities, the formation of OSAs would increase rates of degradation of oil by associated microbes, however, studies of this process are scarce (Arnosti et al., 2016). Bioremediation of spilled oil by PAHs-degrading microbial communities could mitigate bioaccumulation of PAHs by benthic organisms. In our OSA-contaminated environment, Proteobacteria (especially Gammaproteobacteria) responded rapidly to greater concentrations of PAHs by increasing both abundance and diversity. This means that they have potential to degrade PAHs that tend to accumulate on surfaces of OSAs. One of the major insights provided by the results of the present study was that changes in microbial community composition over a 50 day period was observed in the various OSA treatments. As a result, bioaccumulation of PAHs by clams was influenced by several factors, including chemical properties and exogenous degradation such as chemical weathering and/or microbial degradation.

Several studies, in marine environments, have described species of Gammaproteobacteria as key transformers of PAHs and that they respond immediately to crude oil spills, even within a day or so (Redmond & Valentine, 2012; Beazley et al., 2012; Rivers et al., 2013; Kappell et al., 2014; Lamendella et al., 2014). Results of this study generally confirmed this quick microbial response to OSAs. For instance, a rapid recolonization by microbial communities with some selected species was observed, particularly in the presence of OSA_{high}. The associated microbial taxa responding most rapidly to oil-soaked organic-rich suspended particles included mainly the class Gammaproteobacteria *Pseudomonas*, *Porticoccus*, *Cycloclasticus*, *Methylophaga*, and *Alcanivorax* spp. Such rapid

changes in composition in response to OSAs by microbial communities persisted for almost 2 months (50 days in our study). This result suggests that Gammaproteobacteria could be used to control bioaccumulation of PAHs in marine environments.

Similarly, increases in abundances of species of *Cycloslasticus* and *Alcanivorax* have also been reported in environments contaminated by petroleum hydrocarbons (Dyksterhouse et al., 1995; Geiselbrecht et al., 1998; Kasai et al., 2002; McKew et al., 2007; Cui et al., 2008; Wang et al., 2008; Genovese et al., 2014). *Pseudomonas* has been reported to degrade Nap, Ant, Phe, and Flu in various types of terrestrial soils (Tagger et al., 1990; Ashok et al., 1995; Whyte et al., 1997; Aislabie et al., 2000; Andreoni et al., 2004) and is thought to be involved in cometabolization of Flu (Trzesicka-Mlynarz & Ward, 1995). Although *Thioprofundum* was considered to be mesophilic, anaerobic, and sulfur-oxidizing bacterial community occurred in hydrothermal areas (Mori et al., 2011), the decrease of concentrations of Dbt and alkylated Dbt in clams also could be explained by the increase of *Thioprofundum*, which could have accelerated desulfurization of sulfur heterocycles. *P. litoralis* and *P. hydrocarbonoclasticus* have been reported to be specialized hydrocarbon-degrading bacteria living in association with marine phytoplankton (Gutierrez et al., 2012). In this study, by Day 50, at the end of experiment, *P. litoralis* composed about 21% of the entire bacterial composition in the OSA_{high} treatment, which was almost 42-fold greater in relative abundance than in the Control treatment (0.6%). *A. sediminis* has been only recently isolated from marine sediment (Zhao et al., 2015), hence studies of biodegradation by that species are limited. However, *A. sediminis* was considered one of the hydrocarbon degraders because relatively great abundance was evidenced in the OSA treatments compared to that in the Control. Overall, bioaccumulation of PAHs into soft tissues of *M. veneriformis* was related to temporal changes of hydrocarbon-degrading bacterial compositions and abundances. Such an association between bioaccumulation and microbial degradation should be taken into account when handling and utilizing the OSAs in remediating oil spills. Of course, there might be differences in the microbial communities that decompose OSA depending on the type and characteristics of crude oil. In particular, what mechanisms are involved in degradation of PAHs by

microbes is the limit of this study and further studies are needed.

The primary goal of the present study was to address the role of microbial degradation associated with bioaccumulations of PAHs by benthic organisms. The results presented here indicate the importance of *Porticoccus* spp., which can use PAHs as a source of carbon. Some of the results presented here provide insight into how OSAs are related to bioaccumulation by bivalves and biodegradation by microbes. Based on the results of this study, we can consider ways to promote the formation and degradation of OSA by injecting fine sediment particles and oil-degrading bacterial agents in offshore oil spill accidents. To our knowledge, no other study has focused on bioaccumulation of OSAs in association with microbial communities. Thus, the present study appears to be the first step, in developing protocols for OSAs to remediate oil spills.

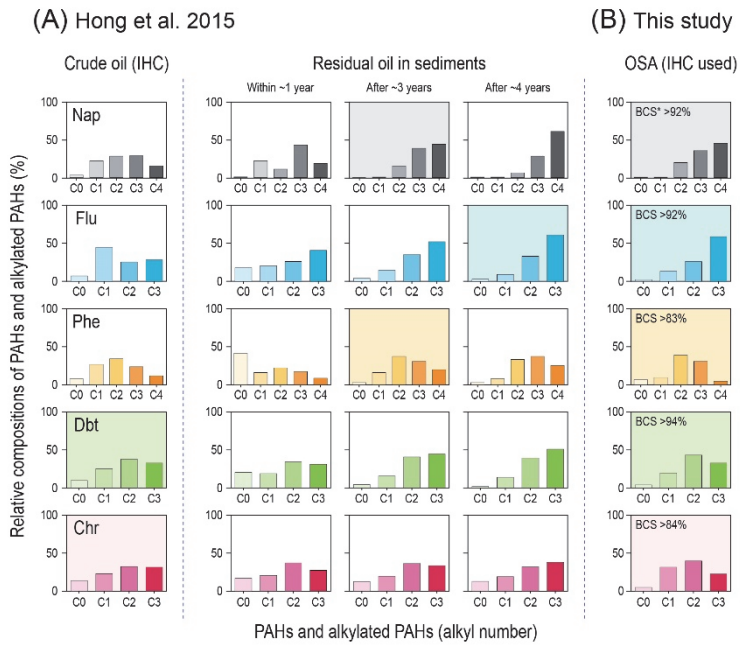

Fig. 5.10. Relative compositions of PAHs and alkylated PAHs in crude oil (Iranian Heavy Crude, IHC), sediments contaminated by Hebei Spirit oil spill, and OSA made of IHC. (A) These results were referenced from a previous study (Hong et al. 2015) and (B) concentration of OSA quantified in this study (*Comparisons of Bray-Curtis similarities (BCS) in relative compositions of PAHs and their alkyl derivatives showed that the most resembled period in weathering of IHC compared to OSA). Acronyms for PAHs given in Table 5.3.

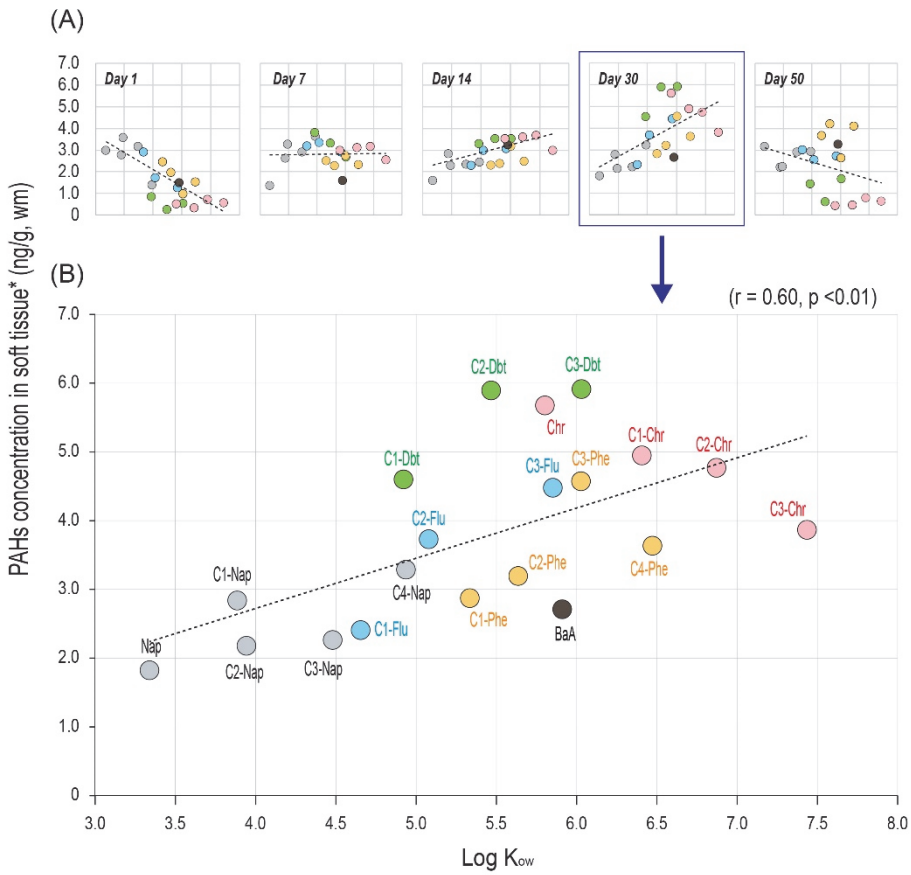

Fig. 5.11. Relationship between Log Kow and concentration of PAHs in soft tissue of clams, Mactra veneriformis. (A) Concentration of PAHs compounds in OSAhigh treatments at Days 1, 7, 14, 30, and 50. (B) The result of OSAhigh treatment at Day 30 as peak concentration of PAHs in soft tissue (*The concentrations were standardized by total, and square root transformed for normality). Acronyms for PAHs given in Table 5.3.

CHAPTER 6.

DISCUSSION AND IMPLICATION

6.1. Summary

In the present study, ecological responses to anthropogenic influences which focused on marine organisms, were evaluated in different spatiotemporal settings in case of the Yellow Sea where various human impacts such as pollution, coastal development, and reclamation have been concentrated over the last decades. Microphytobenthic production has been assessed for the benthic primary productivity and revisited benthic-pelagic coupling in the Yellow Sea large marine ecosystem. In the regional scales, food web dynamics were evaluated in a closed estuary where freshwater free-flow was interrupted for long periods due to the construction of estuaries. Additionally, the structure of fish assemblages in natural and artificial reefs, which is widely installed along the coast, was evaluated. The oil spill accident which is a relatively local scale event but very hazards on marine ecosystem was assessed for bioaccumulation and biodegradation of OSAs. Major findings of the present study are highlighted below:

Chapter 2. Ecological role and significance of benthic-pelagic coupling: Case study in the Yellow Sea

- A global meta-data indicated that the North America and the western Europe showed averagely enriched MPB biomass, whereas he East Asia of tidal flat was characteristic with the elevated MPB productivity.
- Microphytobenthic biomass showed a significant association to pelagic chlorophyll *a* concentration observed in GOCI.
- The benthic-pelagic coupling was identified significantly up to ~10 km offshore in the Yellow Sea.
- Productive zone of benthic-pelagic coupling boundary is primarily attributable to its macrotidal regime, as evidenced by increasing pelagic to benthic ratio following tidal height.

Chapter 3. Influences of estuarine dike on marine food web dynamics

- The stable isotopic signatures of samples indicated dissimilarity in distribution of organic matters between inside and outside of dike, supporting geographical and/or trophic isolation.
- Seasonal feeding chances in compositions of major food sources (microphytobenthos and particulate organic matters) were observed for two target bivalves.
- The temporal variations were further linked to selective feedings that evidenced by age(size)-dependent and/or tissue specific assimilations.
- The present study suggested seasonality, diet preference, and growth-dependent food web dynamics in an estuary characterizing the long-term anthropogenic influences of a sea dike.

Chapter 4. Influences of artificial reef installation of fish assemblages

- More individuals and species of fish were present in artificial reefs compared to control sites.
- Water temperature over the seasons was the most important environmental factor associated with the trophic group composition of fish.
- Macrocarnivores and benthic invertivores/cleaners closely reflected habitat conditions in a consistent manner, and indicator species were found under certain environmental conditions in artificial reefs.
- While, community shifting or low effectiveness for fish recruitment were potential impacts on artificial reef installation.

Chapter 5. Influences of OSA formation in marine environment: PAHs bioaccumulation and biodegradation

- Total concentration of PAHs increased more rapidly during the first week of exposure, peaked at day 30, then gradually declined to the end of experiment.
- Bioaccumulation pattern of PAHs in clams, were identified two major groups, indicating one group of a fairly constant rate of accumulation, while another group of decreasing rate following a bell-shaped.
- Bioaccumulation of PAHs by clams was dependent on changes in abundance of Gammaproteobacteria, in particular, six key species were remarkable.
- The present study firstly demonstrated the interactions of OSAs and macrofauna/microbe in oil cleanup operations.

6.2. Discussion

This dissertation has conducted four case studies on how human activities affect marine life for the overarching research question, ***"How do anthropogenic activities affect to marine organisms?"***. Overall, this study confirmed that human activity affects and changes the structure or function of marine life, and also marine ecosystem showed resilience in the Yellow Sea (Fig. 6.1). The chapters in this study are significant in identifying the responses of marine organisms from bacteria to fish at multiple levels of organization to diverse anthropogenic activities (Table 6.1). In particular, the main contents of the chapters are highlighted in that they complement the limitations of the structure and functions of marine organisms that were not addressed in previous studies.

Benthic-pelagic coupling study addressed not only the distribution of microphyto- plankton and benthos biomass (Chl-a) in the very large marine ecosystem scale, but also the benthic production was emphasized. Despite the effects of human activity accumulated on the Yellow Sea coasts for at present, MPB as a major primary producers living in intertidal coasts has been highly productive and could be actively transferred to the open sea.

In addition, food web study covered various marine biota in estuarine areas, which showed that MPB was used as one of the most important food sources in the environment where the input of terrestrial organic matter was limited due to the construction of the sea dike. Thus, destruction of coastal habitats due to development and/or reclamation will lead to a decline in MPB production, which in turn will lead to reduced productivity of upper levels.

Although the study of artificial reefs has been addressed for fish communities only, it shows that human efforts to restore marine habitat and increase productivity have had an overall positive effect, but side effects have also been identified. This suggests that it is very difficult to restore ecosystems by artificial efforts, but may have side effects.

The OSA study has shown that microbial activity that breaks down OSA (PAHs degradation) has a beneficial effect on PAHs bioaccumulation by benthic organisms. The results of bioaccumulation and biodegradation of the oil-producing

material OSA show the very active self-purificaiton capacity of marine ecosystems. Although the impact of human activity can continue to accumulate in the oceans, it will be sustainable to the extent that the ecosystem can solve itself.

Altogether, this study was able to fill some of the gaps in previous studies under the theme of human activity and marine organisms. In particular, it was confirmed that benthic production, which has been relatively unnoticed before, may be very important for the production of upper trophics. However, the anthropogenic impacts beyond the loads that the ecosystem can accept will eventually return to humans with serious feedback. Therefore, more research afforts for smart management of marine ecosystem will be needed in the future.

6.3. Implication and future direction

From the present study, implications of case studies were suggested focused on marine organisms as presented in Table 6.2. And limitations and study highlights also indicated in Fig. 6.2 to 6.5. in aspects on biota, spatio, and temporal scales.

Of note, the study on bioaccumulation and bioremediation of OSA was firstly featured in a process including from contamination to clean-up, in particular, the bioaccumulation of PAHs in marine bivalves was stabilized in a few months (at least 30 d) by PAHs-degrading bacteria. Such processes could be appealed to the technique for handling and utilizing the OSAs in remediation oil spills. On the food web dynamics study in the closed estuary, Geum River, the utilization of terrestrial POM to marine benthic organisms was limited, and MPB was the most important food source to marine bivalves in the manner. Possibly, in the natural lotic systems without disturbance by the sea-dike, benthic organisms could use potential food sources in the wider ranges. The study on artificial reefs in the Jeju coasts, fish assemblages were more introduced in artificial reef habitats compared to control sites, and certain species showed their preferences depending on the conditions of the artificial reefs. Although there was the positive effect of the artificial reefs for the recruitment of fish individuals, potential impacts on the installation of artificial reefs were found such as community shifting of dominant fishes and low effectiveness on artificial reef introduction as well. Finally, in the scale of the Yellow Sea large marine ecosystem, the present study could provide the revisited zone for benthic-pelagic coupling as ~10 km offshore in the macrotidal regime, it is of great significance as suggesting specific areas for the management of coastal ecosystem.

Based on the current understandings and limitations in the present study, some future research directions were presented below:

- *Shotgun genomic analysis for PAHs degrading microbes*
- *Potential hazard on input of terrestrial toxicants into the estuarine food web*
- *Disturbance of artificial reef installation to the lower trophic organisms*
- *Quantification of the proportion of benthic diatom in pelagic water*
- *Evaluation of loss on marine ecosystem services by anthropogenic activities*

On the OSA study, the contribution of microbial communities was suggested, however the specific process on the bioremediation is still not clear. The shotgun genomic analysis can be the one of solutions to solve such a question, and the method is sufficient to determine the species/strain of the organism where the DNA comes from, provided its genome is already known, by using taxonomic classifier software. Thus, studies of detailed processes in biodegradation of oil-derived chemicals, can provide more accurate knowledge of the microbial communities available at the site of the oil spill accident.

The inside of the estuary dike (freshwater environment) is prone to eutrophication due to the interruption of river flow and the accumulation of terrestrial organic matters. In such an environment, large algal blooming is apt to occur, and red tide in the freshwater environment is a prominent problem because it can produce a high concentration of toxic substances such as microcystin. One way to solve this problem is to control the flow of algal bloomed water into the sea, that is, by controlling it through discharge. Given the potential impact on humans, further studies on the potential risk that potential toxicants were introduced into the estuarine food web, are needed.

Even as a part of marine habitat restoration, artificial reefs introduced into the natural environment can be disturbing native communities, and in fact our research has shown that. Unlike the mobile fishes, lower trophic communities, such as sessile invertebrates and/or meiofauna could be responded more critical to the installation of artificial reefs. Moreover, the organisms are important food sources for the upper trophic levels, thus, the study on these lower trophic organisms would be a necessary

part for sustainable management of fish communities eventually.

Benthic-pelagic coupling boundary was suggested in the present study, however, an accurate proportion of benthic diatoms in the pelagic water column in the coastal area is still unclear. Ubertini et al. (2012) reported that pennate microalgae relatively existed in water column than centric shape, which implying composition of certain microphytobenthos could be a key factor to explain the transportation of benthic productivity to open ocean side. The study on the microphytobenthos contributing to benthic-pelagic coupling has to be a part of field surveys in large-scale ecosystems, which will be labor-intensive and costly. Nevertheless, it is one of the essential parts to understand more detailed benthic-pelagic productivity and is seen as the important task to be solved in future research.

The value that marine ecosystems provide to humans is limited, and the impact of anthropogenic activities is a limiting factor to determine the quantity and quality of marine ecosystem. The global marine ecosystem, as well as the Yellow Sea, is constantly under development pressure, so valuing of marine ecosystem services and marine spatial planning must be strategic for the sustainability of marine ecosystem services. However, Korea's understanding of marine ecosystem services and marine spatial planning is very immature at the moment. Yim et al. (2018) reported that the coastal area of the Yellow Sea reduced by ~36% from 1981 to present, say 1% annual loss. That is, the benefits from the marine ecosystem of the Yellow Sea have been lost forever due to reckless development pressure and reclamation. Therefore, future studies should be supported by specific data that can be used in marine policies (e.g., the estimation of the actual price of marine ecosystem services) for the better management and sustainable development of marine ecosystem.

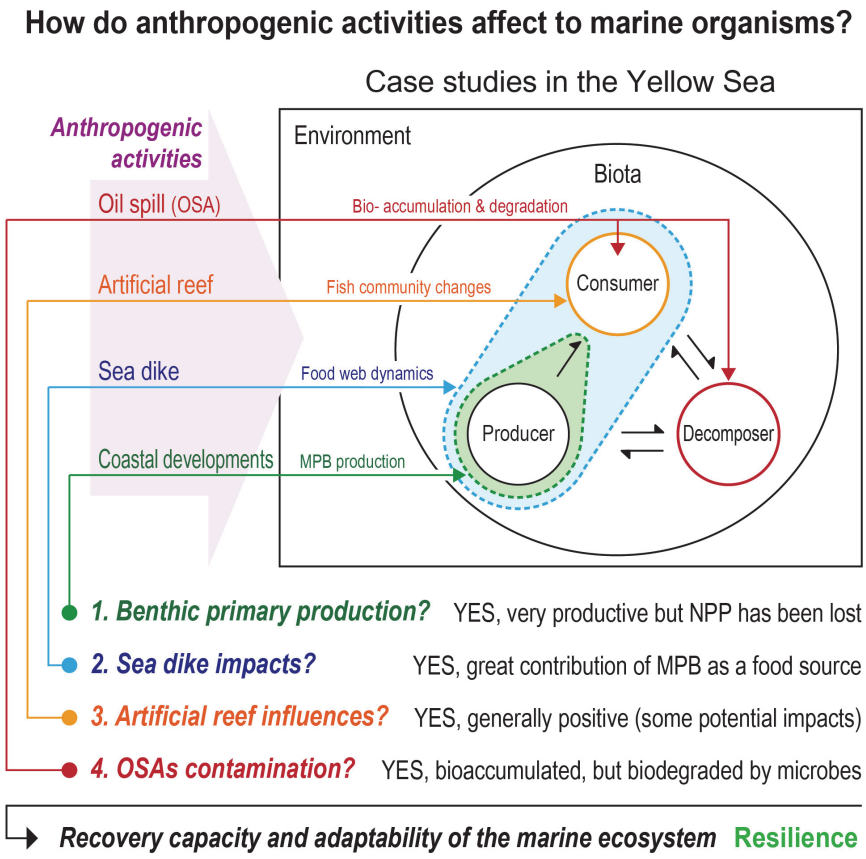

Fig. 6.1. Research questions and key findings in the present study.

Table 6.1. Spatiotemporal scale, marine organisms, and study points of subtopics which focused on this study. The marine organisms studied in each subchapter were presented as positive, negative, and neutral responses.

Spatiotemporal scale*	Marine organisms		Study points		Subtopics (chapters) in this study			
	Taxon		End-point	Remark	Benthic PP** ①	Sea dike ②	Artificial reef ③	OSAs formation ④
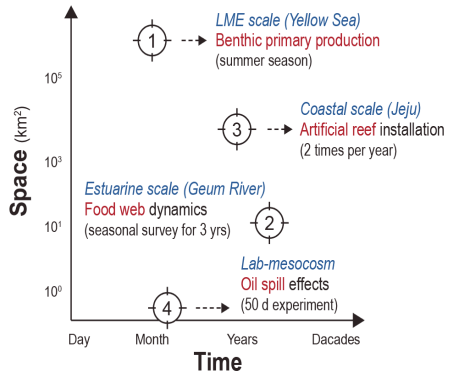	Micro-biota	Bacteria	Stucture	PAHs degraders	-	-	-	+1
			Function	-	-	-	-	-
		Phytoplankton	Structure	Biomass (Chl-*a*)	0	-	-	-
			Function	Food web	-	0	-	-
		Phytobenthos	Structure	Biomass (Chl-*a*)	+1	-	-	-
			Function	Food web	+1	+1	-	-
	Macro-biota	Macrobenthos	Structure	Invertebrates	-	0	-	-
			Function	Food web	-	0	-	-1
		Nekton	Structure	Fishes	-	0	-1, +1	-
			Function	Food web	-	0	-	-

*The numbers in the figure correspond to the subtopic order of this study, **Primary production
'+1': positive, '-1': negative, '0': neutral, '-': not available

Table 6.2. Summary of key-findings and implications in the present study.

Chapter & topics	Target organisms (end-points)	Key-findings	Implication
Chapter. 1 Benthic primary production & benthic-pelagic coupling (in situ, one month during summer)	Marine microphytobenthos (Primary production & benthic-pelagic coupling on Chl-*a* distribution)	• Great primary productivity in the Yellow Sea regime • Benthic-pelagic coupling boundary revisited (~10 km) • Transportation of benthic production by tidal height	1) For future management of coast, we provided a specific range of coastal area (~10 km) covering intertidal to subtidal habitats 2) Indiscreet development and/or alteration of the huge intertidal habitats will lead to a series of declines in entire marine productivity
Chapter. 2 Food web dynamics in a closed estuary by sea dike (in situ, 3 yr seasonal monitoring)	Marine benthos (Dietary contribution to marine benthos in food web)	• MPB & seawater POM dietary contributions (50 to ~100% of MPB, 10 to ~70% of POM)	1) The utilization of terrestrial POM to marine benthic organisms was limited in the closed estuary 2) The various food sources would be used for benthic organisms in natural lotic systems
Chapter. 3 Fish assemblages in artificial reef (in situ, 2 times per a yr for 5 yrs)	Fish communities (Community structure in natural and artificial reefs)	• Artificial reef preferences of fish assemblages • Potential impacts; community shifting & low efficiency	1) Specific fish assemblages could be introduced to certain AR habitats depending on AR preferences 2) Installation of concrete ARs on sand/sand-rocky would not be recommended
Chapter. 4 OSA exposure (lab-mesocosm, 50 d)	Marine bivalve (PAHs bioaccumulation), Marine microbe (PAHs biodegradation)	• >50% PAHs depuration • Increase of PAHs-degrading bacteria in OSA environment	1) Although the bioaccumulation problem, it might be stabilized in a few months by PAHs-degrading bacteria 2) Such processes could be taken into account when handling and utilizing the OSAs in remediating oil spills

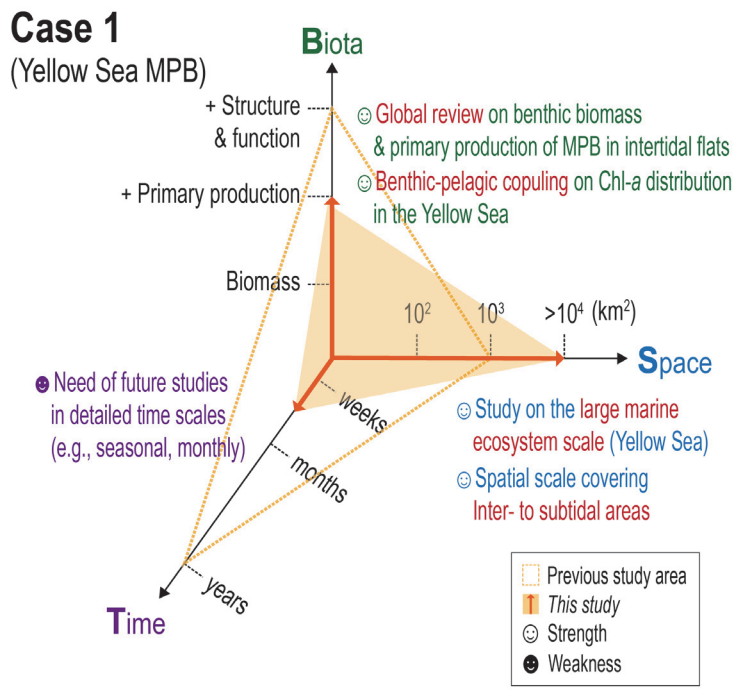

Fig. 6.2. Limitation and highlights of *Case Study 1* in aspects ot biota, time, and space scales.

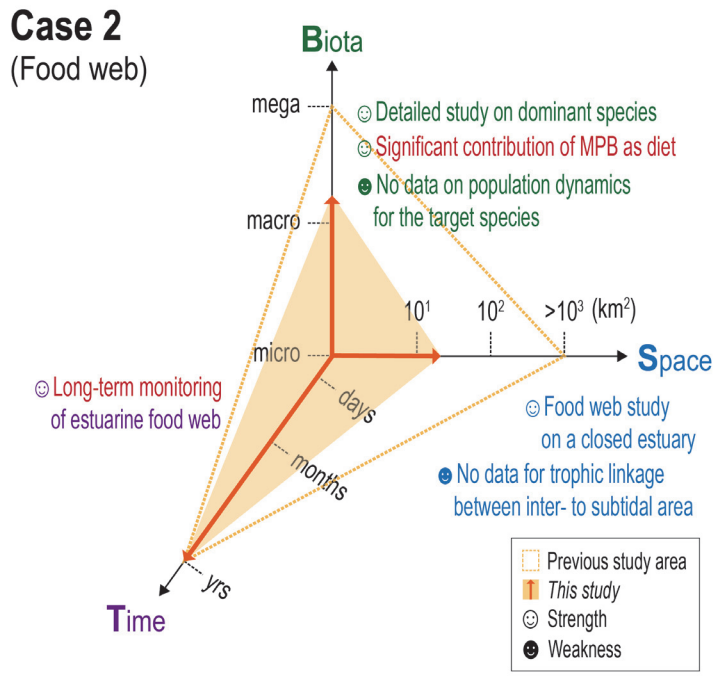

Fig. 6.3. Limitation and highlights of *Case Study 2* in aspects ot biota, time, and space scales.

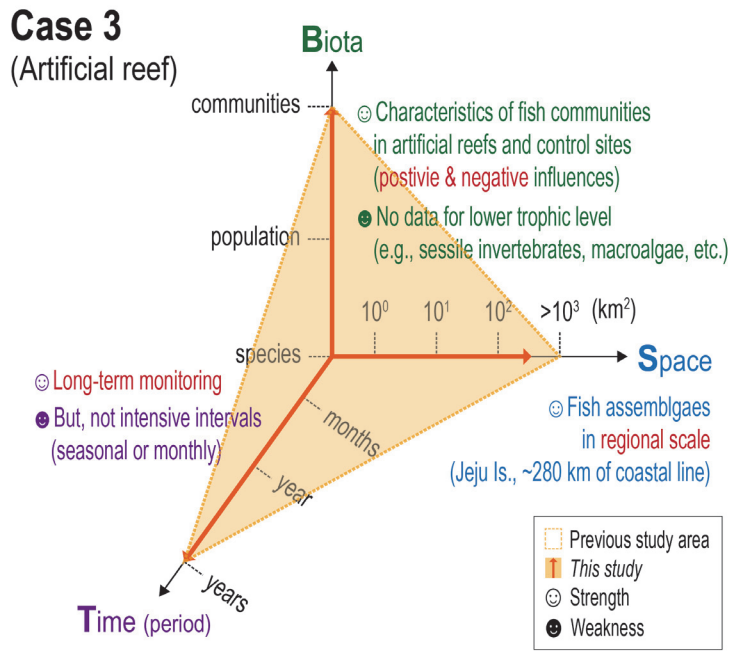

Fig. 6.4. Limitation and highlights of *Case Study 3* in aspects ot biota, time, and space scales.

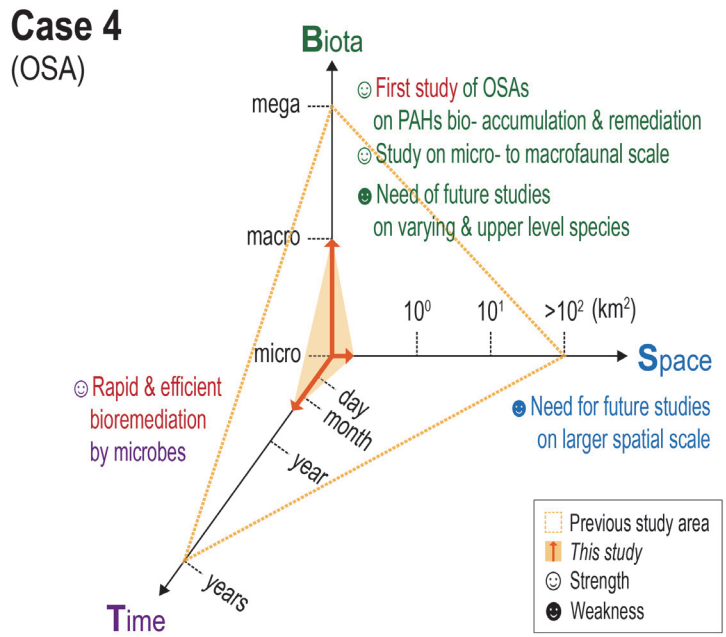

Fig. 6.5. Limitation and highlights of *Case Study 4* in aspects ot biota, time, and space scales.

REFERENCE

Agatz, M., Asmus, R. M., Deventer, B. Structural changes in the benthic diatom community along a eutrophication gradient on a tidal flat. *Helgol. Mar. Res.* **53**, 92–101 (1999).

Aislabie, J., Foght, J., Saul, D. Aromatic hydrocarbon-degrading bacteria from soil near Scott Base, Antarctica. *Polar Biol*. **23**(3), 183–188 (2000).

Ajijolaiya, L. O., Hill, P. S., Khelifa, A., Islam, R. M., Lee, K. Laboratory investigation of the effects of mineral size and concentration on the formation of oil–mineral aggregates. *Mar. Pollut. Bull.* **52**(8), 920–927 (2006).

An, S. Benthic environment and macrofaunal community changes during the dike construction in Saemangeun subtidal area, Korea. *Ocean Polar Res*. **28,** 369–383 (2006).

Anandraj, A., Perissinotto, R., Nozais, C., Stretch, D. The recovery of microalgal production and biomass in a South African temporarily open/closed estuary, following mouth breaching. *Estuar. Coast. Shelf S.* **79**, 599–606 (2008).

Andersen, T. J., Lanuru, M., van Bernem, C., Pejrup, M., Riethmueller, R. Erodibility of a mixed mudflat dominated by microphytobenthos and *Cerastoderma edule*, East Frisian Wadden Sea, Germany. *Estuar. Coast. Shelf S.* **87**, 197–206 (2010).

Anderson, T. W., DeMartini, E. E., Roberts, D. A. The relationship between habitat structure, body size and distribution of fishes at a temperate artificial reef. *B. Mar. Sci*. **44**, 681–697 (1989).

Andreoni, V. et al. Bacterial communities and enzyme activities of PAHs polluted soils. *Chemosphere* **57**(5), 401–412 (2004).

Antonio, E.S. et al. Spatialtemporal feeding dynamics of benthic communities in an estuary-marine gradient. *Estuar. Coast. Shelf S*. **112**, 86–97 (2012).

Ambrose, R. F., Anderson, T. W. Influence of an artificial reef on the surrounding infaunal community. *Mar. Biol.* **107**(1), 41–52 (1990).

Arnosti, C., Ziervogel, K., Yang, T., Teske, A. Oil-derived marine aggregates–hot spots of polysaccharide degradation by specialized bacterial communities. *Deep Sea Res. Part II Top. Stud. Oceanogr.* **129**, 179–186 (2016).

Ashok, B., Saxena, S., Musarrat, J. Isolation and characterization of four polycyclic aromatic hydrocarbon degrading bacteria from soil near an oil refinery. *Lett. Appl. Microbiol*. **21**(4), 246–248 (1995).

Asmus, R. Field measurements on seasonal variation of the activity of primary producers on a sandy tidal flat in the northern Wadden Sea. *Neth. J. Sea. Res.* **16**, 389–402 (1982).

Aya, F.A., Kudo, I. Nitrogen stable isotopes reveal age-dependent dietary shift in the Japanese scallop *Mizuhopecten yessoensis*. *Isot. Environ. Healt. S.* **53**, 80–90 (2017).

Baillie, P. W. Oxygenation of intertidal estuarine sediments by benthic microalgal photosynthesis. *Estuar. Coast. Shelf S.* **22**, 143–159 (1986).

Bandowe, B. A. M. Polycyclic aromatic compounds (PAHs and oxygenated PAHs) and trace metals in fish species from Ghana (West Africa): bioaccumulation and health risk assessment. *Environ. Int.* **65**, 135–146 (2014).

Barhoumi, B. et al. Occurrence of polycyclic aromatic hydrocarbons (PAHs) in mussel (*Mytilus galloprovincialis*) and eel (*Anguilla anguilla*) from Bizerte lagoon, Tunisia, and associated human health risk assessment. *Cont. Shelf. Res.***124**, 104–116 (2016).

Barranguet, C., Kromkamp, J., Peene, J. Factors controlling primary production and photosynthetic characteristics of intertidal microphytobenthos. *Mar. Ecol. Prog. Ser.* **173**,

117–126 (1998).

Bartoli, M., Castaldelli, G., Nizzoli, D., Viaroli, P. Benthic primary production and bacterial denitrification in a Mediterranean eutrophic coastal lagoon. *J. Exp. Mar. Biol. Ecol.* **438**, 41–51 (2012).

Baumard, P. et al. Concentrations of PAHs (polycyclic aromatic hydrocarbons) in various marine organisms in relation to those in sediments and to trophic level. *Mar. Pollut. Bull*. **36**(12), 951–960 (1998).

Baussant, T., Sanni, S., Jonsson, G., Skadsheim, A., Børseth, J. F. Bioaccumulation of polycyclic aromatic compounds: 1. Bioconcentration in two marine species and in semipermeable membrane devices during chronic exposure to dispersed crude oil. *Environ. Toxicol. Chem*. **20**(6), 1175–1184 (2001).

Baussant, T. et al. Bioaccumulation of polycyclic aromatic compounds: 2. Modeling bioaccumulation in marine organisms chronically exposed to dispersed oil. *Environ. Toxicol. Chem*. **20**(6), 1185–1195 (2001).

Bebianno, M. J., Lopes, B., Guerra, L., Hoarau, P., Ferreira, A. M. Glutathione S-tranferases and cytochrome P450 activities in *Mytilus galloprovincialis* from the South coast of Portugal: effect of abiotic factors. *Environ. Int*. **33**(4), 550–558 (2007).

Beazley, M. J. et al. Microbial community analysis of a coastal salt marsh affected by the Deepwater Horizon oil spill. *PloS one* **7**(7), e41305 (2012).

Bennett, M. G., Kozak, J. P., Spatial and temporal patterns in fish community structure and abundance in the largest US river swamp, the Atchafalaya River floodplain, Louisiana. *Ecol. Freshw. Fish.* **25**, 577–589 (2015).

Berman-Frank, I., Erez, J., Kaplan, A. Changes in inorganic carbon uptake during the progression of a dinoflagellate bloom in a lake ecosystem. *Can. J. Bot*. **76**(6) 1043–1051 (1998).

Bigelow, G.W. Primary productivity of benthic microalgae in the Newport River estuary. MS thesis (North Carolina State University, Raleigh, NC, USA, 1977).

Billerbeck, M., Røy, H., Bosselmann, K., Huettel, M. Benthic photosynthesis in submerged Wadden Sea intertidal flats. *Estuar. Coast. Shelf S.* **71**, 704–716 (2007).

Bodin, N. et al. Seasonal variations of a battery of biomarkers and physiological indices for the mussel Mytilus galloprovincialis transplanted into the northwest Mediterranean Sea. *Comp. Biochem. Phys. C*. **138**(4), 411–427 (2004).

Boglaienko, D., Tansel, B. Partitioning of fresh crude oil between floating, dispersed and sediment phases: Effect of exposure order to dispersant and granular materials. *J. Environ. Manage.* **175**, 40–45 (2016).

Bohnsack, J. A., Sutherland, D.L. Artificial reef research: a review with recommendations for future priorities. *B. Mar. Sci.* **37**, 11–39 (1985).

Boldt, J. L. et al. Developing ecosystem indicators for responses to multiple stressors. Oceanography **27**, 116–133 (2014).

Bombace, G., Fabi, G., Fiorentini, L., Speranza, S. Analysis of the efficacy of artificial reefs located in five different areas of the Adriatic Sea. *B. Mar. Sci.* **55**, 559–580 (1994).

Brotto, D., Krohling, W., Zalmon, I. Usage patterns of an artificial reef by the fish community on the northern coast of Rio de Janeiro–Brazil. *J. Coast. Res.* **39**, 1122–1125 (2006).

Brotas, V., Catarino, F. Microphytobenthos primary production of Tagus estuary intertidal flats (Portugal). *Neth. J. Aquat. Ecol.* **29**, 333–339 (1995).

Cadée, G. C., Hegeman, J. Primary production of the benthic microflora living on tidal flats

in the Dutch Wadden Sea. *Neth. J. Sea. Res.* **8**, 260–291 (1974).
Cadée, G. C., Hegeman, J. Distribution of primary production of the benthic microflora and accumulation of organic matter on a tidal flat area, Balgzand, Dutch Wadden Sea. *Neth. J. Sea. Res.* **11**, 24–41 (1977).
Cadée, G. C. Reappraisal of the production and import of organic carbon in the western Wadden Sea. *Neth. J. Sea. Res.* **14**, 305–322 (1980).
Cahoon, L. B. The role of benthic microalgae in neritic ecosystems. *Oceanogr. Mar. Biol.* **37**, 47–86 (1999).
Camus, L. et al. Biomarker responses and PAH uptake in Mya truncata following exposure to oil–contaminated sediment in an Arctic fjord (Svalbard). *Sci. Total. Environ.* **308**(1), 221–234 (2003).
Carmichael, R. H. et al. Assimilation of oil-derived elements by oysters due to the Deepwater Horizon oil spill. *Environ. Sci. Technol*. **46**(23), 12787–12795 (2012).
Charbonnel, E., Serre, C., Ruitton, S., Harmelin, J.-G., Jensen, A. Effects of increased habitat complexity on fish assemblages associated with large artificial reef units (French Mediterranean coast). *ICES J. Mar. Sci.* **59**, S208–S213 (2002).
ChemSpider. database via ACD/Labs Percepta Platform, PhysChem Module 2017. Available: http://www.chemspider.com/ [last accessed: 06/21/17].
Choi, H., Choi, B., Shin, K.-H. Determination of trophic position using nitrogen isotope ratio of individual amino acid in the Geum Estuary. *KJEE* **50**, 432–440 (2017).
Choy, E. J., An, S., Kang, C. K. Pathways of organic matter through food webs of diverse habitats in the regulated Nakdong River estuary (Korea). *Estuar. Coast. Shelf S.* **78**, 215–226 (2008).
Christianen, M. et al. Benthic primary producers are key to sustain the Wadden Sea food web: stable carbon isotope analysis at landscape scale. *Ecology* **98**, 1498–1512 (2017).
Cibic, T., Blasutto, O., Hancke, K., Johnsen, G. Microphytobenthic species composition, pigment concentration, and primary production in sublittoral sediments of the Trondheimsfjord (Norway). *J. Phycol.* **43**, 1126–1137 (2007).
Clarke, K., Gorley, R., 2006. PRIMER v6: user manual/tutorial (Plymouth routines in multivariate ecological research). Plymouth: Primer-E Ltd.
Claudet, J., Pelletier, D. Marine protected areas and artificial reefs: A review of the interactions between management and scientific studies. *Aquat. Living Resour*. **17**, 129–138 (2004).
Cognie, B., Barillé, L., Rincé, Y. Selective feeding of the oyster *Crassostrea gigas* fed on a natural microphytobenthos assemblage. *Estuaries* **24**, 126–134 (2001).
Cohen, R. A., Wilkerson, F. P., Parker, A. E., Carpenter, E. J. Ecosystem-scale rates of primary production within wetland habitats of the northern San Francisco Estuary. *Wetlands* **34**, 759–774 (2014).
Cole, J. R. Ribosomal Database Project: data and tools for high throughput rRNA analysis. *Nucleic Acids Res*. **42**(D1), D633–D642 (2013).
Colijn, F., Dijkema, K. S. Species composition of benthic diatoms and distribution of chlorophyll *a* on an intertidal flat in the Dutch Wadden Sea. *Mar. Ecol. Prog. Ser.* **4**, 9–21 (1981).
Colijn, F., De Jonge, V. N. Primary production of microphytobenthos in the Ems-Dollard Estuary. *Mar. Ecol. Prog. Ser.* **14**, 185–196 (1984).
Collins, K., Jensen, A., Lockwood, A. Fishery enhancement reef building exercise. *Chem.*

Ecol. **4**, 179–187 (1990).

Coosen, J., Seys, J., Meire, P. M., Craeymeersch, J. A. M. Effect of sedimentological and hydrodynamical changes in the intertidal areas of the Oosterschelde estuary (SW Netherlands) on distribution, density and biomass of five common macrobenthic species : *Spio martinensis* (Mesnil), *Hydrobia ulvae* (Pennant), *Arenicola marina* (L.), *Scoloplos armiger* (Muller) and *Bathyporeia* sp.. *Hydrobiologia* **282**, 235–249 (1994).

Costanza, R., et al. The value of the world's ecosystem services and natural capital. *Nature* **387**, 253 (1997).

Costello M. J. et al. A census of marine biodiversity knowledge, resources, and future challenges. *PLoS One* **5**, e12110 (2010).

Couch, C.A. Carbon and nitrogen stable isotopes of meiobenthos and their food resources. *Estuar. Coast. Shelf S.* **28**, 433–441 (1989).

Cui, Z., Lai, Q., Dong, C., Shao, Z. Biodiversity of polycyclic aromatic hydrocarbon-degrading bacteria from deep sea sediments of the Middle Atlantic ridge. *Environ. Microbiol*. **10**(8), 2138–2149 (2008).

Darley, W. M., Dunn, E. L., Holmes, K. S., Larew III, H. G. A ^{14}C method for measuring epibenthic microalgal productivity in air. *J. Exp. Mar. Biol. Ecol.* **25**, 207–217 (1976).

Darley, W. M., Montague, C. L., Plumley, F. G., Sage, W. W., Psalidas, A. T. Factors limiting edaphic algal biomass and productivity in a georgia salt marsh. *J. Phycol.* **17**, 122–128 (1981).

Davenport, J. Size-differential feeding in *Pinna nobilis* L. (Mollusca: Bivalvia): exploitation of detritus, phytoplankton and zooplankton. *Estuar. Coast. Shelf S*. **92**, 246–254 (2011).

Davies, J. L., Clayton, K. M. Geographical variation in coastal development (2nd Ed). London: Longman (1980).

Davoult, D. et al. Spatio-temporal variability of intertidal benthic primary production and respiration in the western part of the Mont Saint-Michel Bay (Western English Channel, France). *Hydrobiologia* **620**, 163–172 (2009).

De Jong, D. J., Nienhuis, P. H., Kater, B. J. Microphytobenthos in the Oosterschelde estuary (The Netherlands), 1981–1990; consequences of a changed tidal regime. *Hydrobiologia*, **282/283**, 183–195 (1994).

De Jong, D. J., De Jonge, V. N. Dynamics and distribution of microphytobenthic chlorophyll-*a* in the Western Scheldt estuary (SW Netherlands). *Hydrobiologia* **311**, 21–30 (1995).

De Jonge, V. N., Van Beuselom, J. E. E. Contribution of resuspended microphytobenthos to total phytoplankton in the Ems estuary and its possible role for grazers. *Neth. J. Sea Res*. **30**, 91–105 (1992).

De Jonge, V. N., Colijn, F. Dynamics of microphytobenthos biomass in the Ems estuary. *Mar. Ecol. Prog. Ser.* **104**, 185–196 (1994).

De Jonge, V. N., Van Beuselom, J. E. E. Wind-and tide-induced resuspension of sediment and microphytobenthos from tidal flats in the Ems estuary. *Limnol. Oceanogr*. **40**, 776–778 (1995).

De Jonge, V. N., de Boer, W. F., de Jong, D. J., Brauer, V. S. Long-term mean annual microphytobenthos chlorophyll *a* variation correlates with air temperature. *Mar. Ecol. Prog. Ser.* **468**, 43–56 (2012).

Delong, M. D., Thorp, J. H., Greenwood, K. S., Miller, M. C. Responses of consumers and food resources to a high magnitude, unpredicted flood in the upper Mississippi River basin. *Regul. River* **17**, 217–234 (2001).

Derbyshire, K., 2006. Fisheries Guidelines for Fish-Friendly Structures. Department of Primary Industries and Fisheries, Queensland.

Dias, E., Morais, P., Cotter, A. M., Antunes, C., Hoffman, J. C. Estuarine consumers utilize marine, estuarine and terrestrial organic matter and provide connectivity among these food webs. *Mar. Ecol. Prog. Ser*. **554**, 21–34 (2016).

Díaz-Castañeda, V., Reish, D. J., 2009. Polychaetes in environmental studies. In: Annelids as Model System in the Biological Sciences. J. Wiley, Sons, p. 205–227.

Dimitriou-Christidis, P., Harris, B. C., McDonald, T. J., Reese, E., Autenrieth, R. L. Estimation of selected physicochemical properties for methylated naphthalene compounds. *Chemosphere* **52**(5), 869–881 (2003).

Dong, Y.-W., Huang, X.-W., Wang, W., Li, Y., Wang, J. The marine 'great wall' of China: local- and broad-scale ecological impacts of coastal infrastructure on intertidal microbenthic communities. *Diversity Distrib*. **22**, 731–744 (2016).

Dos Santos, L. N., Brotto, D. S., Zalmon, I.R. Fish responses to increasing distance from artificial reefs on the Southeastern Brazilian Coast. *J. Exp. Bar. Biol. Ecol*. **386**, 54–60 (2010).

Du, G. Y., Chung, I. K. Estimating areal production of intertidal microphytobenthos based on spatio-temporal community dynamics and laboratory measurements. *Ocean Sci. J.* **44**, 189–197 (2009).

Dubois, S., Orvain, F., Marin-Léal, J. C., Ropert, M., Lefebvre, S. Small-scale spatial variability of food partitioning between cultivated oysters and associated suspensionfeeding species, as revealed by stable isotopes. *Mar. Ecol. Prog. Ser*. **336**, 151–160 (2007).

Dufrêne, M., Legendre, P. Species assemblages and indicator species: the need for a flexible asymmetrical approach. *Ecol. Monogr.* **67**, 345–366 (1997).

Duran, R., Cravo-Laureau, C. Role of environmental factors and microorganisms in determining the fate of polycyclic aromatic hydrocarbons in the marine environment. *FEMS Microbiol. Rev*. **40**(6), 814–830 (2016).

Dyksterhouse, S. E., Gray, J. P., Herwig, R. P., Lara, J. C., Staley, J. T. *Cycloclasticus pugetii* gen. nov., sp. nov., an aromatic hydrocarbon-degrading bacterium from marine sediments. *Int. J. Syst. Evol. Micr*. **45**(1), 116–123 (1995).

Edgar, R. C. Search and clustering orders of magnitude faster than BLAST. *Bioinformatics* **26**(19), 2460–2461 (2010).

Fabi, G., Fiorentini, L. Comparison between an artificial reef and a control site in the Adriatic Sea: Analysis of four years of monitoring. *B. Mar. Sci*. **55**, 538–558 (1994).

Falkowski, P. G., Barber, R. T., Smetacek, V. Biogeochemical controls and feedbacks on ocean primary production. *Science* **281**, 200–206 (1998).

Fang, L. et al. Preliminary Evaluation on Resources Enhancement of Artificial Reef in the East Corner of Zhelang Shanwei. *Asian Agric. Res.* **5**, 111 (2013).

Ferrari, G. M., Bo, F. G., Babin, M. Geo-chemical and optical characterizations of suspended matter in European coastal waters. *Estuar. Coast. Shelf Sci*. **57**(1), 17–24 (2003).

Field, J., Clarke, K., Warwick, R. A practical strategy for analyzing multispecies distribution patterns. *Mar. Ecol. Prog. Ser*. **8**, 37–52 (1982).

Field, C. B., Behrenfeld, M. J., Randerson, J. T., Falkowski, P. Primary production of the biosphere: Integrating terrestrial and oceanic components. *Science* **281**, 237–240 (1998).

Fielding, P. J., Damstra, K. St. J., Branch, G. M. Benthic diatom biomass, production, and

sediment chlorophyll in Langebaan lagoon, South Africa. *Estuar. Coast. Shelf S.* **27**, 413–426 (1988).

Finlay, J. C., Kendall, C., 2007. Stable isotope tracing of temporal and spatial variability in organic matter sources to freshwater ecosystems. p. 283–333. Stable isotope in ecology and environmental science. Wiley.

Fitzhardinge, R., Bailey-Brock, J. Colonization of artificial reef materials by corals and other sessile organisms. *B. Mar. Sci*. **44**, 567–579 (1989).

Fry, B., Sherr, E. B. $\delta^{13}C$ measurements as indicators of carbon flow in marine and freshwater ecosystems. *Contrib. Mar. Sci*. **27**, 13–47 (1984).

Fuji, A., Watanabe, H., Ogura, K., Noda, T., Goshima, S. Abundance and productivity of microphytobenthos on a rocky shore in southern Hokkaido. *Bull. Fac. Fish. Hokkaido Univ.* **42**, 136–146 (1991).

Gallagher, J. L., Daiber, F. C. Primary production of edaphic algal communities in a Delaware salt marsh. *Limnol. Oceanogr.* **19**, 390–395 (1974).

Galván, K., Fleeger, J. W., Fry, B. Stable isotope addition reveals dietary importance of phytoplankton and microphytobenthos to saltmarsh infauna. *Mar. Ecol. Prog. Ser*. **359**, 37–49 (2008).

García-Robledo, E., Corzo, A., Papaspyrou, S., Jiménez-Arias, J. L., Villahermosa, D. Freeze-lysable inorganic nutrients in intertidal sediments: dependence on microphytobenthos abundance. *Mar. Ecol. Prog. Ser.* **403**, 155–163 (2010).

Ge, B. et al. Impact of dike age on biodiversity and functional composition of soil macrofaunal communities in poplar forests in a reclaimed coastal area. *Turk. J. Zool*. **40**, 241–247 (2016).

Geiselbrecht, A. D., Hedlund, B. P., Tichi, M. A., Staley, J. T. Isolation of marine polycyclic aromatic hydrocarbon (PAH)-degrading *Cycloclasticus* strains from the Gulf of Mexico and comparison of their PAH degradation ability with that of Puget Sound *Cycloclasticus* strains. *Appl. Environ. Microb*. **64**(12), 4703–4710 (1998).

Genovese, M. et al. Effective bioremediation strategy for rapid in situ cleanup of anoxic marine sediments in mesocosm oil spill simulation. *Front. Microbiol*., **5**, 162 (2014).

Godoy, E. A. S., Almeida, T. C. M., Zalmon, I. R. Fish assemblages and environmental variables on an artificial reef north of Rio de Janeiro, Brazil. *ICES J. Mar. Sci.* **59**, S138–S143 (2002).

Golubkov, S. M. A relative contribution of carbon from green tide algae *Cladophora glomerata* and *Ulva intestinalis* in the coastal food webs in the Neva Estuary (Baltic Sea) *Mar. Pollut. Bull*. **126**, 43–50 (2018).

Gong, Y. et al. A review of oil, dispersed oil and sediment interactions in the aquatic environment: influence on the fate, transport and remediation of oil spills. *Mar. Pollut. Bull*. **79**(1), 16–33 (2014).

Goto, N., Mitamura, O., Terai, H. Seasonal variation in primary production of microphytobenthos at the Isshiki intertidal flat in Mikawa Bay. *Limnology* **1**, 133–138 (2000).

Goudi, A., 2006. The Human Impact on the Natural Environment: Past, Present and Future. Blackwell. Oxford, RU.

Gould, D. M., Gallagher, E. D. Field measurement of specific growth rate, biomass, and primary production of benthic diatoms of Savin Hill Cove, Boston. *Limnol. Oceanogr.* **35**, 1757–1770 (1990).

Gouleau, D., Blanchard, G., Cariou-Le Gall, V. Production potentielle et consummation

d'oxygène sur une vasière intertidale au cours d'une émersion. *Vie Milieu* **44**, 109–115 (1994).

Gounand, I., Little, C. J., Harvey, E., Altermatt, F. Cross-ecosystem carbon flows connecting ecosystems worldwide. *Nat. Commun.* **9**, 4825 (2018).

Grant, J., Mills, E. L., Hopper, C. M. A chlorophyll budget of the sediment-water interface and the effect of stabilizing biofilms on particle fluxes. *Ophelia* **26**, 207–219 (1986).

Gratwicke, B., Speight, M. R. Effects of habitat complexity on Caribbean marine fish assemblages. *Mar. Ecol. Prog. Ser.* **292**, 301–310 (2005).

Grippo, M. A., Fleeger, J. W., Dubois, S. F., Condrey, R. Spatial variation in basal resources supporting benthic food webs revealed for the inner continental shelf. *Limnol. Oceanogr*. **56**, 841–856 (2011).

Gu, B., Schelske, C. L., Brenner, M. Relationship between sediment and plankton isotope ratios ($\delta^{13}C$ and $\delta^{15}N$) and primary productivity in Florida lakes. *Can. J. Fish. Aquat. Sci*. **53**, 875–883 (1996).

Gu, B. Variations and controls of nitrogen stable isotopes in particulate organic matter of lakes. *Oecologia* **160**, 421–431 (2009).

Gustitus, S. A., Clement, T. P. Formation, fate and impacts of microscopic and macroscopic oil-sediment residues in nearshore marine environments—a critical review. *Rev. Geophys*. **55**(4), 1130–1157 (2017).

Gutierrez, T., Nichols, P. D., Whitman, W. B., Aitken, M. D. *Porticoccus hydrocarbonoclasticus* sp. nov., an aromatic hydrocarbon-degrading bacterium identified in laboratory cultures of marine phytoplankton. *Appl. Environ. Microb*. **78**(3), 628–637 (2012).

Habit, E., Belk, M. C., Parra, O. Response of the riverine fish community to the construction and operation of a diversion hydropower plant in central Chile. *Aquat. Conserv.* **17**, 37–49 (2007).

Hackradt, C. W., Félix-Hackradt, F. C. Assembléia de peixes associados a ambientes consolidados no litoral do Paraná, Brasil: uma análise qualitativa com notas sobre sua bioecologia. *Pap. Avulsos. Zool.* (São Paulo) **49**, 389–403 (2009).

Hackradt, C. W., Félix-Hackradt, F. C., García-Charton, J.A. Influence of habitat structure on fish assemblage of an artificial reef in southern Brazil. *Mar. Environ. Res*. **72**, 235–247 (2011).

Hadas, O., Altabet,. A., Agnihotri, R. Seasonally varying nitrogen isotope biogeochemistry of particulate organic matter in Lake Kinneret, Israel. *Limnol. Oceanogr*. **54**, 75–85 (2009).

Halpern, B. S., Floeter, S. R. Functional diversity responses to changing species richness in reef fish communities. *Mar. Ecol. Prog. Ser.* **364**, 147–156 (2008).

Hao, Q. et al. Standing crop and primary production of benthic microalgae on the tidal flats in Yueqing bay. *J. Ocean Univ. China* **10**, 157–164 (2011).

Hardison, A. K. et al. Microphytobenthos and benthic macroalgae determine sediment organic matter composition in shallow photic sediments. *Biogeosciences* **10**, 5571–5588 (2013).

Hargrave, B. T., Prouse, N. J., Phillips, G., Neame, P. A. Primary production and respiration in pelagic and benthic communities at two intertidal sites in the upper Bay of Fundy. *Can. J. Fish. Aquat. Sci.* **40**, s229–s243 (1983).

Hazen, T. C., Prince, R. C., Mahmoudi, N. Marine oil biodegradation. *Environ. Sci. Technol*.

50(5), 2121–2129 (2016).
Hazen, T. C. et al. Deep-sea oil plume enriches indigenous oil-degrading bacteria. *Science* 2010, **330**(6001), 204–208 (2016).
Heinrich, B. Winter foraging at carcasses by three sympatric corvids, with emphasis on recruitment by the raven, *Corvus corax*. *Behav. Ecol. Sociobiol*. **23**, 141–156 (1988).
Hellebust, J. A., Lewin, J. Heterotrophic nutrition. In The Biology of Diatoms. **13**, 167–197 (1977).
Herman, P. M. J., Middelburg, J. J., Widdows, J., Lucas, C. H., Heip, C. H. R. Stable isotopes as trophic tracers: combining field sampling and manipulative labelling of food resources for macrobenthos. *Mar. Ecol. Prog. Ser*. **204**, 79–92 (2000).
Hogg, R. S., Coghlan, S. M. Jr., Zydlewski, J., Gardner, C. Fish community response to a small-stream dam removal in a maine coastal river tributary. *T. Am. Fish. Soc*. **144**, 467–479 (2015).
Hong, S. et al. Environmental and ecological effects and recoveries after five years of the Hebei Spirit oil spill, Taean, Korea. *Ocean. Coast. Manage.* **102**, 522–532 (2014).
Hong, S. et al. Effect-directed analysis and mixture effects of AhR-active PAHs in crude oil and coastal sediments contaminated by the Hebei Spirit oil spill. *Environ. Pollut*. **199**, 110–118 (2015).
Hubas, C., Davoult, D., Cariou, T., Artigas, L. F. Factors controlling benthic metabolism during low tide along a granulometric gradient in an intertidal bay (Roscoff Aber Bay, France). *Mar. Ecol. Prog. Ser.* **316**, 53–68 (2006).
Hur, J. W., Jang, M.-H., Shin, K.-H., Lee, K.-L., Chang, K.-H. Ecological niche space of fish communities in impounded sections of large rivers: its application to assessment of the impact of weirs on river ecosystems. *Sustainability* **10**, 4784 (2018).
Hwang, J. H., Van, S. P., Choi, B. J., Chang, Y. S., Kim, Y. H. The physical processes in the Yellow Sea. *Ocean Coast. Manage.* **102**, 449–457 (2014).
IOC/UNESCO, FAO, UNDP, 2011. A Blueprint for Ocean and Coastal Sustainability.
Jackson, J. B. C. et al. Historical overfishing and the recent collapse of coastal ecosystems. *Science* **293**, 629–637 (2001).
Jassby, A. D., Platt, T. Mathematical formulation of the relationship between photosynthesis and light for phytoplankton. *Limnol. Oceanogr.* **21**, 540–547 (1976).
Jaxion-Harm, J., Szedlmayer, S. T. Depth and artificial reef type effects on size and distribution of red snapper in the Northern Gulf of Mexico. *N. Am. J. Fish. Manage.* **35**(1), 86–96 (2015).
Jensen, A. Artificial reefs of Europe: perspective and future. *ICES J. Mar. Sci.* **59**, S3–S13 (2002).
Jensen, A., Collins, K., Free, E., Bannister, R. Lobster (Homarus gammarus) movement on an artificial reef: the potential use of artificial reefs for stock enhancement. *Crustaceana* **67**, 198–211 (1994).
Jeppesen, E. et al. Zooplankton as indicators in lakes: a scientific–based plea for including zooplankton in the ecological quality assessment of lakes according to the European Water Framework Directive (WFD). *Hydrobiologia* **676**, 279 (2011).
Jesus, B., Brotas, V., Marani, M., Paterson, D. M. Spatial dynamics of microphytobenthos determined by PAM fluorescence. *Estuar. Coast. Shelf S.* **65**, 30–42 (2005).
Johnson, T. et al. Fish production and habitat utilization on a southern California artificial reef. *B. Mar. Sci.* **55**, 709–723 (1994).

Joint, I. R. Microbial production of an estuarine mudflat *Estuar. Coast. Shelf S.* **7**, 185–195 (1978).

Jordan, L. K., Gilliam, D. S., Spieler, R.E. Reef fish assemblage structure affected by small-scale spacing and size variations of artificial patch reefs. *J. Exp. Mar. Biol. Ecol.* **326**, 170–186 (2005).

Kang, C.-K., Sauriau, P.-G., Richard, P., Blanchard, G. F. Food sources of the infaunal suspension-feeding bivalve *Cerastoderma edule* in a muddy sandflat of Marennes-Oléron Bay, as determined by analyses of carbon and nitrogen stable isotopes. *Mar. Ecol. Prog. Ser*. **187**, 147–158 (1999).

Kang, C.-K. et al. Trophic importance of benthic microalgae to macrozoobenthos in coastal bay systems in Korea: dual stable C and N isotope analyses. *Mar. Ecol. Prog. Ser.* **259**, 79–92 (2003).

Kang, C.-K. et al. Microphytobenthos seasonality determines growth and reproduction in intertidal bivalves. *Mar. Ecol. Prog. Ser*. **315**, 113–127 (2006).

Kang, C.-K., Choy, E. J., Hur, Y.-B., Myeong, J.-I. Isotopic evidence of particle size dependent food partitioning in cocultured sea squirt *Halocynthia roretzi* and Pacific oyster *Crassostrea gigas*. *Mar. Ecol. Prog. Ser.* **6**, 289–302 (2009).

Kang, H.-J. Prediction of ecotoxicity of heavy crude oil: contribution of measured components. *Environ. Sci. Technol.* **48**(5), 2962–2970 (2014).

Kang, C.-K. et al. Linking intertidal and subtidal food webs: consumer-mediated transport of intertidal benthic microalgal carbon. *PLoS One* **10**, e0139802 (2015).

Kang, H. Y., Lee, Y.-J., Lee, W.-C., Kim, H. C., Kang, C.-K. Gross biochemical and isotopic analyses of nutrition-allocation strategies for somatic growth and reproduction in the bay scallop *Argopecten irradians* newly introduced into Korean waters. *Aquaculture* **503**, 156–166 (2019).

Kappell, A. D. The polycyclic aromatic hydrocarbon degradation potential of Gulf of Mexico native coastal microbial communities after the Deepwater Horizon oil spill. *Front. Microbiol*. **5**, 205 (2014).

Karlson, A. M. L., Niemand, C., Savage, C., Pilditch, C. A. Density of key-species determines efficiency of macroalgae detritus uptake by intertidal benthic communities. *PLoS One* **11**, e0158785 (2016).

Karlsson, J. et al. Terrestrial organic matter support of lake food webs: evidence from lake metabolism and stable hydrogen isotopes of consumers. *Limnol. Oceanogr*. **57**, 1042–1048 (2012).

Kasai, A., Nakata, A. Utilization of terrestrial organic matter by the bivalve *Corbicula japonica* estimated from stable isotope analysis. *Fisheries Sci*. **71**, 151–158 (2005).

Kasai, Y. et al. Predominant growth of *Alcanivorax* strains in oil-contaminated and nutrient-supplemented sea water. *Environ. Microbiol*. **4**(3), 141–147 (2002).

Kelley, B. J., McKellar, H. N., Zingmark, R.G. Summary and comparison of component productivities. In South Carolina coastal wetland impoundments ecological characterization, management, status and use. Vol. II. Technical synthesis (R. Devoe, D. Baughman (eds). South Carolina Sea Grant Publication #SC-SG-TR-86-2, 1986).

Khelifa, A. Sediment contamination due to oil-suspended particulate matter aggregation during oil spills in coastal waters. In Contaminated Sediments: 5th Volume, Restoration of Aquatic Environment, *Am. Soc. Test. Mater.* 208–228 (2012).

Khodse, V. B. Distribution and seasonal variation of concentrations of particulate

carbohydrates and uronic acids in the northern Indian Ocean. *Mar. Chem*. **103**, 327–346 (2007).

Kim, J.-W., Kim, H.-W., Huh, S.-H., Kwak, S.-N. Seasonal variation and species composition of fish species in artificial reefs in the Shinyang-Ri coastal waters off Jeju island, Korea. *J. Kor. Soc. Fish. Tech.* **47**(2), 118–127 (2011).

Kim, M. et al. Hebei Spirit oil spill monitored on site by fluorometric detection of residual oil in coastal waters off Taean, Korea. *Mar. Pollut. Bull*. **60**(3), 383–389 (2010).

Kim, Y.-H., Ryou, D.-K. Study on the growth of *Mactra veneriformis* (Reeve). *Bull. Kunsan Fish. J. Coll*. **25**, 41–47 (1991).

Kiørboe, T., Møhlenberg, F. Particle selection in suspension-feeding bivalves. *Mar. Ecol. Prog. Ser*. **5**, 291–296 (1981).

Ko, M.-H., Kwan, Y.-S., Lee, W.-K., Won, Y.-J. Impact of human activities on changes of ichthyofauna in Dongjin River of Korea in the past 30 years. *Anim. Cells Syst*. **21**, 207–216 (2017).

Koh, C.-H. Tidal resuspension of microphytobenthic chlorophyll *a* in a Nanaura mudflat, Saga, Ariake Sea, Japan: flood–ebb and spring–neap variations. *Mar. Ecol. Prog. Ser*. **312**, 85–100 (2006).

Koh, C.-H., Khim, J. S., Araki, H., Yamanishi, H., Koga, K. Within-day and seasonal patterns of microphytobenthos biomass determined by co-measurement of sediment and water column chlorophylls in the intertidal mudflat of Nanaura, Saga, Ariake Sea, Japan. *Estuar. Coast. Shelf S.* **72**, 42–52 (2007).

Koh, C.-H., Khim, J. S. The Korean tidal flat of the Yellow Sea: physical setting, ecosystem and management. *Ocean Coast. Manage*. **102**, 398–414 (2014).

Kojima, S. Fishing for dolphins in the western part of the Japan Sea. II. Why do the fish take shelter under floating materials. *Bull. Jap. Soc. Sci. Fish* **21**, 1049–1052 (1956).

Koo, B. J. et al. Changes in macrobenthic community structure on Gunsan tidal flat after the closing of the Saemangeum 4th dyke. *Ocean Polar Res*. **30**, 497–507 (2008).

KRCC, 2019. Korea Rural Community Corporation (Freshwater Discharge Record).

Korea Fisheries Resources Agency (FIRA), 2014. Report of Artificial reefs management, Jeju Island. FIRA, Jeju.

Korean Coastal Guard (KCG), 2008. White Paper. 11-1530000-000048-10, p. 523.

Kristensen, E., Lee, S. Y., Mangion, P., Quintana, C .O., Valdemarsen, T. Trophic discrimination of stable isotopes and potential food source partitioning by leaf-eating crabs in mangrove environments. *Limnol. Oceanogr*. **62**, 2097–2112 (2017).

Kromkamp, J., Peene, J., Van Rijswijk, P., Sandee, A., Goosen, N. Nutrients, light and primary production by phytoplankton and microphytobenthos in the eutrophic, turbid Westerschelde estuary (The Netherlands). *Hydrobiologia*, **311**, 9–19 (1995).

Kwon, B.-O. et al. Short-term variability of microphytobenthic primary production associated with in situ diel and tidal conditions. *Estuar. Coast. Shelf S.* **112**, 236–242 (2012).

Kwon, B.-O. et al. The relationship between primary production of microphytobenthos and tidal cycle on the Hwaseong mudflat, west coast of Korea. *J. Coastal Res.* **30**, 1188–1196 (2014).

Kwon, B.-O. et al. Temporal dynamics and spatial heterogeneity of microalgal biomass in recently reclaimed intertidal flats of the Saemangeum area, Korea. *J. Sea Res.* **116**, 1–11 (2016).

Kwon, B.-O. et al. Development of temperature-based algorithms for the estimation of microphytobenthic primary production in a tidal flat: a case study in Daebu mudflat, Korea. *Environ. Pollut*. **241**, 115–123 (2018).

Lake, S. J., Brush, M. J. The contribution of microphytobenthos to total productivity in upper Narragansett Bay, Rhode Island. *Estuar. Coast. Shelf S.* **95**, 289–297 (2011).

Lamb, A. L., Wilson, G. P., Leng, M. J. A review of coastal palaeoclimate and relative sea level reconstructions using δ13C and C/N ratios in organic material. *Earth Sci. Rev.* **75**, 29–57 (2006).

Lamendella, R. Assessment of the Deepwater Horizon oil spill impact on Gulf coast microbial communities. *Front. Microbiol*. **5**, 130 (2014).

Lasne, E., Bergerot, B., Lek, S., Laffaille, P. Fish zonation and indicator species for the evaluation of the ecological status of rivers: example of the Loire basin (France). *River Res. Appl.* **23**, 877–890 (2007).

Leach, J. H. Epibenthic algal production in an intertidal mudflat. *Limnol. Oceanogr.* **15**, 514–521 (1970).

Lebata-Ramos, M., Hazel, J., Doyola-Solis, E. F., 2016. Fishery resource enhancement: An overview of the current situation and issues in the southeast Asian region. Consolidating the Strategies for Fishery Resources Enhancement in Southeast Asia. Proceedings of the Symposium on Strategy for Fisheries Resources Enhancement in the Southeast Asian Region, Pattaya, Thailand, 27-30 July 2015. Training Department, Southeast Asian Fisheries Development Center, 124–128.

Le Loc'h, F., Hily, C., Grall, J. Benthic community and food web structure on the continental shelf of the Bay of Biscay (North Eastern Atlantic) revealed by stable isotopes analysis. *J. Marine Syst*. **72**, 17–34 (2008).

Lee, C. H. A study on the primary production of benthic microalgae on Songdo tidal flat, Incheon, West Coast of Korea. MS thesis (Seoul National University, Seoul, Korea, 1991).

Lee, C.-H. et al. Bioaccumulation of polycyclic aromatic hydrocarbons in Manila clam (*Ruditapes philippinarum*) exposed to crude oil-contaminated sediments. *Kor. J. Malacol.* **30**(4), 371–381 (2014).

Lee, H. Y., Jung, M. Distribution of benthic diatoms in tidal flats of Hampyeong bay, Korea. *Korean J. Environ. Biol.* **29**, 17–22 (2011).

Lee, H. Y. Diversity and biomass of benthic diatoms in Hampyeong bay tidal flats. *Korean J. Environ. Biol.* **31**, 295–301 (2013).

Lee, K., Weise, A. M., St-Pierre, S. Enhanced oil biodegradation with mineral fine interaction. *Spill Sci. Technol. B*. **3**(4), 263–267 (1996).

Lee, S. Measured and predicted affinities of binding and relative potencies to activate the AhR of PAHs and their alkylated analogues. *Chemosphere* **139**, 23–29 (2015).

Lee, S. Y. The effect of mangrove leaf litter enrichment on macrobenthic colonization of defaunated sandy substrates. *Estuar. Coast. Shelf S*. **49**, 703–712 (1999).

Leitão, F. Artificial reefs: from ecological processes to fishing enhancement tools. *Braz. J. Oceanogr.* **61**, 77–81 (2013).

Li, K., Liu, X., Zhao, X., Guo, W. Effects of reclamation projects on marine ecological environment in tianjin harbor industrial zone. *Procedia Environ. Sci.* **2**, 792–799 (2010).

Liang, Y., Tse, M., Young, L., Wong, M. Distribution patterns of polycyclic aromatic hydrocarbons (PAHs) in the sediments and fish at Mai Po Marshes Nature Reserve, Hong Kong. *Water. Res.* **41**(6), 1303–1311 (2007).

Lin, T., et al. Effects of clam size, food type, sediment characteristic, and seawater carbonate chemistry on grazing capacity of Venus clam *Cyclina sinensis* (Gmelin, 1791). *Chin. J. Oceanol. Limn*. **35**, 1239–1247 (2017).

Lindeman, R. L. The trophic-dynamic aspect of ecology. *Ecology* **23**, 399–417 (1942).

Liu, W. X. et al. Distribution of persistent toxic substances in benthic bivalves from the inshore areas of the Yellow Sea. *Environ. Toxicol. Chem.* **27**(1), 57–66 (2008).

Liu, W., Zhang, J., Tian, G., Xu, H., Yan, X. Temporal and vertical distribution of microphytobenthos biomass in mangrove sediments of Zhujiang (Pearl River) Estuary. *Acta. Oceanol. Sin.* **32**, 82–88 (2013).

Loh, A., Shim, W. J., Ha, S. Y., Yim, U. H. Oil-suspended particulate matter aggregates: Formation mechanism and fate in the marine environment. *Ocean Sci. J*. **49**(4), 329–341 (2014).

London Convention and Protocol/UNEP, 2009. London Convention and Protocol/UNEP Guidelines for the placement of artificial reefs. London, UK.

Lorenzen, C. J. Determination of chlorophyll and pheo-pigments: spectrophotometric equations. *Limnol. Oceanogr.* **12**, 343–346 (1967).

Lorrain, A. et al. Differential δ13C and δ15N signatures among scallop tissues: implications for ecology and physiology. *J. Exp. Mar. Biol. Ecol*. **275**, 47–61 (2002).

Lowry, M. et al. Response of fish communities to the deployment of estuarine artificial reefs for fisheries enhancement. *Fisheries Manag. Ecol.* **21**, 42–56 (2014).

Lucas, C. H., Widdows, J., Brinsley, M. D., Salkeld, P. N., Herman, P. M. J. Benthicpelagic exchange of microalgae at a tidal flat. 1. Pigment analysis. *Mar. Ecol. Prog. Ser*. **196**, 59–73 (2000).

Lucas, C. H., Holligan, P. M. Nature and ecological implications of algal pigment diversity on the Molenplaat tidal flat (Westerschelde estuary, SW Netherlands). *Mar. Ecol. Prog. Ser.* **180**, 51–64 (1999).

Lundin, C. G., Linden, O. Coastal ecosystems: attempts to manage a threatened resource. *Ambio*, 468–473 (1993).

Ma, Y.-G., Lei, Y. D., Xiao, H., Wania, F., Wang, W.-H. Critical review and recommended values for the physical-chemical property data of 15 polycyclic aromatic hydrocarbons at 25 ºC. *J. Chem. Eng. Data* **55**(2), 819–825 (2009).

Macintyre, H. L., Geider, R. J., Miller, D. C. Microphytobenthos: The ecological role of the "Secret Garden" of unvegetated, shallow-water marine habitats. I. Distribution, abundance and primary production. *Estuaries* **19**, 186–201 (1996).

Magni, P., Montani, S. Development of benthic microalgal assemblages on an intertidal flat in the Seto Inland Sea, Japan: effects of environmental variability. *La mer* **35**, 137–148 (1997).

Makoto, O., Tsutomu, I., 1984. Methods in marine zooplankton ecology. Wiley, New York.

Margalef, R., 1958. Temporal succession and spatial heterogeneity in phytoplankton. University of California press, USA.

Marquiegui, M. A. Aguirrezabalaga, F. Colonization process by macrobenthic infauna after a managed coastal realignment in the Bidasoa estuary (Bay of Biscay, NE Atlantic). *Estuar. Coast. Shelf. S*. **84**, 598–604 (2009).

Marshall, N., Oviatt, C. A., Skauen, D. M. Productivity of the benthic microflora of shoal estuarine environments in southern New England. *Int. Revue ges. Hydrobiol.* **56**, 947–955 (1971).

Maruyama, A. Dynamics of microbial populations and strong selection for *Cycloclasticus pugetii* following the Nakhodka oil spill. *Microb. Ecol*. **46**(4), 442–453 (2003).

Masselink, G., Hughes, M. G. (2014). An introduction to coastal processes and geomorphology. New York: Routledge (2014).

McClelland, J. W., Valiela, I. Changes in food web structure under the influence of increased anthropogenic nitrogen inputs to estuaries. *Mar. Ecol. Prog. Ser*. **168**, 259–271 (1998).

Mcintire, C. D., Amspoker, M. C. Effects of sediment properties on benthic primary production in the Columbia River estuary. *Aquat. Bot.* **24**, 249–267 (1986).

McKew, B. A. et al. Efficacy of intervention strategies for bioremediation of crude oil in marine systems and effects on indigenous hydrocarbonoclastic bacteria. *Environ. Microbiol*. **9**(6), 1562–1571 (2007).

McLusky, D. S., Elliott, M., 2004. The Estuarine Ecosystem: Ecology, Threats and Management. Oxford University Press on Demand.

McTigue, N. D., Bucolo, P., Liu, Z., Dunton, K. H. Pelagic-benthic coupling, food webs, and organic matter degradation in the Chukchi Sea: insights from sedimentary pigments and stable carbon isotopes. *Limnol. Oceanogr*. **60**, 429–445 (2015).

Meador, J., Casillas, E., Sloan, C., Varanasi, U. Comparative bioaccumulation of polycyclic aromatic hydrocarbons from sediment by two infaunal invertebrates. *Mar. Ecol. Prog. Ser*. **123**, 107–124 (1995).

Meire, P. M., Seys, J., Buijs, J., Coosen, J. Spatial and temporal patterns of intertidal macrobenthic populations in the Oosterschelde : are they influenced by the construction of the storm-surge barrier? *Hydrobiologia* **282**, 157–182 (1994).

Micheli, F., Halpern, B. S. Low functional redundancy in coastal marine assemblages. *Ecol. Lett*. **8**, 391–400 (2005).

Middelburg, J. J., Barranguet, C., Boschker, H. T., Herman, P. M., Moens, T., Heip, C. H. The fate of intertidal microphytobenthos carbon: An in situ ^{13}C-labeling study. *Limnol. Oceanogr.* **45**, 1224–1234 (2000).

Migné, A., Spilmont, N., Davoult, D. In situ measurements of benthic primary production during emersion: seasonal variations and annual production in the Bay of Somme (eastern English Channel, France). *Cont. Shelf Res.* **24**, 1437–1449 (2004).

Migné, A. et al. Annual budget of benthic production in Mont Saint-Michel Bay considering cloudiness, microphytobenthos migration, and variability of respiration rates with tidal conditions. *Cont. Shelf Res.* **29**, 2280–2285 (2009).

Miller, D. C., Geider, R. J., Macintyre, H. L. Microphytobenthos: The ecological role of the "Secret Garden" of unvegetated, shallow-water marine habitats. II. Role in sediment stability and shallow-water food webs. *Estuaries* **19**, 202–212 (1996).

Millennium Ecosystem Assessment Synthesis Report, 2005. *Ecosystems and Human Well-Being*, Chpater 3, p. 49

Montani, S., Magni, P., Abe, N. Seasonal and interannual patterns of intertidal microphytobenthos in combination with laboratory and areal production estimates. *Mar. Ecol. Prog. Ser.* **249**, 79–91 (2003).

Moon, J. E. et al. Initial validation of GOCI water products against in situ data collected around Korean peninsula for 2010–2011. *Ocean Sci. J.* **47**, 261–277 (2012).

Mori, K. et al. *Thioprofundum hispidum* sp. nov., an obligately chemolithoautotrophic sulfur-oxidizing gammaproteobacterium isolated from the hydrothermal field on Suiyo Seamount, and proposal of *Thioalkalispiraceae* fam. nov. in the order *Chromatiales*. *Int.*

J. Syst. Evol. Micr. 2011, 61 (10), 2412–2418.

Mueter, F. J., Norcross, B. L. Spatial and temporal patterns in the demersal fish community on the shelf and upper slope regions of the Gulf of Alaska. *Fish. B-NOAA*. **100**, 559–581 (2002).

Murphy, R. J., Tolhurst, T. J., Chapman, M. G., Underwood, A. J. Seasonal distribution of chlorophyll on mudflats in New South Wales, Australia measured by field spectrometry and PAM fluorometry. *Estuar. Coast. Shelf S.* **84**, 108–118 (2009).

Muschenheim, D., Lee, K. Removal of oil from the sea surface through particulate interactions: review and prospectus. *Spill Sci. Technol. B*. **8**(1), 9–18 (2002).

Nadon, M.-O., Himmelman, J. H. Stable isotopes in subtidal food webs: have enriched carbon ratios in benthic consumers been misinterpreted? *Limnol. Oceanogr*. **51**, 2828–2836 (2006).

Naser, H. A. Effects of reclamation on macrobenthic assemblages in the coastline of the Arabian Gulf: A microcosm experimental approach. *Mar. Pollut. Bull.* **62**, 520–524 (2011).

NCDSS, 2019. National Climate Data Service System. http://sts.kma.go.kr/eng/jsp/home/contents/main/
main.do.

Ning, X., Cai, Y., Liu, Z., Hu, X., Liu, C. Standing crop and primary production of benthic microalgae on tidal flats in the Sanggou and Jiaozhou Bays, China. *Acta. Oceanol. Sin.* **22**, 75–87 (2003).

Nixon, S. W., Oviatt, C. A., Frithsen, J., Sullivan, B. Nutrients and the productivity of estuarine and coastal marine ecosystems. *J. Limnol. Soc. S. Afr*. **12**, 43–71 (1986).

Nobriga, M. L., Feyrer, F., Baxter, R. D., Chotkowski, M. Fish community ecology in an altered river delta: spatial patterns in species composition, life history strategies, and biomass. *Estuaries* **28**, 776–785 (2005).

Noether, G. E., 1976. Introduction to statistics: A nonparametic approach. Houghton Mifflin Company, Boston.

Noh, J., Yoon, S. J., Lee, C., Kwon, B.-O., Khim, J. S. Optimal environmental monitoring system for ecosystem assessment in the Geum River estuary, Korea. *J. Korean Soc. Mar. Environ. Energy* **21**, 1–17 (2018).

Normile, D. Restoration or devastation? *Science* **327**, 1568–1570 (2010).

O'Reilly, J. E. et al. Ocean color chlorophyll *a* algorithms for SeaWiFS, OC2, and OC4: Version 4. In Hooker, S.B., Firestone, E.R (eds.), SeaWiFS Postlaunch Calibration and Validation Analyses, Part 3, National Aeronautics and Space Administration Technical Memorandum 2000-206892, **11**, 9–23 (2000).

Oh, S.-J., Moon, C.-H., Park, M.-O. HPLC analysis of biomass and community composition of microphytobenthos in the Saemankeum tidal flat, West Coast of Korea. *J. Kor. Fish. Soc.* **37**, 215–225 (2004).

Oh, T.-Y. et al. Seasonal variation and species composition of fishes communities in artificial reef unit at marine ranching area in the coastal waters off Jeju island, Korea. *J. Kor. Soc. Fish. Tech.* **46**(2), 139–147 (2010).

Oliva, A. L. Distribution and human health risk assessment of PAHs in four fish species from a SW Atlantic estuary. *Environ. Sci. Pollut. R*. **24**(23), 18979–18990 (2017).

Onozato, M., Nishigaki, A., Okoshi, K. Polycyclic aromatic hydrocarbons in sediments and bivalves on the Pacific Coast of Japan: Influence of Tsunami and fire. *PloS one*, **11** (5),

e0156447 (2016).
Orbea, A., Ortiz–Zarragoitia, M., Solé, M., Porte, C., Cajaraville, M. P. Antioxidant enzymes and peroxisome proliferation in relation to contaminant body burdens of PAHs and PCBs in bivalve molluscs, crabs and fish from the Urdaibai and Plentzia estuaries (Bay of Biscay). *Aquat. Toxicol.* **58**(1), 75–98 (2002).
Ouisse, V., Migné, A., Davoult, D. Seasonal variations of community production, respiration and biomass of different primary producers in an intertidal *Zostera noltii* bed (Western English Channel, France). *Hydrobiologia* **649**, 3–11 (2010).
Owens, E. H., Lee, K. Interaction of oil and mineral fines on shorelines: review and assessment. *Mar. Pollut. Bull.* **47**(9), 397–405 (2003).
Owens, N. J. P., 1988. Natural variations in ^{15}N in the marine environment. *Advances in Marine Biology*. Elsevier, p. 389–451.
Paalvast, P., van der Velde, G. Long term anthropogenic changes and ecosystem service consequences in the northern part of the complex Rhine-Meuse estuarine system. *Ocean Coast. Manage*. **92**, 50–64 (2014).
Page, H. M. Importance of vascular plant and algal production to macro-invertebrate consumers in a southern California salt marsh. *Estuar. Coast. Shelf S.* **45**, 823–834 (1997).
Page, H., Lastra, M. Diet of intertidal bivalves in the Ría de Arosa (NW Spain): evidence from stable C and N isotope analysis. *Mar. Biol*. **143**, 519–532 (2003).
Pamatmat, M. M. Ecology and metabolism of a benthic community on an intertidal sandflat. *Int. Revue ges. Hydrobiol.* **53**, 211–298 (1968).
Park, H. J., Choy, E. J., Kang, C. K. Spatial and temporal variations of microphytobenthos on the common reed Phragmites australis bed in a marine protected area of Yeoja Bay, Korea. *Wetlands* **33**, 737–745 (2013).
Park, H. J., Kang, H. Y., Park, T. H., Kang, C.-K. Comparative trophic structures of macrobenthic food web in two macrotidal wetlands with and without a dike on the temperate coast of Korea as revealed by stable isotopes. *Mar. Environ. Res.* **131**, 134–145 (2017).
Park, J. et al. Microphytobenthos of Korean tidal flats: A review and analysis on floral distribution and tidal dynamics. *Ocean Coast. Manage.* **102**, 471–481 (2014).
Park, S. K. et al. Seasonal variation in species composition and biomass of microphytobenthos at Jinsanri, Taean, Korea. *Kor. J. Fish. Aquat. Sci.* **46**, 176–185 (2013).
Park, S. K., Kim, B. Y., Oh, J.-S., Park, K.-J., Choi, H. G. Seasonal variations of microphytobenthos and growth of *Ruditapes philippinarum* at Jeongsanpo and Hwangdo tidal flat, Taean, Korea. *Korean J. Environ. Ecol.* **29**, 884–894 (2015).
Parnell, A., Inger, R., 2016. Stable Isotope Mixing Models in R with SIMMR. https://cran. r-project.org/web
/packages/simmr/vignettes/simmr.html.
Paulet, Y.-M., Lorrain, A., Richard, J., Pouvreau, S. Experimental shift in diet δ13C: a potential tool for ecophysiological studies in marine bivalves. *Org. Geochem*. **37**, 1359–1370 (2006).
Penczak, T. Fish assemblage compositions after implementation of the IndVal method on the Narew River system. *Ecol. Model.* **220**, 419–423 (2009).
Perissinotto, R., Nozais, C., Kibirige, I. Spatio-temporal dynamics of phytoplankton and microphytobenthos in a South African temporarily-open estuary. *Estuar. Coast. Shelf S.* **55**, 47–58 (2002).

Perkol-Finkel, S., Benayahu, Y. Recruitment of benthic organisms onto a planned artificial reef: shifts in community structure one decade post-deployment. *Mar. Environ. Res*. **59**, 79–99 (2005).

Pernet, F. et al. Marine diatoms sustain growth of bivalves in a Mediterranean lagoon. *J. Sea Res*. **68**, 20–32 (2012).

Peterson, B. J., Fry, B. Stable isotopes in ecosystem studies. *Ann. Rev. Ecol. Syst*. **18**, 293–320 (1987).

Pielou, E. C. Species-diversity and pattern-diversity in the study of ecological succession. *J. Theor. Biol* **10**, 370–383 (1966).

Pinckney, J., Zingmark, R. G. Biomass and production of benthic microalgal communities in estuarine habitats. *Estuaries* **16**, 887–897 (1993).

Pinckney, J., Papa, R., Zingmark, R. Comparison of high-performance liquid chromatographic, spectrophotometric, and fluorometric methods for determining chlorophyll *a* concentrations in estaurine sediments. *J. Microbiol. Meth.* **19**, 59–66 (1994).

Poff, N. L. The natural flow regime. *BioScience* **47**, 769–784 (1997).

Pomeroy, L. R. Algal productivity in salt marshes of Georgia. *Limnol. Oceanogr.* **4**, 386–397 (1959).

Pomeroy, W. M., Stockner, J. G. Effects of environmental disturbance on the distribution and primary production of benthic algae on a British Columbia estuary. *J. Fish. Res. Board Can.* **33**, 1175–1187 (1976).

Post, D. M. Using stable isotopes to estimate trophic position: models, methods, and assumptions. *Ecology* **83**, 703–718 (2002).

Pratt, J. R. Artificial habitats and ecosystem restoration: managing for the future. *B. Mar. Sci.* **55**, 268–275 (1994).

Prins, T. C., Smaal, A. C., Pouwer, A. J. Selective ingestion of phytoplankton by the bivalves *Mytilus edulis* L. and *Cerastoderma edule* (L.). *Hydrobiol. Bull*. **25**, 93–100 (1991).

Quadros, G., Sukumaran, S., Athalye, R. P. Impact of the changing ecology on intertidal polychaetes in an anthropogenically stressed tropical creek, India. *Aquat. Ecol.* **43**, 977–985 (2009).

Redmond, M. C., Valentine, D. L. Natural gas and temperature structured a microbial community response to the Deepwater Horizon oil spill. *Proc. Nat. Acad. Sci*. **109**(50), 20292–20297 (2012).

Relini, G., Zamboni, N., Tixi, F., Torchia, G. Patterns of sessile macrobenthos community development on an artificial reef in the Gulf of Genoa (northwestern Mediterranean). *B. Mar. Sci.* **55**, 745–771 (1994).

Rewitz, K. F., Styrishave, B., Løbner-Olesen, A., Andersen, O. Marine invertebrate cytochrome P450: emerging insights from vertebrate and insect analogies. *Comp. Biochem. Phys. C.* **143**(4), 363–381 (2006).

Riccialdelli, L., Newsome, S. D., Fogel, M. L., Fernández, D. A. Trophic interactions and food web structure of a subantarctic marine food web in the Beagle Channel: Bahia Lapataia, Argentina. *Polar Biol*. **40**, 807–821 (2017).

Riera, P., Richard, P. Isotopic determination of food sources of *Crassostrea gigas* along a trophic gradient in the estuarine Bay of Marennes-Ol éron. *Estuar. Coast. Shelf S*. **42**, 347–360 (1996).

Riethmüller, R., Heineke, M., Kühl, H., Keuker-Rüdiger, R. Chlorophyll *a* concentration as an index of sediment surface stabilisation by microphytobenthos? *Cont. Shelf Res.* **20**,

1351–1372 (2000).
Rilov, G., Benayahu, Y. Vertical artificial structures as an alternative habitat for coral reef fishes in disturbed environments. *Mar. Environ. Res*. **45**, 431–451 (1998).
Rios, M. C. et al. Capability of Paraguaçu estuary (Todos os Santos Bay, Brazil) to form oil–SPM aggregates (OSA) and their ecotoxicological effects on pelagic and benthic organisms. *Mar. Pollut. Bull.* **114**(1), 364–371 (2017).
Rivers, A. R. et al. Transcriptional response of bathypelagic marine bacterioplankton to the Deepwater Horizon oil spill. *ISME J.* **7**(12), 2315–2329 (2013).
Riznyk, R. Z., Edens, J. I., Libby, R. C. Production of epibenthic diatoms in a southern California impounded estuary. *J. Phycol.* **14**, 273–279 (1978).
Rizzo, W. M., Wetzel, R. L. Intertidal and shoal benthic community metabolism in a temperate estuary: studies of spatial and temporal scales of variability. *Estuaries*, **8**, 342–351 (1985).
Roh, S. M. Effect of tidal on microalgal distribution and primary production variation in Taean coastal environment. MS thesis (Inha University, Incheon, Korea, 2008).
Rolls, R. J. The role of life-history and location of barriers to migration in the spatial distribution and conservation of fish assemblages in a coastal river system. *Biol. Conserv.* **144**, 339–349 (2011).
Röling, W. F. et al. Bacterial community dynamics and hydrocarbon degradation during a field-scale evaluation of bioremediation on a mudflat beach contaminated with buried oil. *Appl. Environ. Microb*. **70**(5), 2603–2613 (2004).
Rombouts, I. et al. Evaluating marine ecosystem health: case studies of indicators using direct observations and modelling methods. *Ecol. Indic.* **24**, 353–365 (2013).
Rooker, J., Dokken, Q., Pattengill, C., Holt, G. Fish assemblages on artificial and natural reefs in the Flower Garden Banks National Marine Sanctuary, USA. *Coral Reefs* **16**, 83–92 (1997).
Rosenthal, R. An application of the Kolmogorov-Smirnov test for normality with estimated mean and variance. *Psychol. Rep*. **22**, 570 (1968).
Rossi, F., Herman, P. M. J., Middelburg, J. J. Interspecific and intraspecific variation of $\delta^{13}C$ and $\delta^{15}N$ in deposit- and suspension-feeding bivalves (*Macoma balthica* and *Cerastoderma edule*): evidence of ontogenetic changes in feeding mode of *Macoma balthica*. *Limnol. Oceanogr*. **49**, 408–414 (2004).
Rossi, L., Costantini, M. L., Carlino, P., Di Lascio, A., Rossi, D. Autochthonous and allochthonous plant contributions to coastal benthic detritus deposits: a dual-stable isotope study in a volcanic lake. *Aquat. Sci*. **72**, 227–236 (2010).
Rossi, F., Baeta, A., Marques, J. C. Stable isotopes reveal habitat-related diet shifts in facultative deposit-feeders. *J. Sea Res.* **95**, 172–179 (2015).
Ryou, D.-K., Chung, S.-C. Settlement and recruitment of *Mactra veneriformis* R. around the inshore of Kunsan, Korea. *J. Korean Fish. Soc*. **28**, 667–676 (1995).
Ryu, J. et al. The Saemangeum tidal flat: long–term environmental and ecological changes in marine benthic flora and fauna in relation to the embankment. Ocean *Coast Manage* **102**, 559–571 (2014).
Ryu, J.-H., Han, H.-J., Cho, S., Park, Y.-J., Ahn, Y.-H. Overview of geostationary ocean color imager (GOCI) and GOCI data processing system (GDPS). *Ocean Sci. J.* **47**, 223–233 (2012).
Ryu, M. H. Seasonal distribution of microphytobenthos and primary production on an

intertidal mud flat in the Janghwa, Ganghwa Island of Korea. MS thesis (Inha University, Incheon, Korea, 2004).

Sakamaki, T., Richardson, J. S. Effects of small rivers on chemical properties of sediment and diets for primary consumers in estuarine tidal flats. *Mar. Ecol. Prog. Ser*. **360**, 13–24 (2008).

Sammarco, P. W. et al. Distribution and concentrations of petroleum hydrocarbons associated with the BP/Deepwater Horizon Oil Spill, Gulf of Mexico. *Mar. Pollut. Bull*. **73**(1), 129–143 (2013).

Santos, M. N., Oliveira, M. T., Cúrdia, J. A comparison of the fish assemblages on natural and artificial reefs off Sal Island (Cape Verde). *J. Mar. Biol. Assoc. UK*. **93**(2), 437–452 (2013).

Scholz, B., Liebezeit, G. Microphytobenthic dynamics in a Wadden Sea intertidal flat – Part II: Seasonal and spatial variability of non-diatom community components in relation to abiotic parameters. *Eur. J. Phycol.* **47**, 120–137 (2012).

Schubert, C. J., Nielsen, B. Effects of decarbonation treatments on $\delta^{13}C$ values in marine sediments. *Mar. Chem*. **72**, 55–59 (2000).

Scott, M. E., Smith, J. A., Lowry, M. B., Taylor, M. D., Suthers, L. M. The influence of an offshore artificial reef on the abundance of fish in the surrounding pelagic environment. *Mar. Freshwater. Res*. **66**(5), 429–437 (2015).

Seitzinger, S. P. et al. Global river nutrient export: A scenario analysis of past and future trends. *Global Biogeochem. Cycles* **24**, GB0A08 (2010).

Serôdio, J., Catarino, F. Modelling the primary productivity of intertidal microphytobenthos: time scales of variability and effects of migratory rhythms. *Mar. Ecol. Prog. Ser.* **192**, 13–30 (2000).

Shaffer, G. P., Onuf, C. P. Reducing the error in estimating annual production of benthic microflora: hourly to monthly rates, patchiness in space and time. *Mar. Ecol. Prog. Ser*. **26**, 221–231 (1985).

Shaffer, G. P. A comparison of benthic microfloral production on the West and Gulf coasts of the United States: An introduction to the dynamic K-systems model. *Mar. Ecol. Prog. Ser.* **43**, 55–62 (1988).

Shannon, C. E., Weaver, W., 1949. The Mathematical Theory of Communication. Urbana.

Sherman, R. L., Gilliam, D. S., Spieler, R. E., 2002. Artificial reef design: void space, complexity, and attractants. ICES J. Mar. Sci. 59, S196–S200.

Silva, C. S. et al. Potential application of oil-suspended particulate matter aggregates (OSA) on the remediation of reflective beaches impacted by petroleum: a mesocosm simulation. *Environ. Sci. Pollut. R*. 1–13 (2015).

Sirot, C. et al. Combinations of biological attributes predict temporal dynamics of fish species in response to environmental changes. *Ecol. Indic*. **48**, 147–156 (2015).

Siswanto, E. et al. Empirical ocean-color algorithms to retrieve chlorophyll-*a*, total suspended matter, and colored dissolved organic matter absorption coefficient in the Yellow and East China Seas. *J. Oceanogr.* **67**, 627–650 (2011).

Snyder, M. J. Cytochrome P450 enzymes belonging to the CYP4 family from marine invertebrates. *Biochem. Bioph. Res. Co.* **249**(1), 187–190 (1998).

Snyder, M. J. Cytochrome P450 enzymes in aquatic invertebrates: recent advances and future directions. *Aquat. Toxicol*. **48**(4), 529–547 (2000).

Soriano, J. et al. Spatial and temporal trends of petroleum hydrocarbons in wild mussels from

the Galician coast (NW Spain) affected by the Prestige oil spill. *Sci. Total. Environ*. **370**(1), 80–90 (2006).

Spilmont, N., Davoult, D., Migné, A. Benthic primary production during emersion: in situ measurements and potential primary production in the Seine Estuary (English Channel, France). *Mar. Pollut. Bull.* **53**, 49–55 (2006).

Spilmont, N., Migné, A., Seuront, L., Davoult, D. Short-term variability of intertidal benthic community production during emersion and the implication in annual budget calculation. *Mar. Ecol. Prog. Ser.* **333**, 95–101 (2007).

Steele, J. H., Baird, I. E. Production ecology of a sandy beach. *Limnol. Oceanogr.* **13**, 14–25 (1968).

Steimle, F., Foster, K., Kropp, R., Conlin, B. Benthic macrofauna productivity enhancement by an artificial reef in Delaware Bay, USA. *ICES J. Mar. Sci*. **59**, S100–S105 (2002).

Stoffyn-Egli, P., Lee, K. Formation and characterization of oil–mineral aggregates. *Spill Sci. Technol. B.* **8**(1), 31–44 (2002).

Strohmeier, T., Duinker, A., Lie, O. Seasonal variations in chemical composition of the female gonad and storage organs in *Pecten maximus* (L.) suggesting that somatic and reproductive growth are separated in time. *J. Shellfish Res*. **19**, 741–748 (2000).

Sullivan, M. J., Moncreiff, C. A. Primary production of edaphic algal communities in a Mississippi salt marsh. *J. Phycol.* **24**, 49–58 (1988).

Sun, J., Zheng, X. A review of oil-suspended particulate matter aggregation—a natural process of cleansing spilled oil in the aquatic environment. *J. Environ. Monitor*. **11**(10), 1801–1809 (2009).

Sun, J. et al. A laboratory study on the kinetics of the formation of oil–suspended particulate matter aggregates using the NIST–1941b sediment. *Mar. Pollut. Bull*. **60**(10), 1701–1707 (2010).

Sun, J., Khelifa, A., Zhao, C., Zhao, D., Wang, Z. Laboratory investigation of oil–suspended particulate matter aggregation under different mixing conditions. *Sci. Total. Environ*. **473**, 742–749 (2014).

Sundbäck, K., Graneli, W. Influence of microphytobenthos on the nutrient flux between sediment and water: a laboratory study. *Mar. Ecol. Prog. Ser.* **43**, 63–69 (1988).

Svensson, E. et al. Comparison of the stable carbon and nitrogen isotopic values of gill and white muscle tissue of fish. *J. Exp. Mar. Biol. Ecol*. **457**, 173–179 (2014).

Tagger, S., Truffaut, N., Petit, J. L. Preliminary study on relationships among strains forming a bacterial community selected on naphthalene from a marine sediment. *Can. J. Microbiol*. **36**(10), 676–681 (1990).

The National Marine Data and Information Service (eds.), 2018 Tide Tables: From the Yalu River Mouth to the Changjinan River Mouth (Vol.1). Beijing: Ocean Press (2017).

Thom, R. M., Parkwell, T. L., Niyogi, D. K., Shreffler, D. K. Effects of graveling on the primary productivity, respiration and nutrient flux of two estuarine tidal flats. *Mar. Biol.* **118**, 329–341 (1994).

Thom, R. M. Primary production in Grays Harbor estuary, Washington. *Bull. S. Calif. Acad. Sci.* **83**, 99–105 (1984).

Thornton, D. C., Dong, L. F., Underwood, G. J. C., Nedwell, D. B. Factors affecting microphytobenthic biomass, species composition and production in the Colne Estuary (UK). *Aquat. Microb. Ecol.* **27**, 285–300 (2002).

Thornton, D. C., Visser, L. A. Measurement of acid polysaccharides (APS) associated with

microphytobenthos in salt marsh sediments. *Aquat. Microb. Ecol.* **54**, 185–198 (2009).
Thottathil, S. D., Balachandran, K. K., Gupta, G. V. M., Madhu, N. V., Nair, S. Influence of allochthonous input on autotrophic–heterotrophic switch-over in shallow waters of a tropical estuary (Cochin Estuary), India. *Estuar. Coast. Shelf S*. **78**, 551–562 (2008).
Trzesicka-Mlynarz, D., Ward, O. Degradation of polycyclic aromatic hydrocarbons (PAHs) by a mixed culture and its component pure cultures, obtained from PAH-contaminated soil. *Can. J. Microbiol*. **41**(6), 470–476 (1995).
Tuchman, N. C., Schollett, M. A., Rier, S. T., Geddes, P. Differential heterotrophic utilization of organic compounds by diatoms and bacteria under light and dark conditions. *Hydrobiologia* **561**, 167–177 (2006).
Ubertini, M. et al. Spatial variability of benthic-pelagic coupling in an estuary ecosystem: consequences for microphytobenthos resuspension phenomenon. *PLoS One* **7**, e44155 (2012).
Ubertini, M., Lefebvre, S., Rakotomalala, C., Orvain, F. Impact of sediment grain-size and biofilm age on epipelic microphytobenthos resuspension. *J. Exp. Mar. Biol. Ecol.* **467**, 52–64 (2015).
UNEP, 2010. Impact of Climate Change on Marine and Coastal Biodiversity in the Mediterranean Sea: Current State of Knowledge.
Underwood, G. J. C., Kromkamp, J. Primary production by phytoplankton and microphytobenthos in estuaries. In Estuaries. *Adv. Ecol. Res.* **29**, 93–153 (1999).
Underwood, G. J. C. Microphytobenthos. In Encyclopedia of Ocean Sciences (2nd Ed.). 1770–1777 (2001).
Underwood G. J. C. et al. Patterns in microphytobenthic primary productivity: Species-specific variation in migratory rhythms and photosynthetic efficiency in mixed-species biofilms. *Limnol. Oceanogr.* **50**, 755–767 (2005).
Underwood, G. J. C. Microphytobenthos and phytoplankton in the Severn estuary, UK: present situation and possible consequences of a tidal energy barrage. *Mar. Pollut. Bull.* **61**, 83–91 (2010).
Uno, S. et al. Monitoring of PAHs and alkylated PAHs in aquatic organisms after 1 month from the Solar I oil spill off the coast of Guimaras Island, Philippines. *Environ. Monit. Assess*. **165**(1), 501–-515 (2010).
Valentine, D. L. et al. Dynamic autoinoculation and the microbial ecology of a deep water hydrocarbon irruption. *Proc. Nat. Acad. Sci*. **109**(50), 20286–20291 (2012).
Van der Molen, J. S., Perissinotto, R. Microalgal productivity in an estuarine lake during a drought cycle: The St. Lucia Estuary, South Africa. *Estuar. Coast. Shelf S.* **92**, 1–9 (2011).
Van der Oost, R. Bioaccumulation, biotransformation and DNA binding of PAHs in feral eel (*Anguilla anguilla*) exposed to polluted sediments: a field survey. *Environ. Toxicol. Chem.* **13**(6), 859–870 (1994).
Vander Zanden, M. J., Rasmussen, J. B. Primary consumer $\delta^{13}C$ and $\delta^{15}N$ and the trophic position of aquatic consumers. *Ecology* **80**, 1395–1404 (1999).
Van Es, F. B. Community metabolism of intertidal flats in the Ems-Dollard estuary. *Mar. Biol.* **66**, 95–108 (1982).
Van Raalte, C., Stewart, W. C., Valiela, I., Carpenter, E. J. A ^{14}C technique for measuring algal productivity in salt marsh muds. *Bot. Mar.* **17**, 186–188 (1974).
Van Raalte, C. D., Valiela, I., Teal, J. M. The effect of fertilization on the species composition of salt marsh diatoms. *Water Res.* **10**, 1–4 (1976).

Varela, M., Penas, E. Primary production of benthic microalgae in an intertidal sand flat of the Ria de Arosa, NW Spain. *Mar. Ecol. Prog. Ser.* **25**, 111–119 (1985).

Vizzini, S., Sara, G., Michener, R. H., Mazzola, A. The role and contribution of the seagrass *Posidonia oceanica* (L.) Delile organic matter for secondary consumers as revealed by carbon and nitrogen stable isotope analysis. *Acta Oecol*. **23**, 277–285 (2002).

Wang, B., Lai, Q., Cui, Z., Tan, T., Shao, Z. A pyrene-degrading consortium from deep-sea sediment of the West Pacific and its key member *Cycloclasticus* sp. P1. *Environ. Microbiol*. **10**(8), 1948–1963 (2008).

Ware, D. M., Thomson, R. E. Bottom-up ecosystem trophic dynamics determine fish production in the Northeast Pacific. *Science* **308**, 1280–1284 (2005).

Webb, A. P., Eyre, B. D. The effect of natural populations of the burrowing and grazing soldier crab (*Mictyris longicarpus*) on sediment irrigation, benthic metabolism and nitrogen fluxes. *J. Exp. Mar. Biol. Ecol.* **309**, 1–19 (2004).

WEIS, 2019. Water Environment Information System. http://water.nier.go.kr/publicMain/mainContent.do.

Weise, A., Nalewajko, C., Lee, K. Oil-mineral fine interactions facilitate oil biodegradation in seawater. *Environ. Technol*. **20**(8), 811–824 (1999).

Wendker, S., Marshall, H. G. Primary productivity of benthic microalgae in the lower Chesapeake Bay. *Va. J. Sci.* 44, 125 only (1993).

West, J. E. et al. An evaluation of background levels and sources of polycyclic aromatic hydrocarbons in Naturally spawned embryos of Pacific herring (*Clupea pallasii*) from Puget Sound, Washington, USA. *Sci. Total. Environ*. **499**, 114–124 (2014).

Whyte, L. G., Bourbonniere, L., Greer, C. W. Biodegradation of petroleum hydrocarbons by psychrotrophic *Pseudomonas* strains possessing both alkane (alk) and naphthalene (nah) catabolic pathways. *Appl. Environ. Microb*. **63**(9), 3719–3723 (1997).

Wilkinson, V. Production ecology of microphytobenthos populations in the Manukau Harbour. MS thesis (University of Auckland, Auckland, New Zealand, 1981).

Wolfstein, K., Colijn, F., Doerffer, R. Seasonal dynamics of microphytobenthos biomass and photosynthetic characteristics in the northern German Wadden Sea, obtained by the photosynthetic light dispensation system. *Estuar. Coast. Shelf S.* **51**, 651–662 (2000).

Won, E. J., Choi, B., Hong, S., Khim, J. S., Shin, K. H. Importance of accurate trophic level determination by nitrogen isotope of amino acids for trophic magnification studies: a review. *Environ. Pollut*. **238**, 677–690 (2018).

Worm, B. et al. Impacts of biodiversity loss on ocean ecosystem services. *Science* **314**, 787–790 (2006).

Wu, J., Fu, C., Lu, F., Chen, J. Changes in free-living nematode community structure in relation to progressive land reclamation at an intertidal marsh. *Appl. Soil Ecol.* **29**, 47–58 (2005).

Xu, J., Zhang, M. Primary consumers as bioindicator of nitrogen pollution in lake planktonic and benthic food webs. *Ecol. Indic*. **14**, 189–196 (2012).

Yang, W., Li, M., Sun, T., Jin, Y. The joint effect of tidal barrier construction and freshwater releases on the macrobenthos community in the northern Yellow River Delta (China). *Ocean Coast. Manage.* **136**, 83–94 (2017).

Yim, J. Analysis of forty years long changes in coastal land use and land cover of the Yellow Sea: the gains or losses in ecosystem services. *Environ. Pollut*. **241**, 74–84 (2018).

Yin H. et al. Biomass and primary productivity of the microphytobenthos on mudflats of the

Rushan Bay east flow area. *Mar. Fish. Res.* **27**, 62–66 (2006).

Yokoyama, H., Ishihi, Y. Variation in food sources of the macrobenthos along a land–sea transect: a stable isotope study. *Mar. Ecol. Prog. Ser*. **346**, 127–141 (2007).

Yokoyama, H. Variability of diet-tissue isotopic fractionation in estuarine macrobenthos. *Mar. Ecol. Prog. Ser*. **296**, 115–128 (2005a).

Yokoyama, H. Isotopic evidence for phytoplankton as a major food source for macrobenthos on an intertidal sandflat in Ariake Sound, Japan. *Mar. Ecol. Prog. Ser*. **304**, 101–116 (2005b).

Yoon, S. J. Distributions of persistent organic contaminants in sediments and their potential impact on macrobenthic faunal community of the Geum River Estuary and Saemangeum Coast, Korea. *Chemosphere* **173**, 216–226 (2017).

Yoshimuda, N., Fujii, Y. Artificial reef scale and installation conditions. Japanese artificial reef technology. *Aquabio. Fla. Tech. Rep*. **604**, 148–159 (1982).

Zanette, J., Goldstone, J. V., Bainy, A. C., Stegeman, J. J. Identification of CYP genes in *Mytilus* (mussel) and *Crassostrea* (oyster) species: first approach to the full complement of cytochrome P450 genes in bivalves. *Mar. Environ. Res*. **69**, S1–S3 (2010).

Zedler, J. B. Algal mat productivity: comparisons in a salt marsh. *Estuaries* **3**, 122–131 (1980).

Zhao, J.-X., Liu, Q.-Q., Zhou, Y.-X., Chen, G.-J., Du, Z.-J. *Alkalimarinus sediminis* gen. nov., sp. nov., isolated from marine sediment. *Int. J. Syst. Evol. Micr*. **65**(10), 3511–3516 (2015).

ABSTRACT (IN KOREAN)

제목: 황해 해양환경 내 다양한 인간활동이 해양생물에게 미치는 영향에 관한 연구

해양 생태계는 인위적 활동에 의해 여러 스트레스 요인에 의해 지속적으로 영향을 받으며, 그 영향은 다양한 해양 생물들의 생태학적 반응을 통해 평가 될 수 있다. 본 연구에서는 황해에서의 4건의 사례 연구를 통해 인간활동의 영향에 대한 해양생태계의 생태학적 반응을 해양생물을 중심으로 다양한 시공간적 규모에서 평가했다. 본 논문에서는 1) 황해연안의 저서 일차생산 평가 및 저서-대양의 생산성 연결, 2) 하구둑에 의해 담수유통이 인위적으로 저절되는 닫힌 하구 환경에서의 먹이망, 3) 연안환경에 시설되어 있는 인공어초에 서식하는 어류군집구조, 그리고 4) 유류오염된 해양환경 내 서식 생물의 생물축적 및 생분해에 관한 연구를 진행하였다.

황해 연안의 저서생산성에 관한 연구를 통해 황해 연안의 평균적인 저서미세조류의 생체량과 일차생산성에 대한 결과를 얻을 수 있었다. 뿐만 아니라, 저서-대양의 생산성 연결에 대해 재조명 하였다. 연구결과, 저서의 생산성이 재부유 등의 과정에 의해 대양으로 영향을 미칠 수 있는 영역, 즉 연안의 최대 범위는 약 10km까지 공간적으로 연결되어 있음을 확인하였으며, 지역에 따른 조석 에너지(조석 높이)의 세기는 이러한 생산성을 전송할 수 있는 중요한 환경요인 이었다. 따라서, 저서의 생산성은 대양의 생산성과 밀접하게 연관되어 있으며, 무분별한 연안 개발은 생태계 전반의 생산성 손실을 초래할 수 있을 것이다. 닫힌하구의 먹이망 연구에서는 하구에 서식하는 저서생물들의 담수 기원의 유기성 입자물질들의 이용이 제한적임을 알 수 있었다. 특히 저서미세조류는 해양성 조개류의 성장과 계절적 변화에 따라 가장 중요한 먹이원으로 이용되고 있었다. 연안환경 내 시설된 인공어초에 서식하는 어류군집은 상대적으로 대조구 어장에 비해 많은 개체수가

서식하고 있었으며, 인공어초 환경의 특성(수온, 인공어초 재질, 서식지 퇴적물 성상)에 따라 특정 어류 군집들의 서식지 선호도가 있음을 확인하였다. 반면, 특정 인공어초 환경에서는 기존 서식하는 군집 구조를 변화시키거나 인공어초의 시설이 어류 위집효과가 크지 않는 등의 부작용 또한 확인 할 수 있었다. 유류기원 물질 OSAs (oil-suspended particulate matter aggregates)에 노출된 생물 및 환경 내 PAHs 농도변화연구를 통해, 장기 노출된 해양 이매패류의 연조직 내에서 PAHs (다환방향족탄화수소)의 생물축적이 30일 동안 두드러지게 관찰되었다. 이후 생물 내 PAHs 농도는 실험종료시까지(50일차) 1/2 수준이하로 회복되었다. 흥미롭게도, 50일의 노출실험 동안 유류분해성 박테리아의 군집의 꾸준한 증가가 관찰되어 OSA 형성이후 미생물 분해에 따른 유류오염환경 및 생물이 빠르게 회복될 수 있음을 확인할 수 있었다.

본 연구는 다양한 시공간적인 규모에서의 사례 연구를 통해 황해 해양 해양환경이 인간 활동의 영향에 대한 생태학적인 반응에 대해 제시하였다. 네 가지 사례연구를 통해 오염, 개발, 그리고 때로는 서식지 복원을 위한 시도(인공어초)가 해양 생물의 구조와 기능의 변화를 야기할 수 있음을 확인하였다. 지난 반세기동안 인간활동의 영향이 꾸준히 누적되어온 황해저서생태계이지만 저서미세조류에 의한 일차생산은 매우 높다는 것을 확인하였으며, 육상으로부터의 담수유입이 제한적인 환경에서 하구역에 서식하는 저서생물들은 저서미세조류를 먹이원으로 활발히 이용하고 있음을 확인하였다. 반면, 해양생태계 복원의 일환으로 시설되는 인공어초의 어류군집을 위한 긍정적인 효과를 확인하였지만, 잠재적인 위험성도 있음을 확인하였다. 마지막으로, 유류기원물질 OSA 형성이 해양이매패류 내 PAHs 생물축적을 야기하지만, 동시에 미생물에 의한 분해 또한 활발히 이루어짐을 확인할 수 있었다.

종합적으로 본 연구를 통해, 인간활동 영향에 의해 해양생태계의 건강성이 저해될 수 있지만, 여전히 황해생태계는 생산적인 환경이며

현재의 상황에 적응 혹은 대응하면서 작동하고 있음을 확인 하였다. 그러나 지속적인 해양 건강성의 약화는 해양 생태계 전반의 생산성 감소를 가져올 수 있을 것이다. 따라서 연안생태계의 더 나은 미래을 위해 지속 가능한 관리에 대한 과학적인 관심과 꾸준한 노력이 필요하다.

주제어: 해양생태계, 인간활동, 해양생물, 연안개발, 해양오염, 지속가능성
학번: 2015-30104